DESIGN OPTIMIZATION AND OPTIMAL CONTROL OF ENERGY SYSTEMS IN NEARLY/NET-ZERO ENERGY BUILDINGS

LU YUEHONG

Ph.D

The Hong Kong Polytechnic University

2016

The Hong Kong Polytechnic University

Department of Building Services Engineering

Design Optimization and Optimal Control of Energy Systems in Nearly/Net-Zero Energy Buildings

Lu Yuehong

A thesis submitted in partial fulfillment of the requirements for the degree of Doctor of Philosophy

June 2015

CERTIFICATE OF ORIGINALITY

I hereby declare that this thesis is my own work and that, to the best of my knowledge and belief, it reproduces no materials previously published or written, nor material that has been accepted for the award of any other degree or diploma, except where due acknowledgement has been made in the text.

I also declare that the intellectual content of this thesis is the product of my own work, except to the extent that assistance from others in the project's design and conception or in style, presentation and linguistic expression is acknowledged.

_____(Signed)

Lu Yuehong (Name of student)

Department of Building Services Engineering

The Hong Kong Polytechnic University

Hong Kong, P.R. China

ABSTRACT

Abstract of thesis entitled: Design Optimization and Optimal Control of Energy Systems in Nearly/Net-Zero Energy Buildings

Submitted by : Yuehong Lu (1190)

For the degree of : Doctor of Philosophy

at The Hong Kong Polytechnic University in June, 2015.

Nearly/net zero energy buildings (nZEBs) have been attracted increasing attention particularly when high performance is required in terms of energy-saving, indoor thermal comfortable, environment-friendly and grid-friendly. Increasing attention has been paid on how to design nZEBs in a cost/energy efficient and environment-friendly way. However, there is no exact approach at present for the design and control of the buildings to achieve nearly/net zero energy targets. This is mainly due to the complex interplay of electricity generation/consumption system and energy storage system, automatically and manually controlled systems/elements in the highly integrated buildings. Effective optimization methods are essentially needed for the optimal design and control of energy systems in nZEBs.

The aim of this PhD project is to study and develop design optimization methods and optimal scheduling strategies for the energy systems in nZEBs. A comprehensive literature review is presented first. Then, a nZEB simulation platform is developed for

the test and analysis of system design and control optimization. Validation of system models is made on the basis of Hong Kong Zero Carbon Building.

The performance of nearly/net zero energy buildings is largely affected by the renewable energy system design. The sizes of renewable energy systems for nZEBs are optimized by two optimization methods, including a single objective optimization using Genetic Algorithm and a multi-objectives optimization using Non-dominated Sorting Genetic Algorithm (NSGA-II). Building energy system models and renewable energy system models are developed and adopted, allowing the consideration of the interaction between building energy systems and renewable energy systems in optimization. The performance of the buildings with the optimized renewable energy systems is much better than that of the benchmark building in most scenarios. The single objective optimization can provide the "best" solution directly for a given objective while the multi-objective optimization provides rich information for designers to make better compromised decisions.

Due to the intermittent and unstable nature of renewable energy resources, the performance of net zero energy buildings may suffer a great degree of uncertainty compared to traditional buildings without renewable energy systems. Sensitivity analysis is conducted on an optimized renewable energy system (photovoltaic/wind turbine/bio-diesel generator) to investigate the impacts of the variations of input variables on the building performance. Four important design inputs regarding working conditions are concerned in the study, including wind velocity, other load, cooling load and solar radiation. Results show that, with 20% variations in the four variables, the maximum change of the combined objective is about 26.2%. In addition,

wind velocity is the most influential factor on the building performance regarding the total cost and/or CO_2 emissions, while the building loads (other load and cooling load) should be considered with top priority at the design stage concerning the overall building performance. The performance of the energy system, which integrates photovoltaic and bio-diesel generator, has been found not to be the most efficient. But, compared with the other three design options, its performance is the most robust when the working condition changes. The results also indicate that the use of active electricity generation systems in net zero energy buildings could increase the performance robustness of the building energy systems significantly.

The increasing complexity of building energy systems integrated with renewable energy systems requires essentially more intelligent scheduling strategy. An optimal scheduling using nonlinear programming is proposed for the control of energy systems in buildings integrated with electricity generation and thermal energy storage. A case study is conducted to validate the proposed strategy based on the Hong Kong Zero Carbon Building. Two types of grid-connections (i.e., selling electricity to grid is allowed and forbidden respectively) are considered. Results show that significant reductions in carbon dioxide emissions, primary energy consumption and operation cost are achieved by the proposed optimal scheduling strategy.

Considering the discrete working ranges of some energy systems, the mixed-integer nonlinear programming (MINLP) approach is further used to solve the optimal scheduling problems. The enhanced scheduling strategy based on MINLP minimizes the overall operation cost day-ahead, including operation energy cost and cost concerning the plant on/off penalty. Four scenarios are investigated and compared to

evaluate the performance of the enhanced scheduling strategy. Results show that the strategy can reduce operation energy cost greatly (about 25%) compared with a rule-based strategy and the reduction is even increased to about 47% when a thermal energy storage system is used. The strategy can also reduce the on/off frequency of chillers significantly.

PUBLICATIONS ARISING FROM THE THESIS

Journal papers

1. **Lu Y.H**., Wang S.W., Zhao Y., Yan C.C. 2015. Renewable Energy System Optimization of Low/Zero Energy Buildings Using Single-Objective and Multi-Objective Optimization Methods. *Energy and Buildings* 89: 61-75.

2. **Lu Y.H**., Wang S.W., Sun Y.J., Yan C.C. 2015. Optimal scheduling of buildings with energy generation and thermal energy storage under dynamic electricity pricing using mixed-integer nonlinear programming. *Applied Energy* 147: 49–58.

3. **Lu Y.H**., Wang S.W., and Kui Shan. 2015. Design optimization and optimal control of grid-connected and standalone nearly/net zero energy buildings. *Applied Energy* 155: 463-477.

4. Zhao Y., **Lu Y.H**., Yan C.C. and Wang S.W. 2015. MPC-based optimal scheduling of grid-connected low energy buildings with thermal energy storages. *Energy and Buildings* 86: 415-426.

5. Zhao Y., Xiao F., **Lu Y.H**., Wen J. and Wang S.W. 2014. A robust pattern recognition-based fault detection and diagnosis (FDD) method for chillers. *HVAC&R Research* 20 (7): 798-809.

6. Yan C.C., Wang S.W., Shan K., **Lu Y.H**. 2015. A simplified analytical model to evaluate the impact of radiant heat on building cooling load. *Applied Thermal Engineering* 77: 30-41.

Journal papers under review

7. **Lu Y.H**., Wang S.W., Yan C.C. and Kui Shan. 2015. Impacts of renewable energy system design inputs on the performance robustness of net zero energy buildings. Under review by Energy.

Conference papers

8. **Lu Y.H**., Wang S.W., and Zhao Y. 2015. Optimal Scheduling Based on Mixed-integer Nonlinear Approach for Energy Systems in Buildings with Energy Generation and Thermal Storage. *Second International Conference on Sustainable Urbanization (ICSU 2015)*, Hong Kong, China.

9. **Lu Y.H**., Wang S.W. 2014. Design Optimization of Renewable Energy System in Low/Zero Energy Buildings Using Single-Objective and Multi-Objective Optimization Methods. *The 3rd International High Performance Buildings Conference (2014 Purdue Conferences)*, Purdue, USA, 14-18 July 2014.

10. **Lu Y.H**., Wang S.W., Huang Z.J. 2013. Experimental and simulation on the performance and optimization of LiBr liquid dehumidifiers. *CLIMA 2013*, Prague, Czech Republic 16-19 June 2013.

11. Wang S.W., **Lu Y.H**., Xue X. 2013. Experimental investigation on energy demand and generation of zero carbon building in Hong Kong. The 12th international conference on Sustainable Energy Technologies (SET 2013), Hong Kong, China 26-29 August 2013.

ACKNOWLEDGEMENTS

I would like to express my grateful and sincerest appreciation to my supervisor Prof. Shengwei Wang for his patient guidance and continuous support during the last three years of my PhD study. His strict attitude and thinking patterns impress me a lot, which will definitely not only guide me in the research, but also inspire me in my whole life. I would like to thank my co-supervisor Prof. Fu Xiao for her encouragement and continuous support on my research. Also, I would like to thank Dr Guiyi Li, my co-supervisor, for providing me the guidance and essential support on the energy performance study and on-site monitoring on the Hong Kong Zero Carbon Building (ZCB).

I would also like to thank all my fellow members in my research team, especially Dr Zhao Yang for his support and cooperation in developing the optimal scheduling strategy for building energy systems, Dr Yan Chengchu for his support in developing HVAC system models, Dr Shan Kui for his support in performing sensitivity analysis, and Dr Gao Diance for his support in developing system models in TRNSYS. Their talents and diligence always inspire and encourage me to be better.

Finally, I am truly grateful for the love, support and patience from my parents and my brothers. Without them, I would not have been able to thrive in my doctoral program. I am incredibly grateful for those friends who stand by to support me along the way over the last three years.

TABLES OF CONTENTS

LIST OF FIGURES

LIST OF TABLES

NOMENCLATURE

A	area
A'	constant parameter depending on tower size
c	coefficient
CDE	carbon dioxide emissions (kg)
cde	emission factor (kg/kWh)
COP	Coefficient Of Performance
E	energy demand (kW)
F	fuel
f	building-grid interaction
GII	grid interaction index
I	hourly irradiance (kWh/m^2)
J	daily cost (USD)
K	constant parameter depending on tower size
N	fan speed
Δp	pressure drop
P_f	packing factor
PEC	primary energy consumption

PLR	partial cooing load ratio
Q	cold/cooling demand (kW)
T	temperature (℃)
TC	annual total cost (USD)
v	velocity (m/s)
w	weighting factors
W	power (kW)
η	efficiency
ρ	density (kg/m^3)
υ	flow rate (m^3/s)

Subscripts

a	air
ac	absorption chiller
BDG	bio-diesel generator
BB	benchmark building
bio	bio-diesel
ct	cooling tower
c	cooling demand

con	condenser
cwp	cooling water pump
demand	electricity demand
ec	electric chiller
ex	exported
eva	evaporator
ele	electricity
gas	gas consumption
hrs	heat recovery system
HVAC	heating, ventilation and air-conditioning
in	inlet water
im	imported
irra	irradiation
n	nominalized
out	outlet water
oth	other parts of the air system
other	other appliances
PV	photovoltaic
PC	power conditioning

r	recovery
resi	renewable energy system investment
sen	sensor
seq	sequence
supply	electricity supply
wa	water
WT	wind turbine
wb	wet-bulb

CHAPTER 1 INTRODUCTION

1.1 Motivation

Energy conservation and environmental problems are of serious concern to governments, professionals and society. Increasing efforts are made to reduce energy consumption and to protect the environment. It is widely acknowledged that buildings play a significant role in facing the challenges since they account for over 40% of end-use energy in the world and it is even higher (90% of electricity) in Hong Kong. Due to the expansion of population and built area as well as associated energy needs, building energy consumption is continuing to grow over years. In the past two decades, the building energy consumption in China has an annual increase rate of more than 10% (Cai et al. 2009). In the UK and Spain, building energy consumptions have the growing rates of 0.5% and 4.2% per annum respectively. In North American, the growing rate of building energy consumption is 1.9% per annum. In general, it is expected that energy consumption in the service sector in developing countries will be doubled in the next 25 years, with an annual average growth rate of 2.8% (Pe´rez-Lombard et al. 2008), if no serious energy conservation measures are adopted.

With an increasing requirement and heavily dependency on energy, much pressure has been put on conventional energy resources (such as coal, oil and nature gas). However, the limited reserves of conventional energy resources are too expensive and too environmentally damaging to retrieve. Renewable energy resources, such as wind,

solar energy, and geothermal energy and so on, have been attracted great and increasing attention as they are naturally replenished resources. In the past years, hybrid renewable energy systems have been widely applied for remote islands and villages that have no access to electricity from power grid. Renewable energy can be utilized in buildings to relieve the tension between energy demands from power grid and public concerns on environmental pollution.

Figure 1.1 World map of more than 360 international known net zero energy buildings

The terms ‘ZEB’ (zero energy building) and ‘nZEB’ (nearly/net zero energy building) have been recognized as a solution to the energy problems in future for low energy/carbon society construction and sustainable development. Several countries have adopted policies and regulations to promote the development of nZEB as the future buildings such as the “EU Directive on Energy Performance of Buildings” and the “Building Technology Program” of the US Department of Energy. A growing attention has been given to nZEB in recent years and an increasing number of case studies have been conducted worldwide to demonstrate the potential of net zero target. More than 360 nZEB projects in different countries have been recognized, based on

the map of international projects as shown in Figure 1.1. However, there are still many challenges during the development of nZEBs:

Firstly, in the existing literatures, the definition of nZEB is still ambiguous and lacking of common and consistent concept at the international level. There is no standard calculation procedure for nZEBs at present and most of the calculations are just voluntary proposals developed for a particular nZEB case. However, the difference of nZEB definitions would definitely affects significantly the way a building designed and controlled in order to achieve its goal.

Secondly, there is no exact approach or guideline for the design of buildings to achieve the goal of nZEB at present. In general, there are three main steps for achieving the nZEB target, i.e. the use of passive design strategy, energy efficiency technologies and electricity generation technologies. Most of existing design studies aims to obtain the optimal design strategies that minimize the system cost. However, the environmental issues (e.g. CO_2 emissions) and the stress of nZEBs on power grid have not been taken into account in most design optimization.

Thirdly, the integration of on-site electricity generation systems, energy storage systems as well as the two-way communication between nZEBs and smart grid poses great challenges for the energy or cost efficient control of energy systems. The development of intelligent predictive control strategies based on accurate models is essential to perform the dynamic respond to the time-sensitive electricity price under micro/smart grid.

nZEBs will definitely play an increasingly important role in the development of sustainable buildings in future. In fact, there has been significant progress in developing nZEB projects in European and USA. However, it is still urgent and challenging to optimal design and control of nZEBs. The study presented in this thesis is hoped to assist to move the design and control of nZEBs towards a holistic view, ensuring a reliable, gird-friendly, environment-friendly, cost-effective and comfortable building for the living.

1.2 Aim and Objectives

The aim of this PhD project is to study and develop design optimization methods and optimal scheduling strategies for the energy systems in nZEBs. It is accomplished by addressing the following objectives:

1. Develop a nZEB simulation platform and validate the component models developed using the in-situ measurements. The building energy system models and renewable energy system models are used for the test and validation of system design optimization methods and optimal control strategies.

2. Develop and test the design method/approach for optimizing the sizing of the renewable energy systems in nZEBs. The optimization intends to achieve the minimized total cost, the minimized impacts to environment and the minimized grid stress of building energy systems in its life-cycle.

3. Perform sensitivity analysis to investigate the impacts of operation variables on the nZEB performance and to investigate the performance robustness of different

design options for nZEBs. The intention is to identify the most significant factor on nZEB performance and select a design option with robust performance.

4. Develop and validate the optimal scheduling strategy for the control of energy systems in nZEBs. The strategy should generate one-day-ahead schedule trajectories of the control variables for the building energy systems. The strategy should achieve the most cost-efficient operation and satisfy the requirement of operation constraints.

1.3 Organization of the Thesis

This chapter presents the motivation of optimizing renewable energy system design and control in buildings. The development of nZEBs and challenges faced are discussed. Then the aim and objectives of this thesis are presented. The other chapters are organized as follows.

Chapter 2 presents a comprehensive literature review on the design and control issues of nZEB that provide the basis for developing the design optimization and optimal control methods of nZEB. Design optimization is reviewed in terms of design steps, effects of climate and site on design, design optimization methods, and uncertainty/sensitivity analysis for robust design and system reliability. The review on scheduling and control of nZEBs covers the use of high efficiency generation systems, energy storage systems, scheduling and model predictive control methods, smart control technologies, and scheduling/control of energy systems in both grid-connected and standalone buildings.

Chapter 3 presents an overview of the state-of-the-art of the eco-building design and technologies used in Zero Carbon Building (ZCB) in Hong Kong. The ZCB, also a designed nZEB, is studied and used to develop the simulation platform for zero energy building. The building performance is evaluated using one year data (between April 2013 and March 2014). In addition, the performance of ZCB is compared with that of other ZEB projects in terms of their electricity generation systems and energy performance.

Chapter 4 presents building energy system models developed (including the electric chillers, pumps, cooling tower fans and AHU fans) and renewable energy system models developed (including PV, wind turbine and bio-diesel generator). Validation is performed by using the operation data of the energy systems in ZCB.

Chapter 5 presents the method for design optimization of renewable energy systems in nZEBs. Two case studies are conducted on simulation platform to compare capability and effectiveness of two optimization methods (i.e. single objective optimization and multi-objectives optimization).

Chapter 6 presents the impact of operation variables on the performance robustness of energy systems in nZEBs. One-way sensitivity analysis, two-way sensitivity analysis and multiway sensitivity analysis are performed for the typical design options to identify the most significant factor that affects the building performance. In addition, the performance robustness of four design options is compared taking the input variations into consideration.

Chapter 7 presents an optimal scheduling strategy using nonlinear programming (NLP) for the energy systems in nZEBs. Evaluation of the strategy on energy systems is performed in terms of carbon dioxide emission, primary energy consumption and operation cost. Sensitivity analysis is performed to investigate the effect of uncertainties on the building performance by using the proposed strategy. Advantages and limitation of the NLP-based strategy is also discussed.

To address the limitations of the NLP-based strategy, an enhanced optimal scheduling using mixed-integer nonlinear programming (MINLP) for the control of energy systems in nZEBs is presented in Chapter 8. The performance of the energy systems scheduled by the MINLP-based optimal control strategy is compared with that using a rule-based strategy and the NLP strategy respectively.

Chapter 9 presents a summary on the work done in the PhD project and the recommendations for further research and application in the relevant subject area.

CHAPTER 2 LITERATURE REVIEW

The design and control strategies for nearly/net zero energy buildings (nZEBs) are not straight-forward since the buildings may involve complex integration of different energy systems, such as renewable energy generations, energy appliances, energy storages and may also interact with the smart grid. A comprehensive literature view on the design and control issues of nZEBs is essential to assist the development of nZEBs of a high-level performance.

Section 2.1 presents a literature review on the regulatory and policies that aim to promote the development of zero energy buildings in different countries (*Section 2.1.1*) and different definitions found in literature (*Section 2.1.2*).

Section 2.2 presents literature review on design optimization in terms of design steps (*Section 2.2.1*), effects of climate/site on design (*Section 2.2.2*), design optimization methods (*Section 2.2.3*) and uncertainty/sensitivity analysis for robust design and system reliability (*Section 2.2.4*).

Section 2.3 presents literature review on scheduling and control of energy systems in nZEBs, including the use of high efficiency generation systems (*Section 2.3.1*), the use of energy storage systems (*Section 2.3.2*), the use of scheduling and model predictive control methods (*Section 2.3.3*), the use of smart control technologies (*Section 2.3.4*), scheduling and control of energy systems in standalone buildings (*Section 2.3.5*).

Section 2.4 presents an overview of internationally known nZEBs projects (*Section 2.4.1*) and a summary of design features as well as the actual energy performance of buildings in 30 case studies (*Section 2.4.2*).

2.1 An Overview of nZEB Development

2.1.1 nZEB Regulations

Energy consumption of buildings accounts for 40% of the primary energy in USA and Europe, nearly 30% in China and even up to 80% in Hong Kong (Crawley et al. 2009; Aste et al. 2011). Buildings are also one of most significant contributors of greenhouse gases. Nearly/net zero energy buildings (nZEBs), an innovative concept for sustainable buildings, has attracted increasing attentions, which is regarded as a mean to energy-saving and carbon emission reduction. By applying energy sufficiency measures and the integration of renewable energy systems in buildings, it is possible to achieve the target of nearly/net zero energy balance and maintain a sustainable, healthy and grid-friendly building (Li and Wen 2014; Sun et al. 2015; Aelenei and Gonçalves 2014).

Plenty of efforts have been made on establishing regulations and quite a few regulations on nZEBs have been proposed and promoted at the international level, such as:

- Under the umbrella of international energy agency (IEA) solar heating and cooling program (SHC), researchers and experts from Australia, Austria, Belgium, Canada, Denmark, Finland, France, Germany, Italy, Korea, New Zealand, Norway,

Portugal, Singapore, Spain, Sweden, Switzerland, United Kingdom and USA have been working together on the task 40 “Towards net zero energy solar buildings”. The aim of the task is to study nearly/net zero energy buildings and to develop a common understanding and a harmonized international definition framework as well as tools, innovative solutions and industry guidelines (SHC TASK 40 2008).

- In Europe, the Directive on Energy Performance of Buildings establishes the goal of ‘nearly net zero energy buildings’ for all the new buildings from 2020 (EBPD 2010).
- ZEBRA 2020 (Nearly zero energy building strategy 2020) covering 17 countries, was launched in 2014 aiming at creating an observatory for nZEBs based on market studies and various data tools and therefore generates data and evidences for optimization and policy evaluation (Zebra 2014).
- In United Kingdom, the ambition is to have zero carbon homes by 2016.
- In France, all new buildings should comply with energy positive by 2020.
- The California Public Utilities Commission of the USA has set a net zero energy target for all new residential buildings by 2020 and for all new commercial buildings by 2030 (Crawley et al. 2009).
- Similar promotion proposals and developments can be also observed in Japan, China and Australia (Sustainable buildings in Japan; Sustainable buildings in Australia; Sustainable buildings in China).

More than 360 internationally known net zero energy buildings are listed and edited in a world map (World Map of nZEBs 2013). A net zero energy building database also provides some demonstration projects containing realistic experiences of design, operation and test (nZEBs database).

The rigorous regulations and programs also promote the research progress of nZEBs. Marszal et al. (2010) presented a review on the definitions and calculation methodologies of zero energy buildings (ZEBs). Deng et al. (2014) summarized the widely-used research methods, tools and performance evaluation indicators for ZEBs. Li et al. (2013) presented a review on zero energy buildings and sustainable development implications. Kolokotsa et al. (2011) reviewed the technological developments in various ingredients for buildings towards intelligent net zero/positive buildings.

2.1.2 nZEB Definitions

Consistent nZEB definitions are definitely needed for the design, operation, and performance evaluation of nZEBs since the way to define a nZEB affects significantly the way to design the building in order to achieve the target. In the existing literature, the definition/framework of nZEB is still ambiguous and lacking of common and consistent concept at the international level (Marszal et al. 2011). The definition involves different elements, such as: boundary, weight, metrics and criteria etc. Based on individual considerations on local climate, the feasibility of on-site renewable energy sources or cost, different designers could choose specific elements at different levels to form the definition in accordance with the local requirements. Torcellini et al. (2006) indicated that several factors have critical effects on the nZEB definition: (1) the project goals, (2) the intentions of the investor, (3) the energy cost and (4) the concerns about the greenhouse gas emissions and the climate. Therefore, four different nZEB definitions are proposed by them, including site nZEB, source nZEB, emissions nZEB and cost nZEB. Kilkis (2007) also indicated that ‘zero’ should take into

consideration of the quantity and quality (exergy). Therefore, the definition of zero exergy building was proposed. These five typical ZEB definitions are listed below.

- Site nZEB: A site nZEB produces at least as much energy as it uses in a year, when accounted for at the site.
- Source nZEB: A source nZEB produces at least as much energy as it uses in year, when accounted for at the source. Source energy refers to the primary energy used to generate and deliver the energy to the site.
- Emissions nZEB: A net-zero emissions building produces at least as much emissions-free renewable energy as it uses from emissions-producing energy sources.
- Cost nZEB: In a cost nZEB, the amount of money the utility pays the building owner for the energy the building exports to the grid is at least equal to the amount the owner pays the utility for the energy services and energy used over the year.
- Exergy nZEB: a building, which has a total annual sum of zero exergy transfer across the building-district boundary in a district energy system, during all electric and any other transfer that is taking place in a certain period of time.

  There is also no global or universally-agreed definition of low energy building (LEB). But a better energy performance should be achieved in LEB than the standard building energy codes. This generally indicates that a mixture of passive techniques or/and efficient active energy systems is used to minimize building energy use (Low Energy Buildings in Europe 2009). A net zero energy building is commonly regards as a building in which the annual electricity consumption

equals to its annual electricity generation (Iqbal 2004; Li et al.2013; Lu et al. 2015; Sun 2015).

2.2 Design Optimization of nZEBs

2.2.1 Design Steps

Although there is no exact approach for designing and realizing nZEBs, most nZEBs share several common design elements and some consensus. William et al. (2014) proposed an approach involving twelve-steps for the design of nZEBs as shown in Figure 2.1. These twelve steps form a thorough design process containing foundational procedures, design methodology, mechanics and implementation as well as enjoying what you have created. An explicative diagram of a "nearly/net zero energy building" is shown in Figure 2.2. The three main steps for achieving the nZEB target are the use of passive design strategy (e.g. building envelope, orientation, geometric/ratios), energy efficiency technologies (e.g. HVAC, hot water, lighting, appliances and equipment) and electricity generation technologies (e.g. combined cooling and/or heat and power, fuel cells, hydroelectric power, photovoltaic panel, wind turbine) (Rodriguez-Ubinas et al. 2014; Doust et al. 2012).

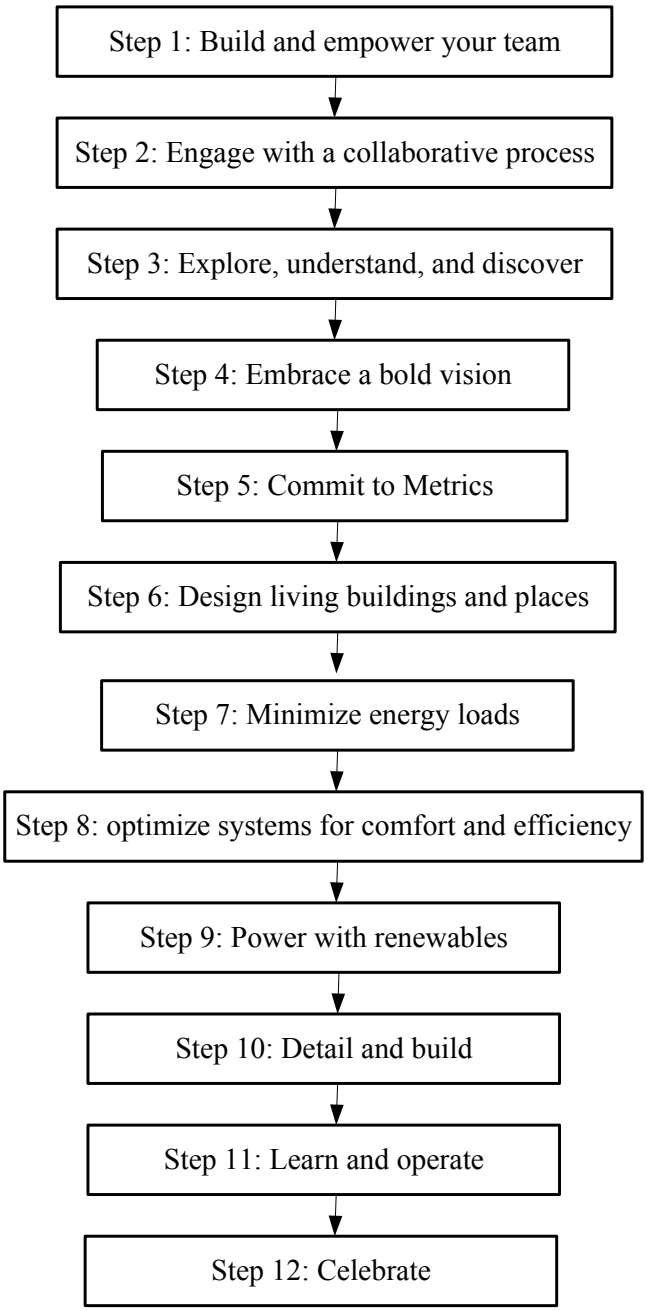

Figure 2.1 Twelve steps to nZEB

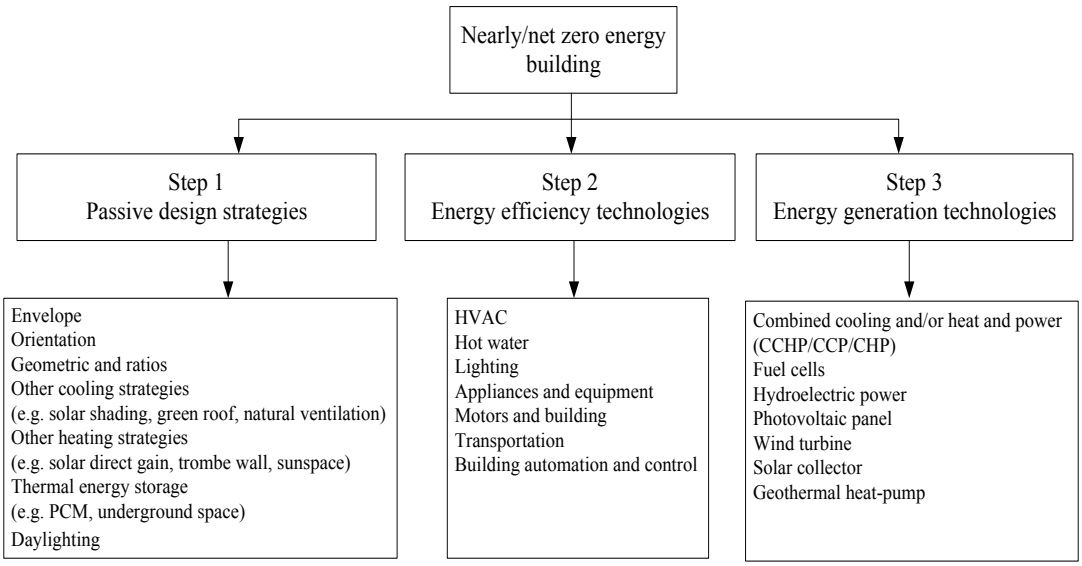

Figure 2.2 The main elements to be designed for nZEB

nZEB researches and projects have been promoted aggressively all over the world. Table 2.1 shows a summary of some recent researches on the design optimization of nZEB in different climate zones including cold climate, warm climate and tropical climate. Detailed description of the individual buildings, measures applied and performance evaluation can be found in the corresponding references. The optimization methods applied, uncertainty/sensitivity analysis involved for robust design and major findings are discussed in the following sections.

Table 2.1 Summary of recent researches on design optimization for nZEBs

Ref	Journal	Country	Electricity generation systems	Optimization Methods/software	Uncertainty/ Sensitivity analysis	Performance indicates
Iqbal (2004)	Renewable energy	Newfoundland	wind turbine	HOMER	Y	annual energy consumption and generation
Bucking et al. (2014)	Building performance simulation	Eastman	photovoltaics & geothermal heat-pump	Back-tracking search	Y	importance factor
Hamdy et al. (2013)	Energy and buildings	Finland	PV, ground source heat pump	A modified multi-objective genetic algorithm PR_GA	Y	life-cycle cost, primary energy consumption
Hassoun et al. (2014)	Energy and buildings	Lebanon	PV, WT, generator, battery	HOMER	Y	net present cost
Rezzouk et al. (2015)	Renewable and sustainable energy reviews	Algeria	PV–diesel–battery	HOMER	Y	Net present cost
Lu et al. (2015)	Energy and buildings	Hong Kong	PV, WT, bio-diesel generator	GA, NSGA-II	N	Total cost, CO2 emission, grid interaction index

Tina et al. (2006)	Solar energy	Italy	PV-WT	Probabilistic approach	Y	energy index of reliability
Ai et al. (2003)	Renewable energy	Hong Kong	PV-WT-battery	Graphical construction method	N	total cost
Kaabeche et al. (2011)	Energy	Algeria	PV-WT-battery	Iterative approach	N	different desired system reliability requirements, the levelised unit electricity cost
Avril et al. (2010)	Energy	France	PV-hydrogen-battery	Particle swarm optimization (PSO)		the total levelized cost
Ramoji et al. (2014)	Advanced research in electrical, electronics and instrumentation engineering	India	PV-WT-battery	Genetic algorithm (GA)	N	total cost
Sun (2015)	Energy and buildings	Hong Kong	PV-WT-battery	Exhaustive search approach	Y	overall initial cost
Ekren et al. (2010)	Applied energy	Turkey	PV-WT-battery	Simulated annealing algorithm/heuristic approach	N	system total cost

Li et al. (2013)	Energy	Urumqi, China	PV-WT-battery	HOMER	Y	The total net present cost
Bambrook et al. (2011)	Energy and buildings	Sydney	PV	IDE Indoor Climate and Energy	N	The life cycle cost
Baglivo et al. (2014)	Energy and buildings	Italy	-	Multi Objectives Genetic Algorithm	N	decrement factor, periodic thermal transmittance, time shift, areal heat capacity
Ismail et al. (2013)	Energy conversion and management	Malaysia	PV-diesel-battery	Genetic algorithm (GA)	Y	Total cost
Kurnitski et al. (2011)	Energy and building	Estonia	PV-solar collector-ground source heat pump	Seven-step procedure + IDE Indoor Climate and Energy	Y	Net present cost
Kapsalaki et al (2011)	Energy and building	Portugal	PV-WT-solar collector	Artificial intelligence method	N	life-cycle cost, initial cost
Dekker et al. (2012)	Electrical power and energy systems	South Africa	PV/diesel/battery	HOMER	Y	Net present cost

2.2.2 Effects of Climate/site on Design

The effects of climate/site cannot be neglected at the beginning of the nZEB design stage due to the fact that the passive design and electricity generation system design for buildings have strong dependence on climate and site (Li et al. 2013; Bernal-Agustín et al. 2009). Many studies have been conducted on the passive design strategies for minimizing the building load and maximizing the use of renewable energy resources available for electricity generation in different climate areas.

In the cold climate areas with heating dominated, insulation in general tends to be more effective (in terms of environmental and cost benefits) than that in cooling-dominated areas. In Europe, a technology of multi-layered walls is adopted in nZEB design. The multi-layered walls use structural materials with good thermal isolation, low density, low specific weight, low mass accumulation and wide thickness in order to bring down winter heating costs and approach very low steady thermal transmittances (Baglivo et al. 2014; Al-Sanea and Zedan 2012). Some studies found that the increase in the shape factor (more external building surface for the same volume, low compactness index) is a good representation of energy consumption and should be careful determined in cold climate zones. Pikas et al. (2014) and Thalfeldt et al. (2013) studied energy efficient fenestration design solutions for a low energy building in the cold Estonian climate. The results indicate that a smaller window to wall ratio, triple glazing and argon filling and 200mm thick insulation for walls are energy efficient and cost optimal within 20 years in this cold climate.

In the warm climate areas, shape factor is no longer a key parameter relevant to energy consumption. As mentioned by Pacheco et al. (2012) and Depecker et al. (2001), the

proportion of the increase in the shape factor to the increase in the energy required for heating was not direct. Eshraghi et al. (2014) conducted a design study of a solar zero energy building, i.e. a detached house located in moderately warm climate. Trombe-wall, roller shading and thermal mass were applied as the main passive strategies and 42% load reduction in a large bedroom was obtained by applying trombe-wall. Bambrook et al. (2014) conducted a design optimization using a building energy simulation program IDA ICE for a detached low energy house in the mild warm Sydney climate. The aim of the optimization was to reduce the building heating and cooling demand to the level at which the heating and cooling system was no longer necessary. Baglivo et al. (2014) carried out a multi-objective analysis to obtain several types of high energetic efficiency external walls for zero energy buildings through the combination of various materials. They pointed out that the superficial mass of the external wall was important for achieving the best building performance in the warm climate compared with the application of multi-layered walls to yield the benefits of typical passive heating systems in Europe.

In the Mediterranean climate, the application of multi-layered walls in buildings does not yield typical passive heating system benefits since surfaces with thermal accumulation mass are not large enough. Panao et al. (2013) discussed the energy required by a nearly zero energy building in a Mediterranean climate (Lisbon). The thermal insulation thickness from 40 to 60 mm and double glazing of 6/16/6 mm are found to be the cost-optimal solutions for most real houses studied. Silva et al. (2013) proposed and studied a new prefabricate retrofit module solution for the existing building facades to meet the nZEB standards in Portuguese. Ismail et al. (2013)

investigated different components constructing the hybrid system for remote houses in a Malaysian village in the tropical climate. They pointed out that the optimal scenario is the system integrating PV panels, a diesel generator and a battery bank. In hot and humid climate, Fong and Fong and Lee (2014) proposed a hybrid renewable cooling system utilizing both the solar energy and the ground source for an office building. The proposed hybrid system could have 40%~70% of primary energy saving compared with the sole system and conventional air conditioning system. As the solar energy and wind energy are abundant in the subtropical Hong Kong, Fong and Lee (2012) also conducted a case study on feasibility of net zero energy target in three-storey houses. This study reveals a possible direction towards realizing the target: PV panels and BIPV with nominal efficiencies of more than 13% as well as good human behaviors involved.

Many studies have been conducted on the effects of different climates on the efficient designs of nZEBs. Kapsalaki et al. (2012) studied the influence of three climate contexts (i.e. climates with cold winter, very mild winter and very mild winter but warm summer respectively) on the economic efficient design solutions for residential net zero energy buildings. The results indicated that more energy efficient solutions and more PV area are required for the optimal design solutions for cold winter climates, which tends to be more costly compared with the design solutions for the mild winter climates. Economic analysis of hybrid PV-diesel power system in different climate zones of South Africa was investigated by Dekker et al. (2012). They found that the arid interior is the optimum climate zone for installing a PV/diesel hybrid power system in South Africa, based on the net present cost (NPC) of all simulations. Robert

and Kummert (2012) investigated the role of climate change on the design of nZEB in two different locations. They also suggested that using individual years that present some variability while including the general trend of climate change is clearly a better option than rewinding a typical reference year representing the past climate.

Zhao et al. (2015) studied the influences of different envelope parameters on the energy use for heating and cooling in different climate zones in China. According to the results, window U-value, air tightness and insulation thickness of external walls should be paid more attention in the cold zone. In the hot summer and cold winter zone, window to wall ratio on the south façade, infiltration rate and U-value of the external walls are crucial. In the hot summer and warm winter zone, insulation thickness of external walls, the shading coefficient of windows and solar protection are the important parameters.

2.2.3 Design Optimization Methods

The biggest challenge for the design of a nZEB, which is integrated with different types of energy systems, is that multiple design parameters must be decided simultaneously. Some researchers therefore divided the design into several steps with the goal of achieving a high performance. Visa et al. (2014) introduced a three steps method for the transform of existing buildings with already implemented renewable energy systems to be nZEBs. The possible alternatives were identified and optimized for a solar house on the basis of the technical and economic criteria. They then extended the method to be four steps and applied it for an R&D laboratory building, several optimal energy mixes were identified using the proposed method (Moldovan et al. 2014). Pikas et al. (2014) employed a three step approach to determine the cost

optimal and most energy efficient fenestration design solutions for achieving nZEB levels in Estonian climate. Kurnitski et al. (2011) developed seven-step procedure combining energy simulation tool IDE-ICE, without using iterative approach or optimization algorithm, to determine the cost optimal solutions for nZEB. In another study (Hamdy et al. 2013), the multi-stage simulation-based optimization method was further introduced to find the cost-optimal design solutions for nZEB in Finland. The design options involve the building-envelope parameters, heating/cooling systems, heat-recovery units and sizes of thermal/ photovoltaic solar systems.

Many efforts have been paid on the applications of graphical construction method (Borowy and Salameh 1996), probabilistic approach (Gordon 1987), iterative approach (Kellogg et al. 1988) and artificial intelligence method (Koutroulis 2006) for the optimum sizing of stand-alone hybrid solar-wind power generation systems, which are explained as follows.

- The graphical technique has been investigated by Borowy and Salameh (1996), Bin et al. (2003), Markvart (1996) and Kaabeche et al. (2006) to optimally size the component capacity of a solar-wind hybrid power generation system. However, the graphical methods utilized only account for two parameters (either PV and batter, or PV and wind turbine) in the optimization process while important factors (such as the wind turbine installation height and PV module slope angle) are ignored completely.
- Probabilistic approach could account the effects of the wind speed and solar radiation variations on sizing the solar-wind hybrid systems. A probabilistic approach based on the convolution technique Karaki et al. (1999) was presented

by Tina et al. (2006), incorporating the fluctuating nature of the load and the resources, to assess the long-term performance of a solar-wind hybrid system for both grid-connected and stand-alone applications and the need for time-series data was eliminated. However, the probabilistic approach cannot represent the dynamic performance of the hybrid systems.

- Iterative method was used by Kaabeche et al. (2011) to optimally size the capacity of a grid-independent PV/wind/battery hybrid energy system. The proposed method was then demonstrated by conducting a case study to design a hybrid energy system for a residential household situated in Algeria. Yang et al. (2003) (2007) proposed an iterative optimization technique to select the number of the PV module, wind turbine and battery. The system cost was minimized while providing the satisfactory of electricity demand and power reliability.
- Ekren et al. (2010) performed simulated annealing algorithm, using a stochastic gradient search, for optimizing the size of PV/wind hybrid system with battery storage. In this study, the simulated annealing algorithm was demonstrated to give a better result compared with the response surface methodology. Ramoji and Kumar (2014) proposed a new approach, GA&TLBO-based optimization technique, to optimally size a PV/wind/battery system to minimize the total cost for the system components while ensuring the system was kept reliable to supply power.

The design optimization software, HOMER, has been used extensively to facilitate the design optimization of renewable energy systems based on net present cost in previous studies (Iqbal 2004; Hassoun and Dincer 2014; Rezzouk and Mellit 2015; Li et al. 2013; Dekker et al. 2012; Ekren et al. 2010]. Iqbal (2004) employed HOMER to select

the optimum energy systems for achieving a zero energy home located in Newfoundland. Hassoun and Dincer (2014) compared various power design options for a net-zero energy house located in Lebanon. Comprehensive simulations were carried out using HOMER and the aim was to achieve the least total net present cost and maximum renewable energy fraction. Rezzouk and Mellit (2015) conducted a study on the optimal configuration of hybrid energy system (photovoltaic-diesel-battery) for a research unit located in the north of Algeria. The power system was optimally designed to get a maximum output power at a low cost for each scenario, while the photovoltaic penetration was varied from 0% to 100%. Askari and Ameri (2012) used HOMER to analyze three renewable energy systems (i.e. PV/battery, wind/batter and PV/wind/battery) for supplying the electricity demand of a remote community in Iran. The results recommend the PV/battery system as the optimal system combination to supply the power requirement in that study. HOMER is relatively simple and easy to be used for designing renewable energy system since it contains a mix of energy production systems (generator, wind turbines, solar photovoltaics, batteries, fuel cells, hydropower and others). However, HOEMR can only address single objective function for minimizing the net present cost while the multi-objectives problem cannot be addressed. In addition, the building energy consumption can be inputted as a file of fixed data only. As mentioned by Lu et al.(2015), HOEMR cannot be used to optimize the design of renewable energy systems in buildings where the design of some renewable energy system affects electric consumption of other energy systems.

Genetic algorithm (GA) is the most favored method for single objective and multi-objective optimizations of hybrid energy systems in previous studies. Kalantar and Mousavi (2010) investigated the design optimization of the wind-micro turbine-PV-battery hybrid system using GA to minimize the annualized cost of system. Yang et al. (2008) developed an optimal sizing method to optimize the configurations of a hybrid solar–wind system with battery banks based on a GA. Ould Bilal et al (2010) applied the multi-objective genetic algorithm to optimally size the solar-wind-battery hybrid system with the objective of minimizing the annualized cost and minimizing the loss of power supply probability. In order to compare the capability and effectiveness between the single objective optimization and multi-objectives optimization methods, Lu et al (2015) presents a comparison study on two design optimization methods, i.e. single objective optimization using GA and multi-objectives optimization using Non-dominated Sorting Genetic Algorithm (NSGA-II), for optimal designing the renewable energy systems in buildings to minimize the total cost, CO_2 emissions and the stress on the power grid. It is found that the computation time for optimization calculations is more than 1 h for GA and more than 10 h for NSGA-II optimization respectively.

The second favorite method in recent papers for the design optimization of energy systems is particle swarm optimization (PSO). Avril et al. (2010) proposed a multi-objective code based on particle swarm optimization to search the best combination of different energy devices. The proposed method performs numerical optimization without explicating the gradient of the variables to be optimized and the calculation time can be reduced by making a parallelization of the code. Moghaddas-Tafreshi and

Hakimi (2009) presented a novel intelligent method based on PSO algorithm for optimal sizing of a hybrid power system with the aim of minimizing the total cost of the system. They further pointed out that the PSO algorithm is faster and less complicated than GA or ant colony algorithm. Besides the GA and PSO algorithm, other methods are also investigated. Sun (2015) proposed an exhaustive search approach for the design of renewable energy system and storage system in a nZEB to minimize the overall initial investment. Sreeraj et al (2010) proposed a novel method combining the deterministic approach and probabilistic approach to find the minimum battery capacity for a renewable hybrid system. Maheri (2014) proposed a robust design methodology for a standalone wind/PV/diesel hybrid system to find the most reliable system and the most cost-effective system respectively.

Several novel method/design tools have been developed for aiding the optimal design of the nZEB. Hamdy et al (2011) proposed a modified multi-objective optimization approach which is combined with IDA ICE (building performance simulation program) to minimize the investment and the equivalent CO_2 emissions for a family house including its HVAC system. O'Brien et al. (2009) developed a design tool for a solar house design. The proposed design tools could cover the optimal design of the form and fabric of a house as well as active solar systems. Attia et al. (2012) presented a simulation-based design support tool (namely ZEBO). A sensitivity analysis is embedded in this tool to facilitate decision making of nZEB design in Egypt. The ZEBO tool can be linked to other optimization algorithms and was developed to address zero-energy target for the buildings in hot climate zones. Kapsalaki et al. (2012) developed a methodology and a new tool based on Matlab program to identify

the economic efficient design solutions for residential net zero energy building design. Silva et al. (2013) presented a new prefabricated retrofit module (PRM) solution and different simulation tools (i.e. 3D CAD, THERM, WUFI, eQuest) were used to optimize the building performance. The application of the PRM solution integrated with retrofit strategy could result in a reduction of 83% and 76% of total energy needs for single-family and multi-family buildings respectively. Wang et al. (2009) investigated the optimal design solutions for zero energy building design in UK. Optimal design strategies and energy systems, including passive design parameters (external walls, window to wall ratios and orientations) and energy efficient mechanical systems as well as renewable energy systems, were provided by employing EnergyPlus and TRNSYS 16 simulation software.

2.2.4 Uncertainty and Sensitivity Analysis for Robust Design and System Reliability

The main research efforts on this subject could be summarized into three categories including: effects of uncertainties on the design of nZEBs, identification of the key parameters to which nZEBs performance is sensitive, and investigation on the parameters which may determine the preferred configuration of hybrid energy systems.

Effects of uncertainties are important to be considered at design stage. The deterministic methods of design optimization may lead to non-optimal design of energy systems in the absence of the uncertainties in energy demand, renewable resources, and power modelling, etc. Zhou et al. (2013) proposed a two-stage stochastic programming model based on the GA algorithm and Monte Carlo method to optimally size the distributed energy systems. A small difference between the

deterministic design and the stochastic design was found. The results also indicate that the introduction of energy storage technologies and grid connection for distributed energy systems may improve the inherent robustness for the systems. Maheri (2014) proposed a robustness design methodology for a standalone wind/PV/diesel hybrid system involving uncertainties, considering both cost and reliability measures. The parameter, margin of safety (MoS), was introduced and determined through probabilistic analysis. This proposed robustness design method could be used to find the most reliable system subject to a constraint on the cost and most cost-effective system subject to constraints on reliability measures respectively.

Another important issue is to identify the key parameters to which the performance of the systems is sensitive. Reliable knowledge on the variations of key parameters under different conditions is of great importance for robust performance-based design. In the modelling and designing process of nZEBs, understanding the parameter variations that cause large discrepancies between predicted and realized building performance is very important to ensure the target of net-zero energy consumption. Bucking et al. (2014) proposed a methodology to identify the influential variations on the building performance. A back-tracking search identified that 8 of 26 variables have significant effects on the net-energy consumption in a net-zero energy house case-study, especially solar orientation, variables related to the sizing of a roof-based PV system and energy-related occupant behavior. Sun (2015) studied the impacts of macro-parameters of buildings and systems (such as wall thickness, window to wall ratio, system COP) and their variations in a nZEB on the system design through a systematic sensitivity analysis. He found that the indoor temperature set-point is the most

significant factor in determining all building system sizes and the overall initial investment cost, followed by the system COP and internal gain intensity. Ismail et al. (2013) analyzed the effect on cost of energy (COE) due to the variations in the PV capital cost, diesel price, discount rate, project life time and main capital costs. Results show that the cost of energy is more sensitive to the variations in the capital cost, discount rate and project life time. Li et al. (2015) considered the effects of wind speed, global solar radiation and primary load on an autonomous hybrid power system. Solar energy was found to contribute more efficiently than the wind energy to the proposed system. Ren et al. (2009) investigated the optimal sizing of grid-connected photovoltaic system in residential buildings concerning the uncertainties in the capital cost, PV efficiency, electricity sale price and interest rate. They observed that the capital cost is the key factor affecting the optimal capacity of the system and the payback period is affected greatly by the capital cost, PV efficiency and electricity sale price. The feasibility study of diesel-PV hybrid system shows that the levelized electricity cost is very sensitive to the fuel intake and the price of fuel (Khelif et al. 2012)

Great attention should be paid to some parameters because the configuration of the hybrid energy system may even change due to the variations of them. Rezzouk and Mellit (2015) studied the effects of input variables on the design size and performance of a hybrid energy system (HES). The hybrid energy system was found not profitable any more at the diesel price above 0.25 $/L. Rehman and Al-Hadhrami (2010) explored a PV/diesel/battery hybrid power system for a remotely village. They concluded that the hybrid system is preferred compared with the diesel-only system at

the diesel price of above 0.6 $/L. Bekele and Tadesse (2012) studied the influence of PV panel price and diesel price on the system types chosen for off-grid rural electrification in Ethiopia. The results show that wind/hydro/generator/battery system is favored when the diesel price decreases, and the most economical system is insensitive to PV capital multiplier at low diesel prices. Hamdy et al. (2013) investigated optimal combination options of energy-saving measures and energy-supply systems at different energy price escalation rates using a comparative framework methodology. The cost of fuel cell should be concerned if the fuel cell is considered as an available option. Khan and Iqbal (2005) found that the wind-diesel-battery hybrid system is the most suitable solution for a remote house in Newfoundland, Canada, while a wind-fuel cell system would become a superior choice with the reduction of fuel cell cost to 15% of its current value.

2.3 Scheduling and Control of nZEBs

Optimal control of energy systems is another key task that plays an important role in achieving the goal of nZEBs. The energy systems in a building must be well managed and controlled in order to guarantee a high building performance. In this section, it is intended to review and summarize some dominant methods for the effective control of the energy systems in nZEBs.

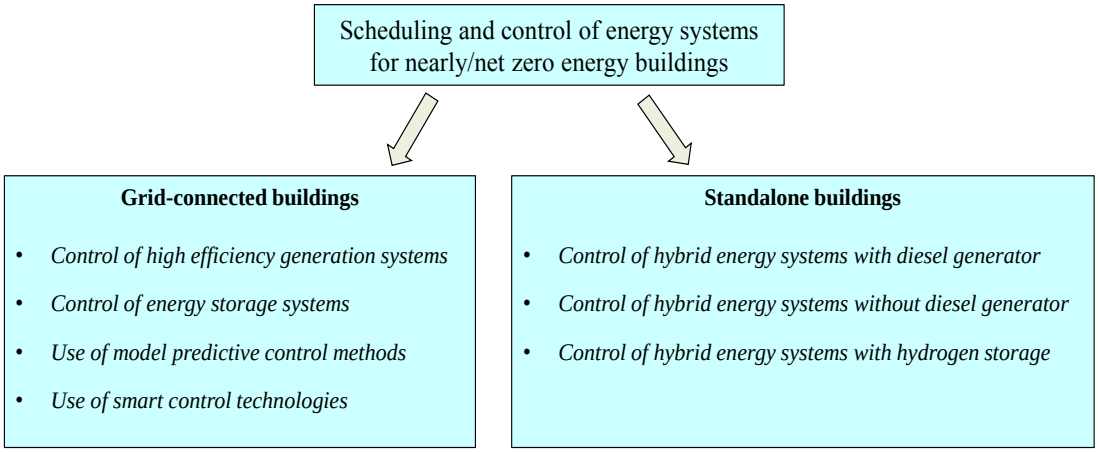

Figure 2.3 Control of energy systems for grid-connected and standalone nZEBs

In nZEBs, the integration of on-site electricity generation systems, energy storage systems as well as the two-way communication between the buildings and smart grid poses great challenges for the efficient control of the energy systems. It is urgent and indispensable to develop optimal scheduling and control methods to maintain the energy balance, cost-saving, energy efficiency and high power reliability for both the buildings and smart grid. As shown in Figure 2.3, regarding the grid-connected buildings, attentions are focused on four main aspects related to the control of energy systems, including: (1) control of high efficiency generation systems for efficient energy conversion and alleviating the peak load, (2) control of energy storage systems for surplus energy storage and/or peak load shifting, (3) use of model predictive control method for effective response to the grid, (4) use of smart control technologies for enhancing the system management and control. With respect to the standalone buildings, this section reviews the control methods used in three types of hybrid energy systems, i.e. hybrid energy systems with diesel generator, hybrid energy systems without diesel generator, and hybrid energy systems with hydrogen storage.

2.3.1 Control of High Efficiency Generation Systems

Electricity generations of many renewable energy systems (e.g. PV panels and wind turbines) are weather-dependent and therefore difficult to be controlled to follow the building demand during operation (Lu et al. 2015), thus the control issue of these generation systems themselves is not discussed in this study. In contrast, the control of another electricity generation system (i.e. CCHP (combined cooling, heating and power system), CHP or CCP) is addressed in this study as CCHP/CHP/CCP can be controlled effectively to improve the efficiency of energy conversion and particularly alleviate the peak load on the grid (Chandan et al. 2012; Facci et al. 2014). In the following, CCHP is used representing the three systems without differentiation.

CCHP is an attractive option for power supply in nZEBs since it can generate electrical energy and useful thermal simultaneously, bringing economic benefits as well as reducing air pollutant emissions dramatically. In general, there are two basic operation strategies for CCHP systems: following the electric load (FEL), and following the thermal load (FTL) (Wang et al. 2011; Guo et al. 2013; Mago et al. 2009; Mago et al. 2010). The two operation modes were evaluated by Mago et al. (2009) and they found that the CCHP system under FTL reduced the primary energy consumption while, under FEL, it always increased the primary energy consumption. However, the two basic strategies may not guarantee the best performance of the system. Some other strategies were developed based on these two basic strategies. For instance, a following seasonal strategy (FSS) was developed which switches the operation strategy between FEL and FTL depending on the monthly electric to thermal load ratio (Fang et al. 2012). Another optimal strategy, i.e. hybrid electric-thermal load strategy,

was introduced by Mago and Chamra (2009). The proposed strategy was demonstrated to have good reduction of cost, PEC and CDE for CCHP system operation.

Based on the specific goal of a nZEB, some other optimized operational/control strategies of CCHP systems may also be helpful. Examples of them are: an optimal operational strategy based on an integrated performance criterion (IPC) (Fang et al. 2012), an emission operational strategy aiming at reducing the carbon dioxide emissions (Fumo et al. 2009), a primary energy saving strategy that can increase thermal energy produced (Cardona and Piacentino 2003), an energy island model operational strategy that can provide an off-grid facility with all the electrical needs (Gu et al. 2012), a new operational strategy based on the ratio of the cooling generated to actual building cooling load (Liu et al. 2012) and a novel operation strategy aiming at minimizing an integrated index (Zheng et al. 2014).

In general, CCHP systems can be integrated with renewable and alternative energy sources (e.g. solar photovoltaics, wind turbine, fuel cells, heat pump and thermal storage) to serve the electric load for a building or an isolated island. However, the mismatch between electricity generation and electricity demand still exists, which is also a major challenge for developing optimal control strategies for building energy systems. Optimal scheduling and control strategies of energy systems are discussed in Section 2.3.3.

2.3.2 Control of Energy Storage Systems

Thermal storage system and electricity storage system have been recognized as two proven technologies in electrical load management by shifting the electricity demand

to a later time, as shown in Figure 2.4. Batteries, with the ability of charging and discharging energy, are commonly employed to complement the renewable energy systems and autonomous energy supply systems, especially in stand-alone building systems. Ma et al. (2014) provided a basic control method for renewable system with battery bank. If the load was less than generation, the excess energy would be charged to battery bank. Otherwise, the energy would be released from battery bank to satisfy the load. Agarwal et al. (2013) proposed a similar control strategy to control a system with solar-PV, battery bank, and diesel. If the solar generation is adequate, excessive power is be used to charge the batteries. If the solar generation is not adequate, battery discharges to supply power. Diesel generator is operated only when the solar generation is not enough and the state of charge of the battery is low.

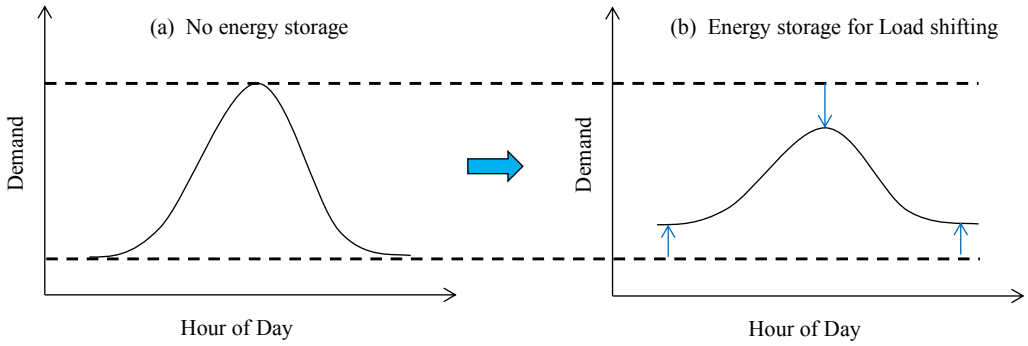

Figure 2.4 Use of energy storage system for load shifting

The implementation of thermal storage in buildings can effectively contribute to shifting the peak load and relieving the power imbalance, which is strongly recommended for thermal demand optimal control and building energy management. Regarding the active thermal storage systems (e.g. ice, water), the control is usually based on a stable control variable. Optimal control strategies are developed to improve the performance of building energy systems with thermal storage. Most of these

strategies are mainly based on day-ahead electricity prices and operation arrangement. Regarding the passive thermal storage systems (e.g. PCM-enhanced building structure, building thermal mass), it is relatively complicated to develop the control strategies due to the physical properties of the thermal mass, although the control strategies developed generally do not depend on a fixed phase changing temperature (Wang et al. 2014).

The thermal storage system could contribute as much as 20-30% electrical peak load reduction Hazran and Rani (2005). In the study of Henze et al. (2004) and Zhou et al. (2005), up to 26% of energy cost can be saved by using the thermal storage systems for shifting peak loads.

Hydrogen is another possible alternative backup system for building energy systems. The basic control rules used are load following, fuzzy logic and five steps charge controllers (Zhou et al. 2005; Ulleberg et al. 2004; Miland 2005). These control rules consider the state of charge (SOC) of the electric and hydrogen storage systems but without taking into account the prediction of the main system parameters. Milo et al. (2011) proposed an adaptive optimization-based energy management strategy to minimize the operation cost of a hydrogen-based nZEB. This strategy could offer additional functionalities as peak-shaving, back-up service and reactive power ancillary services. However, hydrogen has not been employed commonly as the storage system in the buildings at present, mostly due to the high cost of the electrolyzers and fuel cells, and the low conversion efficiency.

2.3.3 Scheduling and Model Predictive Control Methods

Model predictive control (MPC), an advanced control method, is a very commonly used on-line control method for addressing the forecast errors and reducing the impacts of undesired dynamic properties of energy systems. The concept of MPC method is depicted in Figure 2.5. Where a short term planning is repeated each hour and the first hour control trajectory is selected as the schedule for the coming hour. It has various advantages compared with other control approaches, such as peak load shifting capability (Ma et al. 2011), transient and steady-state response improvement (Lü et al. 2007), system efficiency improvements (Elliott 2008) and robustness to disturbances and fluctuations during operation conditions (Privara et al. 2011). Model predictive control method adopted in building energy systems can provide an efficient demand response to the grid.

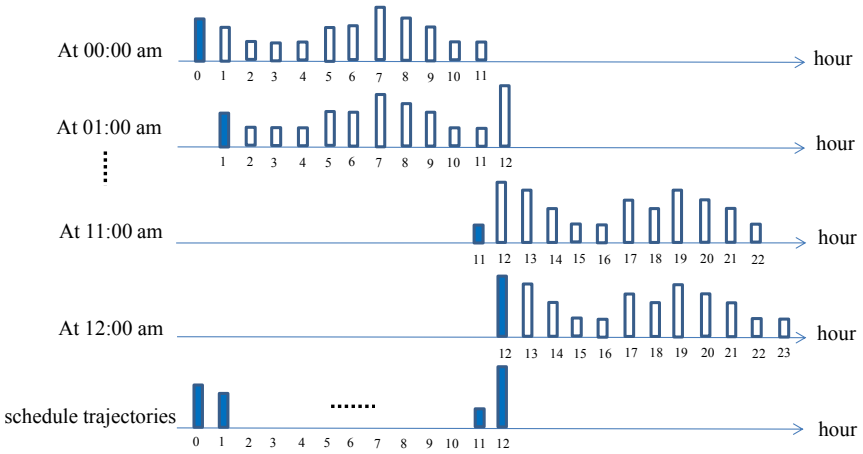

Figure 2.5 Short term prediction based on MPC method

The MPC method has been widely used for optimal control of HVAC systems since the HVAC systems are the most crucial systems which consume more than 30% of building energy and also influence the indoor thermal comfort significantly. The

MPC-based techniques have been employed in zone temperature control (Candanedo and Athienitis 2011), damper process control (Huang 2011), supply air temperature control (Rehrl and Horn 2011), evaporator pressure and cooling set point generation (Elliott 2008), ventilation control (Yuan and Perez 2006). In the study of Ma et al. (2011), the MPC method was employed for zone temperate control. Compared with the baseline night setup strategy used, 28% of savings was achieved by using the MPC method, which was higher than other optimal strategies (set-up strategy achieved 24% saving and line-up strategy achieved 17% saving).

There are also considerable studies conducted on MPC-based optimal scheduling of energy storage systems (Kashima and Boyd 2013) and/or distribute energy generation systems (Chandan et al. 2012; Zhao et al. 2015; Mitra et al. 2013). Zhao et al. (2015) and Lu et al. (2015) adopted the MPC method, using nonlinear programming algorithm and mixed-integer nonlinear programming respectively, to optimize the operation of integrated energy systems in low energy buildings under day-ahead electricity price. Significant reductions in operation cost, primary energy consumption and CO_2 emissions were achieved by the proposed optimal scheduling strategy.

2.3.4 Use of Smart Control Technologies

Smart control might have different contents in different fields and/or to different people. In this thesis, it refers to the energy conservation measures on the building energy systems, implemented by using digital control systems particularly the advanced information technologies. The complex interplay of electricity generation/consumption and energy storage systems as well as the automatically and manually controlled building components call for the development of more intelligent

control technologies taking into account all these interactions. Advanced technologies, such as smart meters, smart sensors/controllers, home energy management systems (HEMS) can play efficient roles in communication and energy coordination between the buildings and smart grid (Wang et al. 2014).

Energy meters in conventional buildings are based on a unidirectional communication, which can collect the historical energy data but do not have the predictive ability. Smart meters are based on a bidirectional communication and can be employed as advanced "automation systems" in buildings. Based on the history and real time data collected/stored, the smart meter systems can analyze and schedule the priorities of house appliances for power demand response (Doostizadeh and Ghasemi 2012; Gans et al. 2013). Thus the systems can also be used to predict the next-day energy consumption/generation.

Home energy management system (HEMS) is an effective tool for demand response, which can be used in a home to shift and cut down its load providing an appropriate response to the grid. Different names can be found for such system in the existing literature, such as, demand-side management system (DMS) (Costanzo et al. 2012), energy management system (EMS) (Lujano-Rojas Juan et al. 2012), home energy management system (HEMS) (Beaudin and Zareipour 2015), smart home controller (Dehnad and Shakouri 2013). As conventional electricity grid cannot satisfy the communication requirements of HEMS, smart grid is proposed to enable the employment of HEMS by improving the communication layer of the grid (Zhu et al. 2012; U.S. Department of Energy 2008).

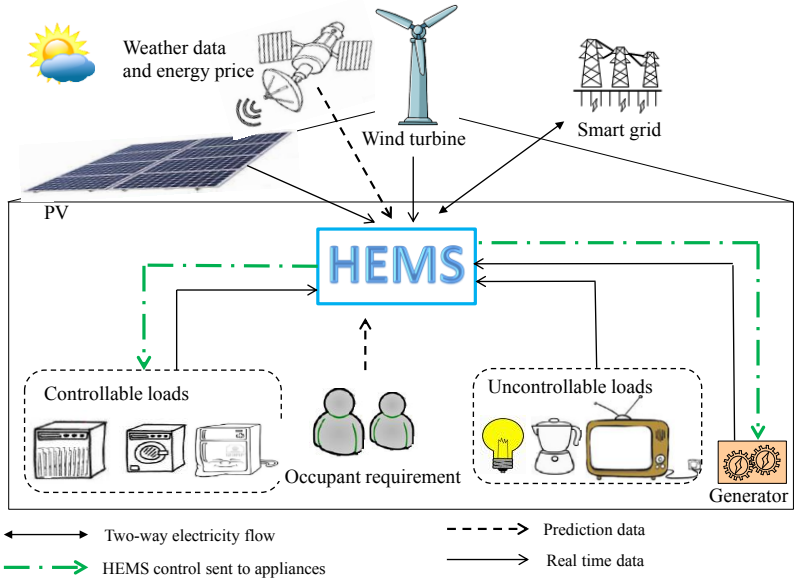

Figure 2.6 Application of HEMS in nZEB

In nZEBs, the HEMS can communicate with different household devices (e.g. HVAC system, lighting, refrigerator), electricity generation systems (e.g. PV, wind turbine, generator) and receive the dynamic electricity price from the smart grid (Missaoui et al. 2014)), as shown in Figure 2.6. With the help of HEMS, the electricity generation/consumption schedule will be optimized and the benefits can be maximized. Ozkan (2015) presented a real time home power management system for a smart home. The proposed system was demonstrated to significantly reduce the operation cost and avoid the high peak demand problem simultaneously. In another study (Long et al. 2012), the global model based anticipative building energy management system (GMBA-BEMS) is general enough to manage a large set of electric appliances such as washing machine, fridge, and electrical heater. The GMBA-BEMS is able to achieve an optimized compromise between energy cost and user comfort, incorporating forecasts of uncertainties such as PV/wind power

generation, weather conditions, occupancy, and energy consumption behavior (RTE 2011).

Therefore, the implementation of advanced metering and energy management systems (e.g. HEMS) in nZEBs could enable the users or the system itself to modify the settings of energy-influencing elements in order to minimize the building energy consumption, maintain the indoor thermal comfort and increase the responsiveness of electricity consumers.

2.3.5 Scheduling and Control of Energy Systems in Standalone Buildings

There are some remote islands and villages having no access to electricity from electrical grid (Bekele and Tadesse 2012; Dufo-López et al. 2007). Buildings in these areas are usually recognized as stand-alone zero energy buildings which can autonomously supply themselves with hybrid renewable energy systems. As these buildings have no access to the electrical grid, energy storage systems (e.g. batteries) are usually integrated with hybrid energy systems to take care of electricity deficits and ensure uninterrupted electricity supply to the end-users. Optimal scheduling/control of hybrid energy systems is necessary since their electricity generations are highly depending on the renewable energy resources of intermittent and unstable nature (e.g. solar radiation, wind velocity). There have been many studies conducted on developing optimal strategies for stand-alone hybrid energy systems.

For the hybrid systems without diesel generators, the control strategy is very simple in general: when the electricity generations excess the building demand, the surplus energy will be stored in the battery, and when the electricity generation cannot satisfy

the building demand, reserved energy will be discharged from the battery (Bernal-Agustín and Dufo-López 2009). Figure 2.7 shows the schematic of a typical hybrid energy system employed in standalone buildings.

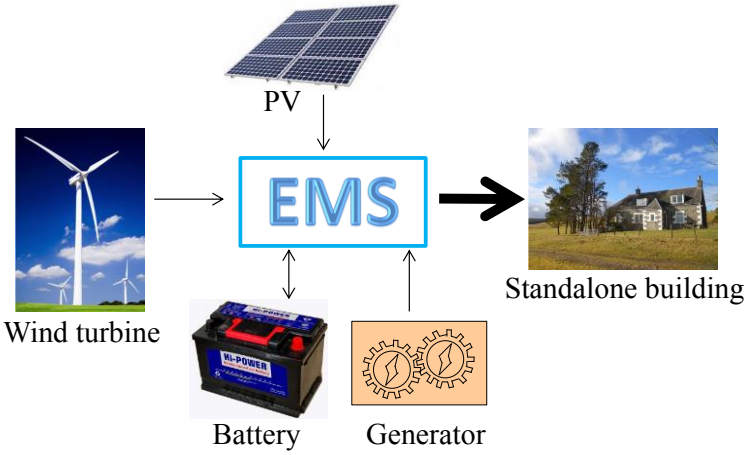

Figure 2.7 Schematic of hybrid energy systems in standalone buildings

However, when a diesel generator is included in the hybrid system, the control strategy can become very complex as it is necessary to determine which system has the priority to supply electricity and how the batteries are charged. Barley et al. (1995) provided various control strategies for PV/diesel/battery hybrid systems. Three basic control strategies proposed were zero-charge strategy, full cycle-charge strategy and predictive control strategy. Based on these control strategies, Barley and Winn (1996) proposed four control strategies, including frugal dispatch strategy, load following strategy, SOC_setpoint strategy and operation strategy of diesel generator (at maximum power for a minimum time). Kang and Won (2009) proposed a power management strategy for a hybrid stand-alone system (PV/FC/battery). The developed strategy could reduce the operation mode changes and thus more effective than the conventional strategy.

Concerning the hybrid systems with hydrogen storage, a few control strategies were also developed. Ulleberg (2004) compared alternative control strategies for PV-Hydrogen systems based on the performance of the fuel cell and the electrolyzer. He also made some recommendations on developing the control strategies which should increase the lifetime of various components (electrolyzer, fuel cell and battery). Dufo-Lo´pez et al. (2007) proposed a novel control strategy based on genetic algorithms for the control of stand-alone hybrid systems with hydrogen storage. The proposed strategy optimizes how the spare energy is used and determines the most economical way to meet the energy deficit. More studies on the control strategies for the hybrid energy system including hydrogen storage can be found in (Milo et al. 2011; Ulleberg 2004; Miland 2005).

2.4 Development of nZEBs Worldwide

2.4.1 An Overview of Nearly/Net Zero Energy Buildings Worldwide

The projects of nZEB have been largely popularized all over the world in the past few years and the number of completed buildings have been kept rising continuously each year. More than 360 nZEBs have been recognized based on the map of international projects (World Map of nZEBs 2013). The information such as name of project, climate type, building typology and its location are provided for each project in this map, in which the nZEB projects can be counted and sorted according to its locations as shown in Fig. 8. It can be observed that the projects in European and USA account for more than 90% of all the projects, especially in German, US, Switzerland and France. The rapid and continuous growth of nZEB projects in European may be stimulated by plenty of policies, programs and regulations on nZEBs that are proposed

and promoted by the government and/or organizations, e.g. International Energy Agency (IEA), US department of energy (DOE), and the Directive on Energy Performance of Buildings (DEPB). However, the development of nZEB in Korea, Japan and China is much slower than European and American, with only 4, 3 and 3 projects respectively. More policies and legislation are definitely helpful in supporting the vigorous development of nZEB at its early stage in Asia and Africa areas. These projects can be categorized as seven groups as shown in Figure 2.9. Small residential buildings and office buildings account for about 54.6% of all these buildings. Apartment buildings, educational buildings and special typologies (hotel, hospital, sports hall) make up approximately 10% in each typology. The remaining 4.9% and 7.0% are contributed by settlements (building group and row houses) and other buildings.

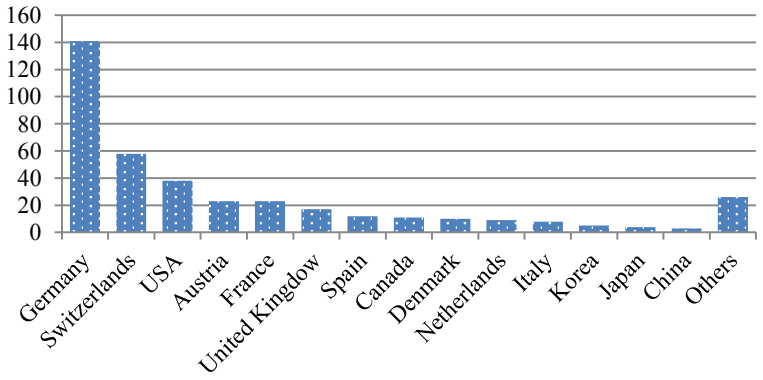

Figure 2.8 Numbers of identified nZEB worldwide

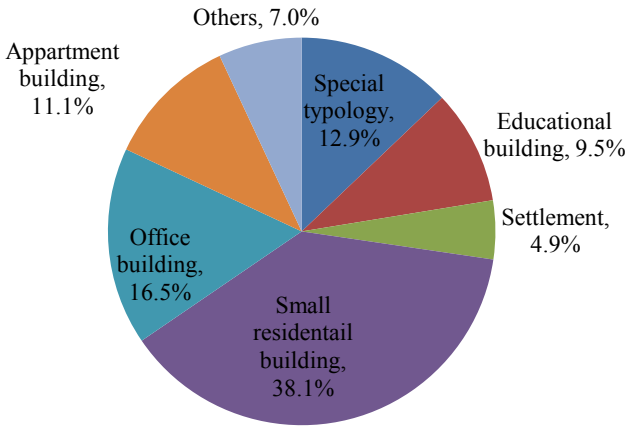

Figure 2.9 Distribution of different building typologies

2.4.2 An Overview on Design Features and Actual Energy Performance

30 nZEB case studies from a report of IEA task 40/Annex 52 are studied here to investigate the design strategies applied and to evaluate the building performance. Passive approaches, energy efficiency systems and electricity generation systems used in the 30 nZEBs are summarized in Table 2.2. The number of the houses which applied the corresponding approaches/systems is also listed in the brackets. It is found that more than half of these houses employed the design approaches of window to wall ration, optimized floor plan, advanced envelop, passive solar heat gain and thermal mass, effective ways to minimize indoor heat gain in summer and reduce the heat loss in winter. In terms of the energy efficiency system, energy efficient lighting, load management and mechanical air heat recovery are favored in most buildings which help reduce building load effectively. More than 70% of the buildings applied solar thermal, photovoltaic and building footprint concerns of the electricity generation systems. Compared with the eighteen houses in the Solar Decathlon Europe 2012 competition located in Madrid climate, 83% of them applied exterior insulation layer and 87% of the houses used one or more thermal energy storage system. Evaporative

cooling systems, as a key strategy for cooling periods in Madrid, are employed in 67% of the houses (Rodriguez-Ubinas et al. 2014). The performance of nZEBs is evaluated in terms of energy consumption and generation as shown in Figure 2.10. Thirteen buildings out of the 30 case studies are labeled as positive energy buildings according to the measured electricity generations and consumptions. The applications of passive approaches and energy efficiency systems help to reduce building load and thus achieve low or even zero/plus energy building. There is still a great potential to reduce the building energy consumption for most houses.

Table 2.2 Design options employed in 30 nZEBs studied in IEA Annex 52

Passive approaches	**Energy efficiency systems**	**Energy supply and integration of renewable energy**
Window to wall ratio (16) Skylights (7) Solar tubes (4) Blinds for glare control (2) Optimized floor plan (28) Thermal zoning (9) Advanced envelope (27) Advanced glazing (11) Passive solar heat gain (23) Thermal mass (23) Solar shading (29) Site vegetation (3)	Energy efficient lighting (24) Efficient appliances (14) Efficient office equipment (13) Advanced lighting controls (8) Load management (15) Mechanical air heat recovery (20) Hot water heat recovery (9) Displacement ventilation (2) Radiant cooling (11) Air source heat pump (10) Ceiling fans/evaporative cooling (6)	Solar thermal (21) Photovoltaic (29) Wind turbine (2) Biomass CHP (6) Biomass-fired boilers (4) Geothermal (14) Building footprint (27)

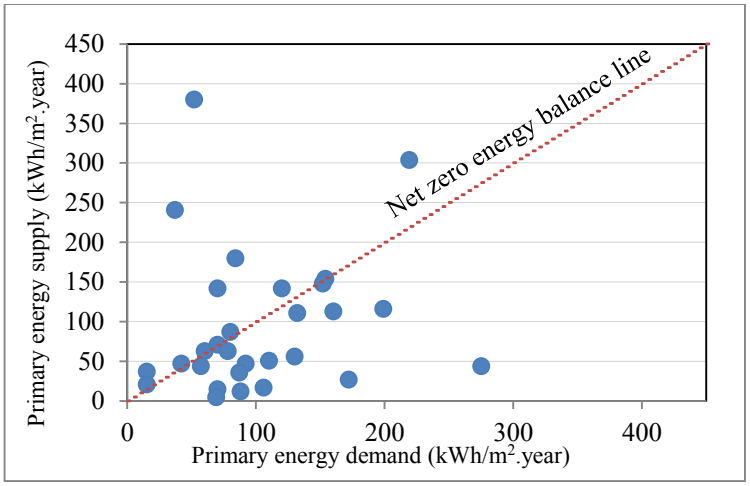

Figure 2.10 Primary energy balance of 30 nZEBs studied in IEA Annex 52

2.5 Discussions and Recommendations

Although there is significant progress in the application of passive design strategies, energy efficiency technologies and hybrid energy systems in buildings, many challenges still exist in the development of nZEBs, especially the urgent needs of a comprehensive approach for optimal design and control of energy systems in nZEBs. Recommendations and challenges faced in developing future nZEBs are summarized as following:

- The definition of nZEB is still lack of common and consistent concept in the existing literature. It may be a challenge to have a consistent nZEB definition since the levels of boundary, criteria, metric, etc., may be different depending on the local climate, economic factor and local requirement. However, the difference of nZEB definitions would definitely affects significantly the way a nZEB is designed and controlled in order to achieve its goal. Therefore, clarification of

definitions will certainly helpful for developing effective design and control strategy of nZEB with a clear objective.

- In the design of climate-sensitive nZEB, design options of passive design strategies and renewable energy available should be carefully considered to cater for the local climate. As a rule of thumb, the target of zero net energy is easy to be achieved for low rise buildings with less energy use intensity and large roof space for solar photovoltaic. However, the question is: can the net zero energy be achieved in high-rise buildings or buildings with high energy use intensity?
- The application of CCHP system and/or energy storage system, integrating with intelligent control system, could provide an effective and active way for buildings to not only reduce and shift peak load on the grid, but also enable fast response to the dynamic electricity price. However, there is still a lack of systematical control strategies for the accurate prediction and effective control of the nZEB system dynamic response. Simulation models that incorporate all the elements of a building are essential for developing effective control strategies, identifying energy-efficiency measures and providing real-time response of energy systems.
- Optimal solutions for nZEB should take into account both system design and control strategies. Unfortunately, the complex interplay of all the intelligent systems in nZEB and various uncertainties, such as strong dependence of energy production /consumption on weather and occupants actions, challenge the conventional way of designing and operating/controlling the buildings. It is necessary to develop a generic decision tool that move the design and control of building towards a holistic view, ensuring a reliable, cost-effective, environment-

friendly and gird-friendly building providing the living and/or working environment of good quality.

- There is significant progress in developing the smart control technologies such as smart meters, smart sensors/controllers and home energy management systems, which can enable effective communication between different types of systems/components in the buildings and the smart grid to achieve optimal operation. Still there are some difficulties in the system integration. The bidirectional connections and two-way information flow between the buildings and smart grid bring some new challenges for system optimization, operation and scheduling.

2.6 Summary

This chapter provides a literature review on design optimization and optimal control of energy systems in nZEBs. A comprehensive review of design optimization and control techniques for nZEBs is presented. Design optimization issue involves the effects of climate/site on design, design optimization methods, the uncertainties/sensitivities for robust design. Control issue involves the use/control of high efficiency generation systems and energy storage systems, scheduling and model predictive control methods, smart control technologies. An outline of the progress of nZEBs is presented by summarizing the internationally known nZEBs identified, including 30 case studies on the design strategies applied and the actual building performance. There are already many researches on the definitions and nZEB demonstration projects worldwide. However, there is still no exact approach for the

design and control of buildings to achieve the nearly/net zero energy target. The complex integration of different energy systems, such as renewable energy generations, energy appliances, energy storages and may also interact with the smart grid in nZEBs make the design and control methods of conventional buildings no longer feasible for nZEBs.

There is still a long way for nZEB developers and researchers to go to address the design and control of nZEBs with a holistic view in order to achieve high-level performance buildings concerning energy-efficiency, environmental friendliness and grid-friendliness.

CHAPTER 3 INTRODUCTION OF ZERO CARBON BUILDING IN HONG KONG AND ITS PERFORMANCE EVALUATION

This chapter presents an overview of the state-of-the art of eco-building design and technologies used in the "Zero Carbon Building" (ZCB) in Hong Kong, which is used to develop the dynamic simulation platform for zero energy building. The actual performance of ZCB is investigated to verify if the target of annual energy balance is achieved in this building.

Section 3.1 presents an overview of the Zero Carbon Building in Hong Kong.

Section 3.2 presents the passive design strategy, active building and system design strategy and electricity generation technology employed in the ZCB. Schematics of the interaction between the energy systems in the building and the control strategies are presented.

Section 3.3 presents the energy performance evaluation of the ZCB using the measurement in one year. A comparison between the ZCB and other ZEB projects is also made in terms of electricity generation system design and energy performance.

3.1 An Overview of Zero Carbon Building (ZCB) in Hong Kong

Hong Kong Zero Carbon Building (ZCB), which is developed by the Hong Kong Construction Industry Council (CIC) in collaborating with the Hong Kong government, which covers a total land area of 14,700 m^2. It comprises of a three-story building with total floor area of 1,520 m^2. This building is integrated with various passive design (wind catcher, earth cooling tube, high performance glazing and others), active design (high volume low speed fans, active skylight and others), and on-site electricity generation systems (PV and bio-diesel generator). Figure 3.1 shows the aerial view of the ZCB. The layouts of ground floor and mezzanine floor are shown in Figure 3.2 and Figure 3.3 respectively. The main specifications of the building and energy systems are given in Table 3.1.

Figure 3.1 Aerial view of Zero Carbon Building in Hong Kong (cycle ZCB in the photo)

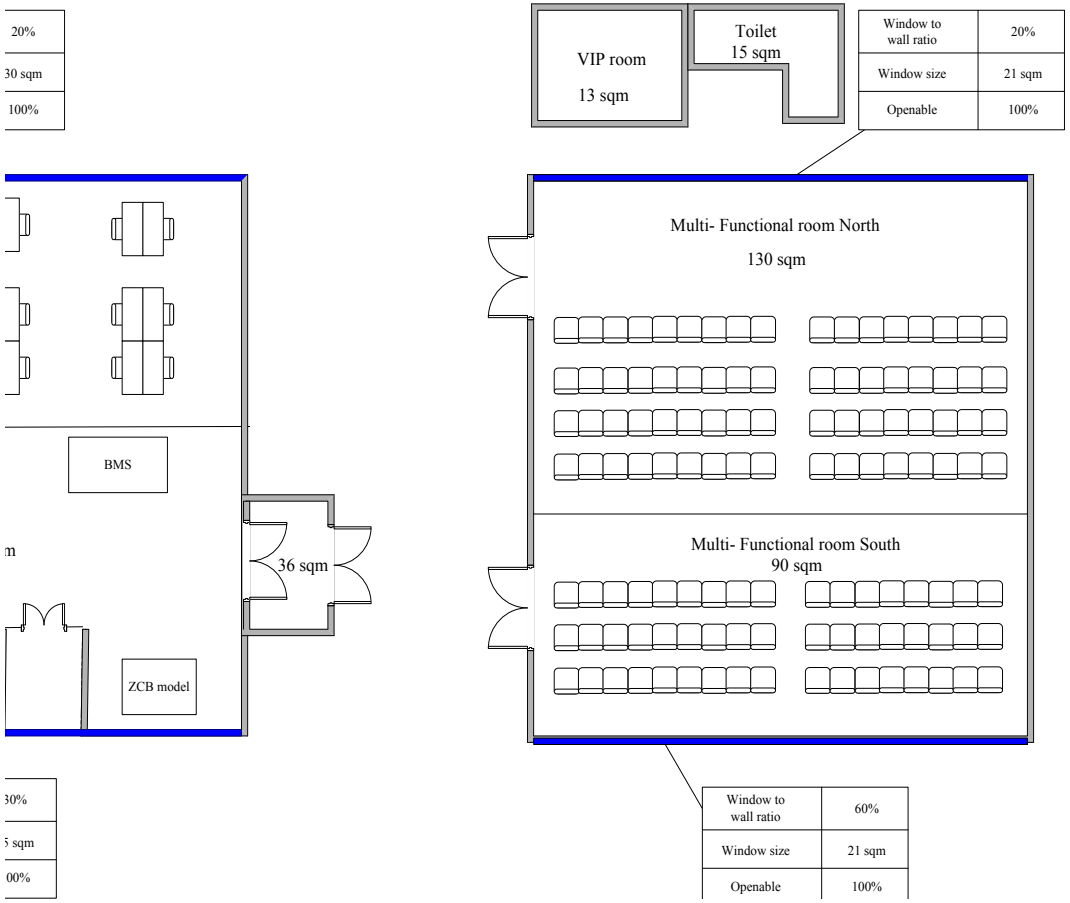

Figure 3.2 Ground floor plan

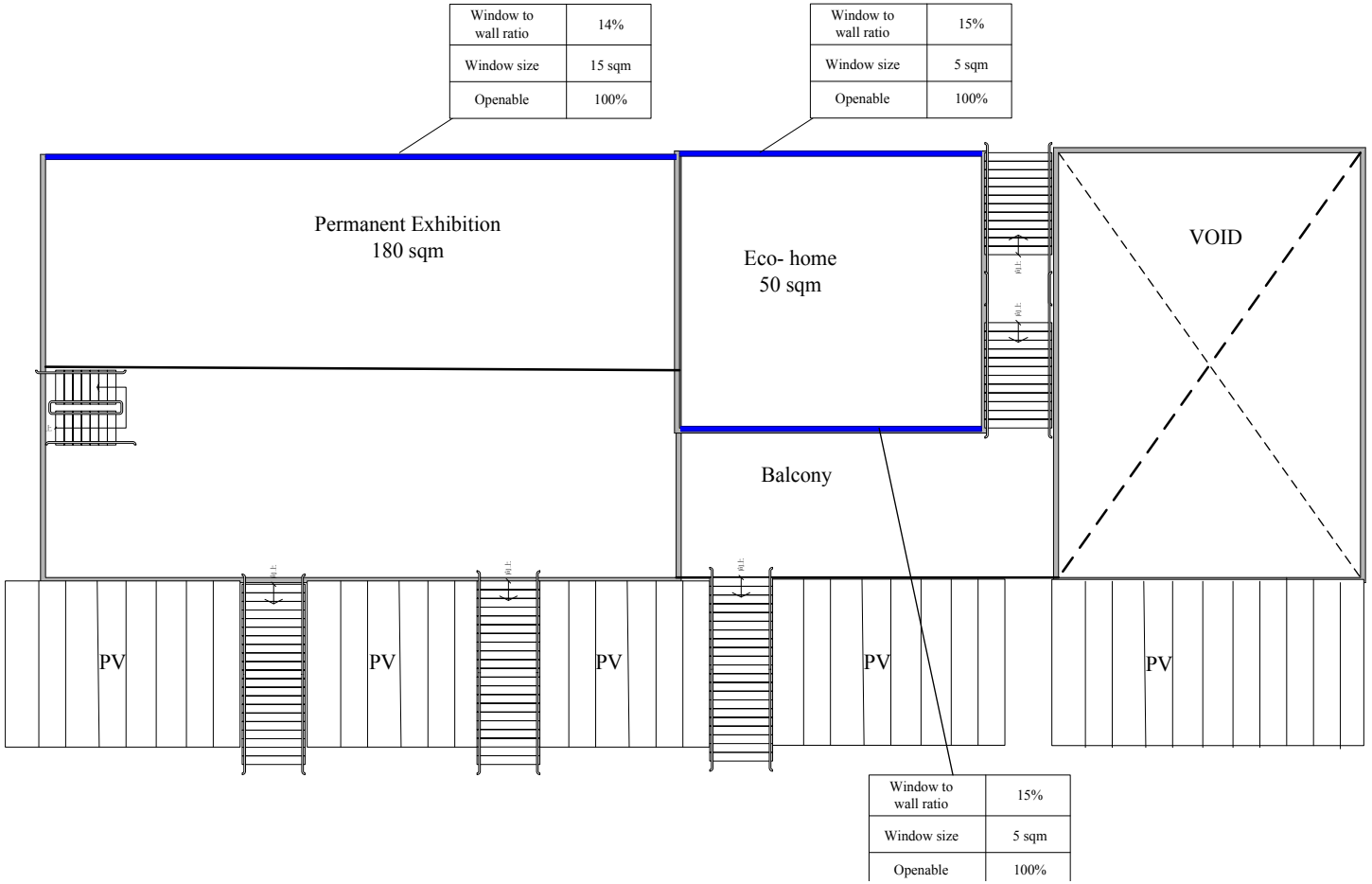

Figure 3.3 Mezzanine floor plan

Table 3.1 Main specifications of ZCB and its energy systems

Feature	Specification
Orientation	South-east
Total net floor area (m^2)	1,520
Window-to-wall ratio	<10- 40%
Shading	45° (angle)
Wall U value (W/(m^2K))/absorption	<1.0 / <0.4
Roof U value (W/(m^2K))/absorption	<1.0 / <0.3
Design peak cooling load (kW)	163
PV (m^2)	1,015
Peak output of PV (kWp)	150
Rated power of bio-diesel generator (kW)	100
Rated power of electric chillers (kW)	70 × 3
Rated power of adsorption chiller (kW)	70 × 1
Maximum no. of occupants (including visitors)	200

3.2 Implementation of Advanced Eco-building Design Technologies

3.2.1 Passive Building Design

Passive design is a design approach that uses natural elements such as sunlight and wind to heat, cool, or light a building. Systems with the passive design require little maintenance and reduce the energy consumption of a building by eliminating the mechanical systems used to regulate indoor temperature and lighting.

In the ZCB, various design measures lead to an energy saving of 20% compared to similar buildings of the current standard design. The design methods include: cross-ventilation layout, wind catcher, earth cooling tube, high performance glazing, ultra-low thermal transfer, north glazing, light shelf, light pipes, heat reflecting shade, cool paint, optimized window to wall ratio, external shading and clerestory for daylighting.

Cross-ventilation layout: It refers to a form of naturally occurring ventilation in a building. The most common options are the windows and wall vents that can allow the fresh air move from one side of a building or room to the other side. One of the benefit is that the process occurs without using ant extra energy and can adjust the humidity in the summer months.

Wind catcher: It is a device used to improve the ventilation in areas far from the windows (Figure 3.4). A small tower on the roof contains an opening where wind velocity is greater than that at the lower area of the building. The cooler air at the opening is forced down from the wind catcher to cool the air in the building. The local air speed can be improved by about 25% using the wind catcher.

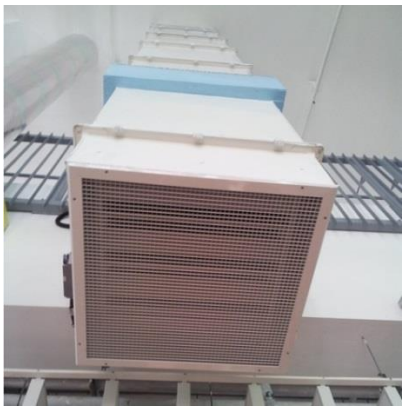

Figure 3.4 Wind catcher

Earth cooling tube: It is a pipe that is buried underground and can provide naturally pre-cooled air for the building (Figure 3.5). The fresh air is drawn through the buried pipe and thus cooled by making use of the naturally low temperature underground. The cooled fresh air will reduce the energy needed for the air conditioning system of the building.

Figure 3.5 Earth cooling tube

High performance glazing: It can offer good optical and thermal performance to reduce the cooling load and the reliance on artificial lighting (Figure 3.6). It performs better than normal glazing with respect to the solar heat control and thermal insulation, thus the energy consumption is reduced.

Figure 3.6 High performance glazing

Ultra-low thermal transfer: the deep overhang over the south facade, heat minimized windows/facades, external shading fins in the north facade as well as the shaded and insulated roof provide a high-performance envelop with the ultra-low overall thermal transfer value of 11 W/m^2, which is 80% lower than the maximum value required under the current standard in Hong Kong. A lower ultra-low overall thermal transfer value represents a higher energy efficiency of the building.

North glazing: The ZCB is built in tapered form which can draw stronger airflow across the building. It can also reduce the solar heat gain from the south facade and increase the daylight from the north facade.

Light shelf: The device, based on sun path geometry used to bounce light off a ceiling, induces the light deeper into a room, distributes and diffuses the light to generate a uniform light level in the interior spaces. The device is strategically positioned in the ZCB at an angle of about 20 degrees to reflect the light to the interior spaces of the building.

Light pipes: They are highly reflective tubes using the domes on the roof of the building to capture the light and then bring the light to the space far away from the windows inside the building (Figure 3.7).

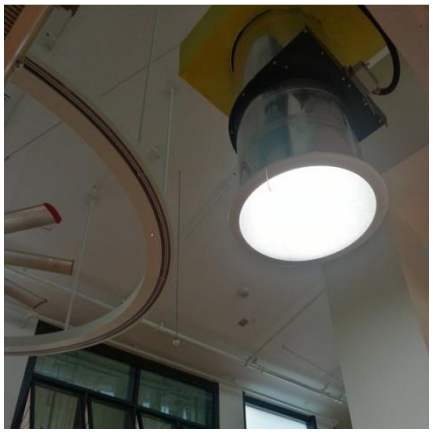

Figure 3.7 Light pipe

Heat reflecting shade: A metalized polyethylene sheet is involved in the device which can reflect solar heat gain back through windows when required. With the aluminum sheet, 3% to 5% of radiant heat absorbed is emitted mainly due to its low emissivity. In summer, solar heat can be reflected out. In winter, heat loss can be reduced.

Cool paint: The device can reflect and emit the solar heat back to the outside, lower heat transfer to indoor space and reduce the surface temperature by up to 5 °C.

Optimized window to wall ratio (WWR): Three types of WWR are adopted effectively that can reduce the cooling load of the air conditioning as well as provide a good natural ventilation and views for occupants.

- High WWR (>65%) on the north-west façade, coupled with external shade and fritted glass, with high transparency to enhance the light from north and the view.
- High WWR (>70%) on the south-east façade, coupled with a deep overhang, for large openable windows and good views.
- Low WWR on north-east facade (<25%) and south-west facade (about 10%) to minimize the solar heat gain.

External shading and clerestory for daylighting: The following external shading methods are used to reduce the solar heat gain and glare.

- Deep overhang projection on the south-east facade is used to block high-angled sunlight;
- Trellises are used to provide additional shade on the south-east facade;
- Vertical shading fins on the north-west facade are used to block the low angle sunlight in the late afternoon:
- Light-colored external shading is used to reduce the risk of solar glare.

Clerestory for daylighting: The light shelf can reflect light onto light-colored and angled ceiling soffit, which improves the daylight distribution. Nature light is well used to reduce the electricity load of artificial lighting and the corresponding contribution to the cooling load.

3.2.2 Active Building and System Design Strategies

Active building and system design strategies refer to the use of electrical and mechanical systems, such as the heating, ventilation and air-conditioning (HVAC) systems and lighting systems. The energy efficient active systems in the ZCB reduce energy consumption by 25% compared to similar buildings of the current standard design in Hong Kong.

High-volume-low-speed fans: The device can generate high volume of air flow at a low speed with a low noise from the fan blade movement (Figure 3.8). The large air volumes are moved effectively by the huge ceiling fans, which can effectively enhance the evaporation for human comfort and reduce the duration of air-conditioning.

Figure 3.8 High volume low speed fan

High temperature cooling system: This system is comprised of the underfloor displacement cooling, chilled beams and desiccant dehumidification (Figure 3.9). Cooling and dehumidification is handled separately, that improves the system efficiency compared to the combined cooling and dehumidification system.

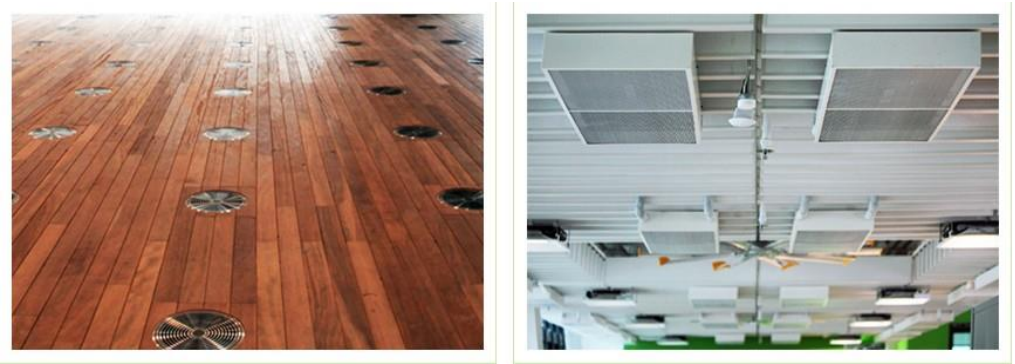

Figure 3.9 High temperature cooling system

Intelligent lighting management: It refers to the automatic control of the lighting based on individual needs, occupancy and natural lighting level. Energy can be saved by monitoring and intelligent control of the lighting.

Active skylight: It refers to a roof window frame set with inclined shading fins, which are controlled by sensors (Figure 3.10). Daylighting and solar control can be optimized by adjusting the shading angles to reduce the direct sunlight at different angles.

Figure 3.10 Active skylight

Task lighting: It can provide high level of illumination in an energy efficient and controllable way by using the white-colored and high luminous efficacious LEDs. The energy use of general lighting is reduced.

Regenerative lift: It refers to a lift equipped with a regenerative convert. A feedback path is provided for generating energy by the regenerative converter. When the lift is down-operation with full/heavy load or up-operation with no/little load, power is regenerated.

Adsorption chiller: It is a heat-operated regeneration unit driven by the hot water coming from recovered heat of bio-diesel generator. Compared with conventional air conditioners driven by electricity, they can be driven by waste heat or solar energy and also use environmentally friendly fluids as refrigerants.

Some other features are also adopted including: water use management, low carbon materials & construction, Eco-workplace & Eco-home, smart controls/building management system, micro climate monitoring stations.

3.2.3 Electricity Generation Technology

Renewable energy is natural energy that will never run out. Renewable energy can be used and does not have a limited supply. The renewable energy sources include solar energy, wind energy, biomass, hydro energy, geothermal energy, wave energy and tidal energy.

In the ZCB, renewable energy is generated on site from solar energy by PV/BIPV/ CIGS and biofuel made of waste cooking oil.

PV system: It is a device that can generate electricity from sunlight (Figure 3.11). Three types of PV panels are installed in the ZCB, including: BIPV-thin film covering the viewing platform, multi-crystalline on the inclined roof, and cylindrical CIGS thin film integrated in the air-tree. The total area of PV panels is about 1015m^2 and 87 MWh of electricity can be generated per year.

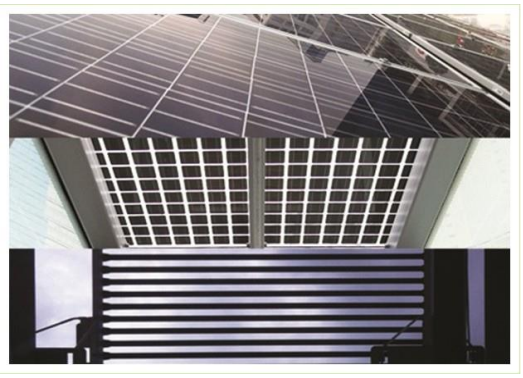

Figure 3.11 PV system

Bio-diesel generator system: It is also called Tri-generation system or combined cooling, heating and power system (Figure 3.12). Electricity is generated using biofuel made of the waste cooling oil and the waste heat is provided for the cooling and dehumidification. Over 143 MWh of electricity is generated per year.

Figure 3.12 Bio-diesel generator system

3.2.4 Schematic of Building Energy Systems

Schematic of the ZCB integrated with power grid is shown in Figure 3.13. PV is responsible for providing electricity. Bio-diesel tri-generator can generate both electrical and thermal energy to meet building electricity load and cooling load. The building electricity consumption is divided into three parts: air handling units (AHUs) & pumps, chillers, other load (lighting, socket etc.). Power grid is a backup power supplier and receiver. When electricity generation from PV and bio-diesel tri-generator is not sufficient for the building electricity load, the power grid will supply electricity to the building. The surplus power from the renewable energy systems will be sent to the power grid. Table 3.2 provides the chiller specifications (three electric chillers and one adsorption chiller).

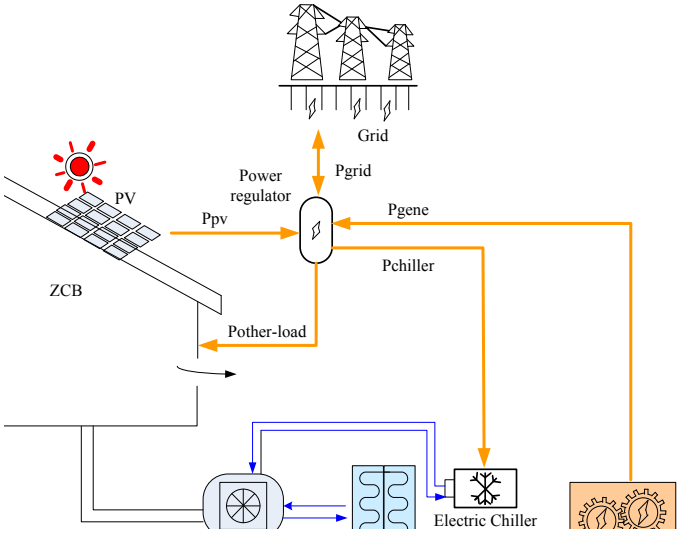

Figure 3.13 Schematics and outlook of HK ZCB integrated with power grid

Table 3.2 Specifications of chillers

Types of chiller	Condenser	Cooling capacity	Chilled water flow rate
Electric Chiller 1	Water cooled	70kW	3.4 l/s
Electric Chiller 2	Water cooled	70kW	3.4 l/s
Electric Chiller 3	Water cooled	70kW	3.4 l/s
Adsorption Chiller	Water cooled	70kW	3.4 l/s

3.3 Energy Performance of Zero Carbon Building

A building management system (BMS) is adopted to monitor operation and the electricity consumption and generation of different energy systems in the building. The window operation, lift system, fire service system, plumbing and drainage system as well as roller blind system are also monitored and controlled by the BMS. More

than 2800 sensors were installed in the building. The detail information and control of central chiller system is monitored in central control and monitoring system (CCMS). In this study, one year data, i.e. 01 April 2013 to 31 March 2014 (365 days), are used to evaluate the performance of the ZCB. Table 3.3 and Figure 3.14 show the monthly electricity consumption and electricity generation of the ZCB in a year. It is found that the on-site electricity generation is higher than the building electricity consumption from July to October. The annual regular building electricity consumption (RBEC) is about 214,615 kWh, and the annual electricity generation is 216,377 kWh. Therefore, electricity generation can satisfy the regular energy demand of the building. It should be mentioned that the regular building electricity consumption includes the energy consumption from ground floor lighting and power, mezzanine floor lighting and power, multipurpose room lighting and power, eco-office lighting and power, shop on landscape, store room, eco-cafe; air-side and water-side of air-conditioning (AC) system, window actuator and lift control. The electricity consumption from basement floor lighting, power and ventilation, fire services, emergency lighting and power, recycling water plant, landscape lighting and PD tanks and pumps is not included in the regular building electricity consumption.

Table 3.3 Monthly electricity consumption and generation in a year (04/2013-04/2014)

Month-Year	Total Electricity Consumption (kWh)	Regular Building Electricity Consumption (kWh)	PV Generation (kWh)	BDG Generation (kWh)	Electricity Input from Power Grid (kWh)
04/2013	18,506.0	9,459.9	5,967	0	3,492.9
05/2013	33,052.1	18,513.9	7,731	0	10,782.9
06/2013	41,045.3	23,494.2	6,567	5,537	11,390.2
07/2013	48,167.6	28,881.2	10,828	19,032	-978.8
08/2013	44,281.3	26,821.0	10,237	21,157	-4,573.0
09/2013	43,969.1	26,522.0	11,242	31,206	-15,926.0
10/2013	40,177.2	26,014.7	13,963	31,901	-19,849.4
11/2013	25,327.7	15,279.0	7,229	2,366	5,684.0
12/2013	17,731	8,562.0	6,596	16	1,950.0
01/2014	19,763.4	10,474.0	8,555	1,744	175.0
02/2014	15,564	10,666.0	7,028	0	3,638.0
03/2014	17,733.5	9,927.0	7,475	0	2,452.0
Total	**365,318**	**214,614.8**	**103,418**	**112,959**	**-1,762.2**

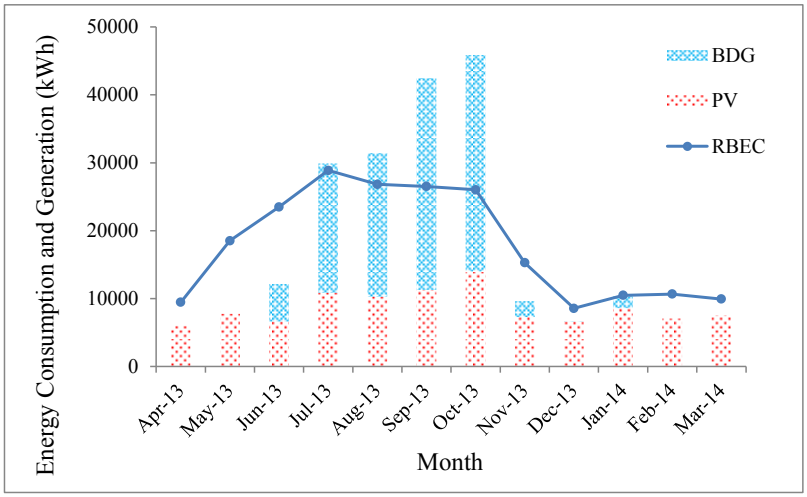

Figure 3.14 Monthly electricity consumption and generation in a year (04/2013-04/2014)

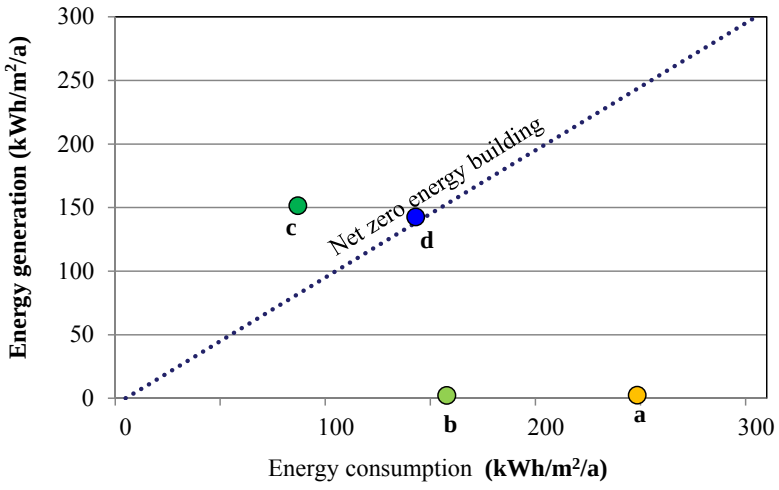

Figure 3.15 Means towards net zero energy performance in ZCB

Figure 3.15 shows the means towards net zero energy performance in the ZCB. Generally, energy use intensity (EUI) of typical existing office buildings in HK is between 250 and 350 kWh/m^2/a (Point *a*). The average building energy use is 157 kWh/m^2/a (Point *b*) if complied with the ASHRAE 90.1–2004. At the design stage of the ZCB, the electrical energy use of the ZCB is estimated to 86 kWh/m^2/a, and electricity generation is estimated to 151 kWh/m^2/a (Point *c*), while the actual regular

building electricity consumption is 141.2 kWh/m^2/a, and electricity generation is 142 kWh/m^2/a (Point *d*). There is still great potential to improve the building performance since the building is still at its commissioning stage.

The regular building electricity consumption is divided into eleven parts as shown in Figure 3.16. Energy used by AC-air side and AC-water side counts for the most portion, 65% of the total regular building electricity consumption. It is followed by the ground floor lighting and small power as well as mezzanine floor lighting and small power, each make up 9% of the total regular building electricity consumption. Therefore, HVAC system consumes the largest amount of energy in the building and should be paid more attention in terms of energy saving.

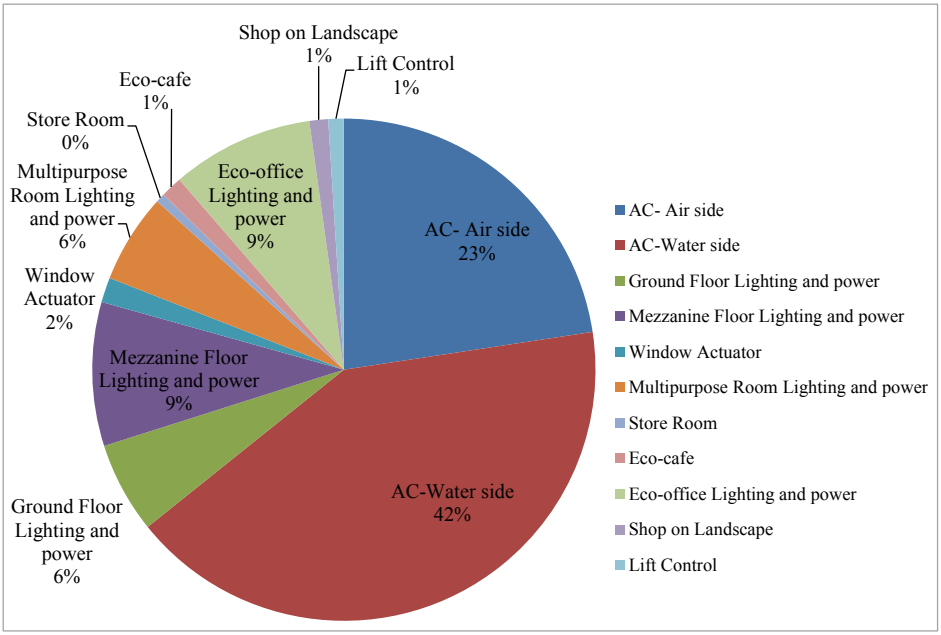

Figure 3.16 Distribution of regular building energy consumption

Regular building electricity consumption in four representative months, i.e. April, July, October and January, are shown in Figure 3.17-3.20 respectively. During night,

regular building electricity consumption is generally less than 10 kW, and it is around 20 kW in the daytime of most days in April and January while it is between 50 kW and 90 kW in the daytime of most days in July and October.

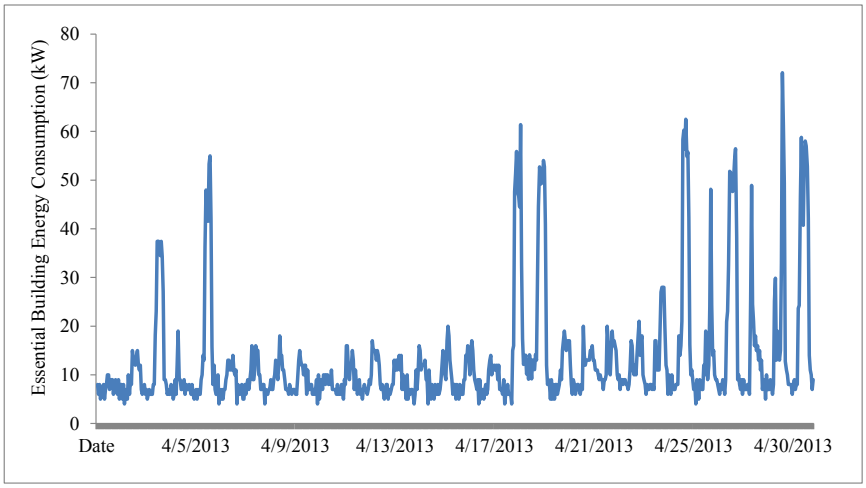

Figure 3.17 Regular building electricity consumption in April

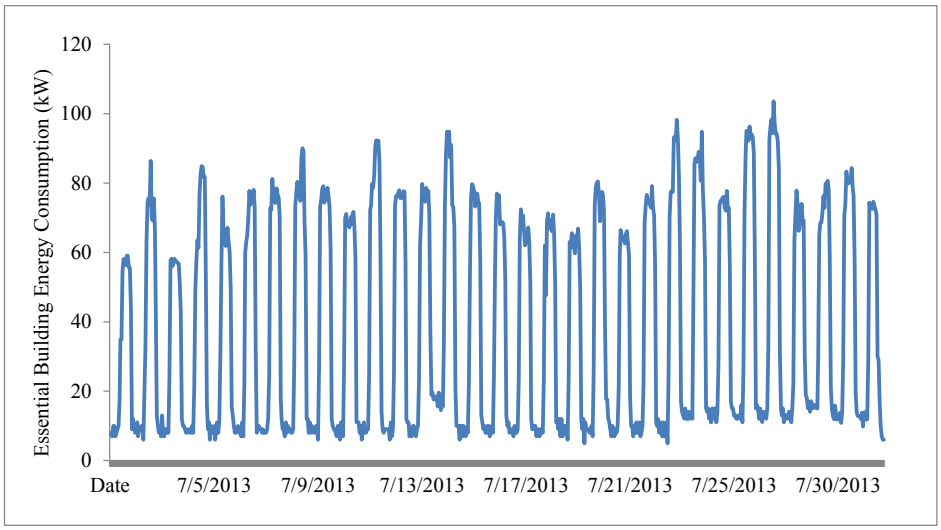

Figure 3.18 Regular building electricity consumption in July

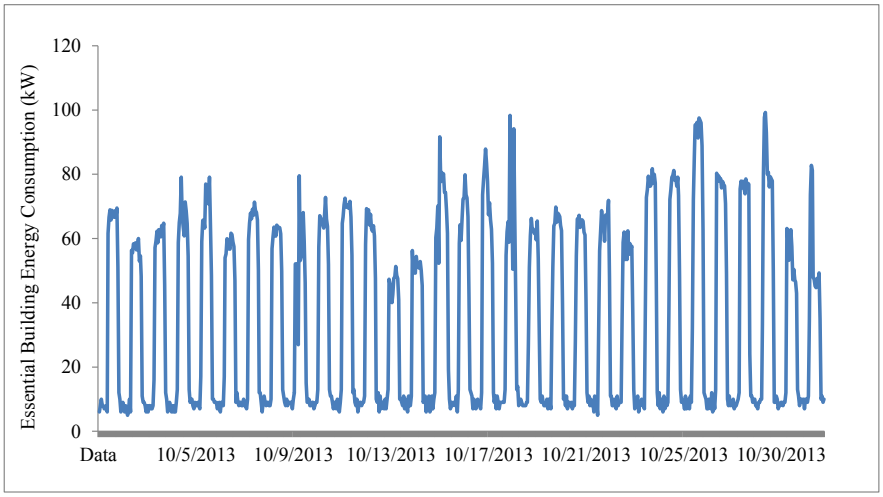

Figure 3.19 Regular building electricity consumption in October

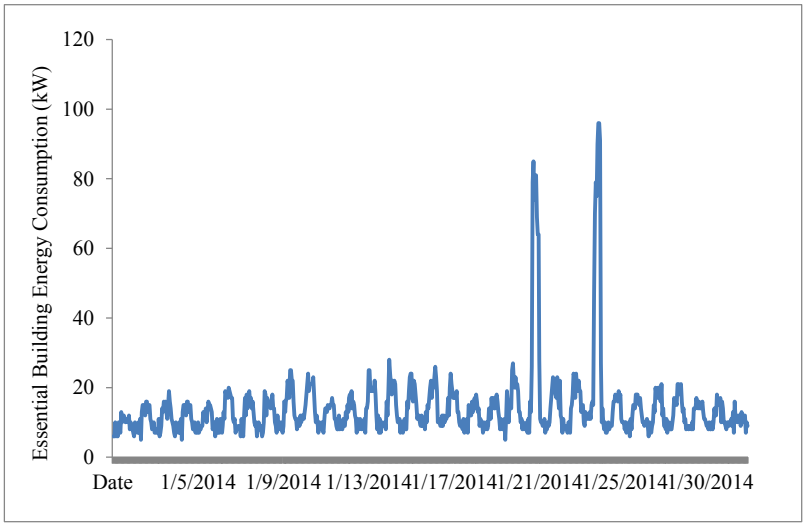

Figure 3.20 Regular building electricity consumption in January

The design peak cooling load of the ZCB is 163 kW. According to the measured outlet water temperature and inlet water temperature, the actual cooling load is calculated using Equation (3.1) and shown in Figure 3.21. It is found that there are still 155 hours in a year when the cooling load is larger than the design peak value.

$$Q_c = \mathrm{c}_w \times \mathrm{m}_w \times (t_{w,outlet} - t_{w,inlet}) \tag{3.1}$$

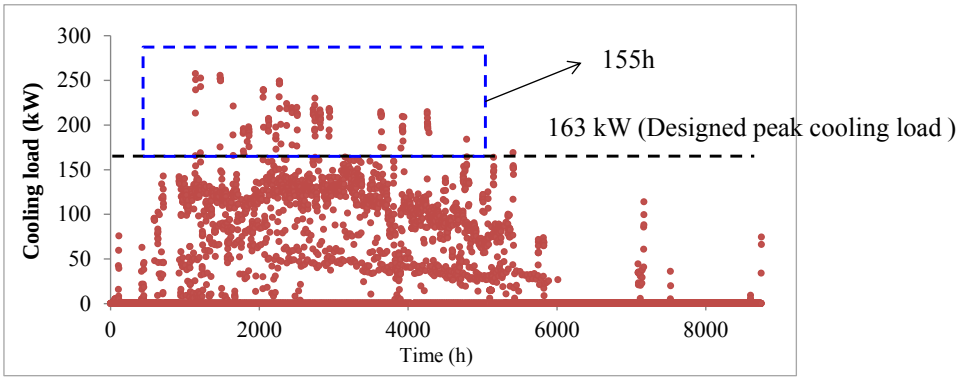

Figure 3.21 Measured cooling load of ZCB

In order to evaluate the ratio of the power demand which is covered by the on-site electricity generation, a load match index is defined as shown in Equation (3.2). Where, *i* represents the time interval (hour, day, month). It is obvious that a large load match index is preferred. When the on-site generation is larger than the load demand, the value is equal to 1.

$$f_{load,i} = \min\left[1, \frac{on\ site\ generation}{load}\right] \times 100(\%) \tag{3.2}$$

Figures 3.22 - 3.24 show monthly, daily and hourly load match indexes respectively. The average monthly, daily and hourly load match indexes are 0.78, 0.74 and 0.35 respectively. During the summer period, especially in July, August, September and October, the high cooling load calls for the operation of BDG which provides a large amount of electrical and thermal energy for the building. Therefore, the load match index in these four months achieves the maximum (Figure 3.22). The daily load match index has a large fluctuation as shown in Figure 3.23. This is because even in the same month, the change of weather condition may cause a large difference in daily load demand and electricity generation in the building. During the daytime, a large amount

of energy can be provided by PV and/or BDG, while the electricity generation is not available during the night. Thus, a low average hourly load match index of 0.35 is obtained (Figure 3.23).

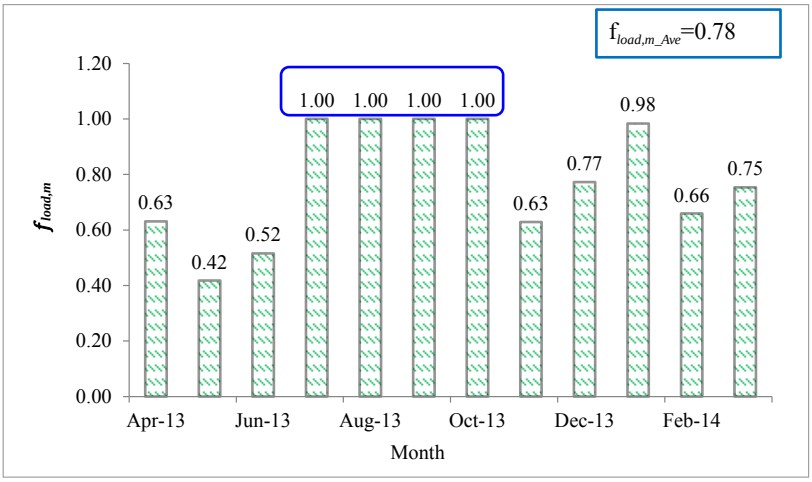

Figure 3.22 Monthly load match index

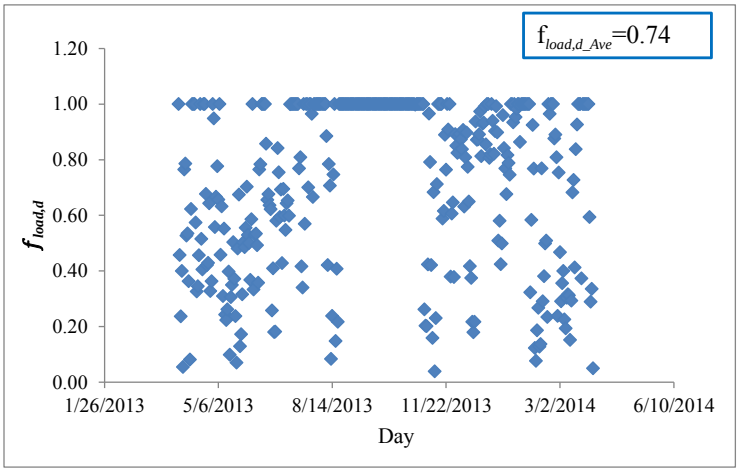

Figure 3.23 Daily load match index

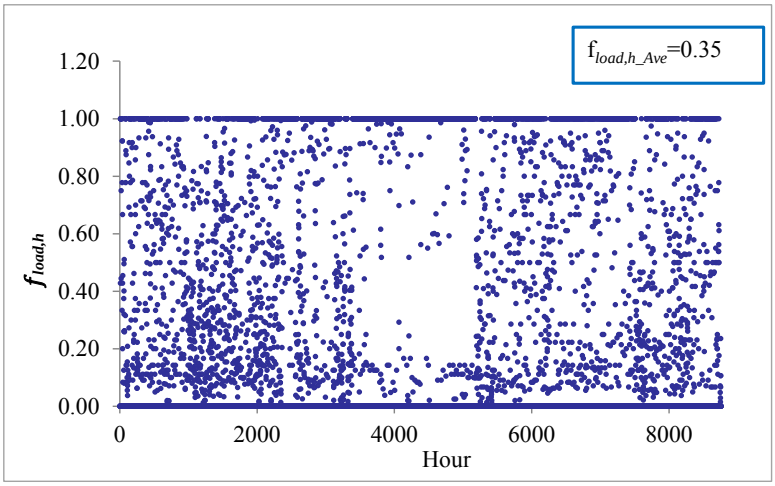

Figure 3.24 Hourly load match index

In order to have a better understanding on the distribution of load match index, the load match index is further divided into five regions, i.e. A (0-0.2), B (0.2-0.4), C (0.4-0.6), D (0.6-0.8), E (0.8-1.0). Figure 3.25 shows the distribution of load match index in each month. In September and October, the load match index is located only in Region E. In February, March, April and May, a large portion of the load match index is located in Region A and B due to the fact that few generations are provided by the BDG in these months. The distribution of hourly load match index in working days (only) in a year is shown in Figure 3.26. The hourly load match index has a high portion in Region E during the midday (e.g. between 11:00 am and 15:00 pm) when the solar radiation is high and the BDG is usually in operation in the summer. In contrast, the hourly load match index is relatively low at both the beginning and the end of the working days, with high portion in Region A.

Table 3.4 presents a few ZEB projects in the world which are provided by U.S. Department of Energy - Energy Efficiency and Renewable Energy. The building information, renewable energy systems installed as well as the energy performance

are provided and compared with that in the ZCB in Hong Kong. The annual generation of the ZCB is achieved nearly the same as the design value. But the annual purchased electricity is much higher than its design value. This is because the actual building electricity consumption is much higher than expected. Detailed information of each building can refer to the website (Zero Carbon Building in Hong Kong 2012).

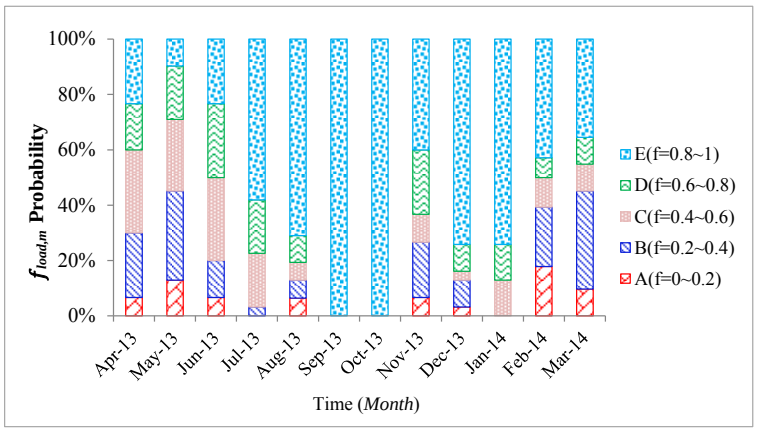

Figure 3.25 Distribution of daily load match index in 12 months

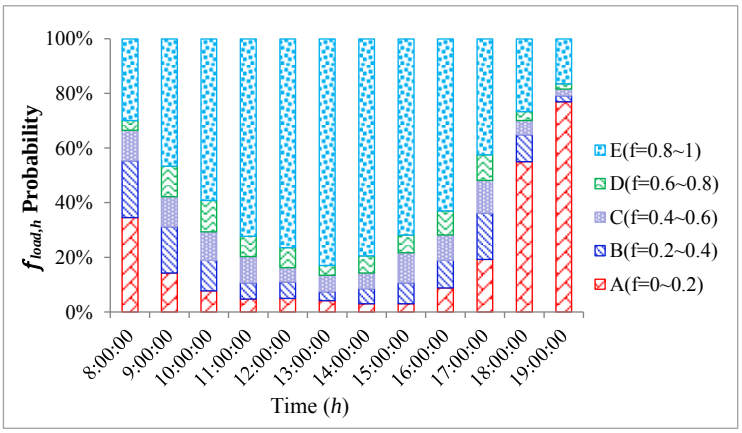

Figure 3.26 Distribution of hourly load match index in working days in a year

Table 3.4 Comparison between Zero Carbon Building and other ZEB projects in the world

Name	**Location**	**Building Type**	**Floor Area** (ft2)	**Renewable Energy System**	**Annual Energy Production** (kBtu/ft2)	**Annual Purchased Energy** (kBu/ft2)
Zero Carbon Building	Hong Kong, China	Office, Visitor education center, Demonstration home	16,386	PV, bio-diesel generator	45.1 (design value: 47.9)	-0.4 (design value: -20.6)
Science House	St. Paul, MN, United States	Interpretive Center	1,530	PV	17.6	0
Steinhude Sea Recreation Facility	Steinhude, Germany	Recreation	3,190	PV, solar hot water collectors, cogeneration microturbine	64.3	0
Omega Center for Sustainable Living	Rhinebeck, NY	Laboratory; Interpretive Center	6,200	PV	21.5	-8.26
Oberlin College Lewis Center	Oberlin, OH	Higher education; Library; Assembly; Campus	13,600	PV	36.4	-4.23
ORNL Office Building 3156	Oak Ridge, TN	Commercial office; Campus	6,940	PV	33.4	-1.47
Las Vegas Cyclery	Las Vegas, NV	Retail	9,790	PV, Wind Turbine	32	-3.87

Hawaii Gateway Energy Center	Kailua-Kona, HI	Commercial office; Interpretive Center; Assembly; Other	3,600	PV	31.1	-3.46
Environmental Tech. Center, Sonoma State	Rohnert Park, CA	Higher education; Laboratory	2,200	PV	3.79	-1.47
Ellis-Scott Family Pavilion	Kingston, TN	Recreation; Interpretive Center; Assembly; Park; Community	2,330	PV	3.39	-2.89
Challengers Tennis Club	Los Angeles, CA	Recreation	3,500	PV	9.17	-0.1
Aldo Leopold Legacy Center	Baraboo, WI	Commercial office; Interpretive Center	11,900	PV	17.6	-2.02

3.4 Summary

This chapter introduces the Hong Kong ZCB and the building energy performance is evaluated. Based on analyzing one year energy data, it can be found that on-site electricity generation is much higher than the building electricity demand in summer. However, electricity generation in winter cannot satisfy the building electricity demand which is mainly due to the fact that the BDG is not in operation. But in general, annual electricity generation can satisfy the regular electricity demand of the building.

The electricity use of the ZCB is estimated to 86 kWh/m^2/a and electricity generation is estimated to be 151 kWh/m^2/a at the design stage. The actual electricity use is 141.2 kWh/m^2/a, and electricity generation is 142 kWh/m^2/a. There is still great potential to improve the building energy performance since the analysis of building energy performance is made when the building is still under commissioning.

Load match index is further used to evaluate how much of power demand is covered by the on-site electricity generation. It is observed that the monthly load match indexes in summer (i.e. July, August, September and October) are the highest while the daily and hourly load match indexes have large fluctuations.

CHAPTER 4 ENERGY SYSTEM MODELS AND THEIR VALIDATION

In order to determine the optimal sizes of the renewable energy systems (in Chapter 5) and optimal control of these energy systems in nZEBs (in Chapter 7 and 8), energy system models are required. The energy system models are therefore developed and validated prior to construct the optimal design and optimal scheduling methods/strategies in this study. This chapter presents the models of the energy systems and the validation of the models.

Section 4.1 presents a brief overview of the reference building and its energy systems. The relationship of energy flows among the integrated energy systems and energy balance between electricity generation and energy consumption are described. In *Section 4.2*, HVAC component models, including electric chiller model, absorption chiller model, pump model, AHU fan model and cooling tower model, are described. In *Section 4.3*, simplified renewable energy system models, including PV model, wind turbine model and bio-diesel generator model, are presented. In *Section 4.4*, the HVAC component models and renewable energy system models are validated by using the measured on-site data. A summary of this chapter is given in *Section 4.5*.

4.1 Reference Building and Its Energy Systems

The building energy systems used in this optimization study are proposed on the basis of the energy systems of the Zero Carbon Building, shown in Figure 4.1. Several modifications/assumptions are made to the existing building energy systems: 1. Absorption chiller is used instead of the adsorption chiller and all the waste heat from bio-diesel generator is used by the absorption chiller. 2. A wind turbine is used to provide electricity for the building. 3. The bio-diesel generator is controlled according to the building cooling load. When the cooling provided by the absorption chiller is not sufficient, extra cooling load is undertaken by the electric chillers. 4. The grid is the backup power supplier and receiver. The building electricity consumption comes from the HVAC system (fans, pumps, cooling towers and chillers) and other appliances (lighting, office equipment and others).

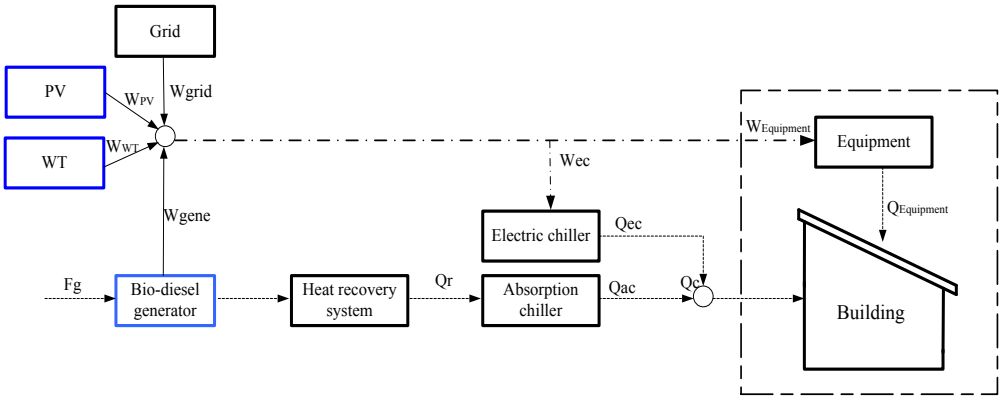

Figure 4.1 Energy flows among the energy systems

Cooling load: Cooling demand of the studied building (Q_c) is satisfied by the absorption chiller (Q_{ac}) and electric chillers (Q_{ec}) as shown in Equation (4.1). When the building cooling load is less than the capacity of absorption chiller ($Q_{ac,design}$), the total cooling load will be fully covered by the absorption chiller, as shown in Equation

(4.2). Otherwise, the absorption chiller will work on its full capacity and the rest of the cooling load will be met by the electric chillers, as shown in Equation (4.3). At the heat recovery system, the heat required by the absorption chiller (Q_r) can be given by Equation (4.4). The capacity of the absorption chiller ($Q_{ac,design}$) is selected according to the capacity of the bio-diesel generator ($Q_{bio,design}$), the efficiency of the heat recovery system (η_{hrs}) and the rated COP of the absorption chiller ($COP_{ac,design}$), as shown in Equation (4.5).

$$Q_c = Q_{ec} + Q_{ac} \tag{4.1}$$

$$Q_{ac} = Q_c|_{\,Q_c<Q_{ac,design}} \tag{4.2}$$

$$Q_{ac} = Q_{ac,design}|_{Q_c>Q_{ac,design}} \tag{4.3}$$

$$Q_r = \frac{Q_{ac}}{COP_{ac}} \tag{4.4}$$

$$Q_{ac,design} = Q_{bio,design} \times \eta_{hrs} \times COP_{ac,design} \tag{4.5}$$

The balance between the electricity supply (W_{supply}) and demand (W_{demand}) is assumed in the building, as shown in Equation (4.6). The electricity consumption/demand in this building comes from two sub-systems: HVAC (W_{HVAC}) and other appliances (W_{other}) as shown by Equation (4.7). The electricity supply is satisfied by the PV (W_{PV}), wind turbine (W_{WT}) and bio-diesel generator (W_{BDG}) while the power grid (W_{grid}) is assumed as the energy storage to store surplus electricity and to cover the power shortage, as shown in Equation (4.8). Where, W_{other} includes power consumed by the lighting, socket outlet, fuse spur, etc. W_{HVAC} represents the power consumed by the

electric chillers (W_{ec}), pumps (W_{pump}), cooling tower fans (W_{ct}) and AHU (air handling unit) fans (W_{fan}) of the HVAC system, as shown in Equation (4.9).

$$W_{demand} = W_{supply} \tag{4.6}$$

$$W_{demand} = W_{HVAC} + W_{other} \tag{4.7}$$

$$W_{supply} = W_{PV} + W_{WT} + W_{BDG} + W_{grid} \tag{4.8}$$

$$W_{HVAC} = W_{ec} + W_{pump} + W_{ct} + W_{fan} \tag{4.9}$$

The power grid can be treated as a backup power supplier and receiver for the building. The actual power supply from grid depends on the building power demand and renewable energy generations as shown by Equation (4.10). $W_{grid} > 0$ represents that the grid supplies electricity to the building. $W_{grid} < 0$ means that the building exports surplus electricity to the power grid.

$$W_{grid} = W_{HVAC} + W_{other} - (W_{PV} + W_{WT} + W_{BDG}) \tag{4.10}$$

4.2 HVAC Component Models

Electric chiller model: The electricity consumption of an electric chiller is calculated based on COP_{ec}, as shown in Equation (4.11). Usually, lower partial cooling load results in lower COP_{ec}. The COP_{ec} of the electric chiller varies depending on the partial cooing load ratio (PLR) and an empirical model is adopted as shown in Equation (4.12) (Hong et al. 2014). Where, a=-1.6757, b=0.3083, c=3.5093, d=0.853. These parameters (a, b, c and d) are identified by fitting the models with the site data of the

chillers in the ZCB with R^2 equal to 0.9. COP_N is the nominal capacity of the chiller and the value is 4.2 in this study. The outlet water temperature of the evaporator ($T_{eva,out}$) is set to be 7℃ in simulation tests, and the inlet water temperature of condenser ($T_{con,in}$) is assumed to have a difference of 5 K with the wet-bulb temperature of the cooling tower inlet air ($T_{wb,in}$) as shown in Equation (4.13).

$$W_{ec} = \frac{Q_{ec}}{COP_{ec}} \tag{4.11}$$

$$COP_{ec} = COP_n \times \frac{T_{eva,out}}{T_{con,in} - T_{eva,out}} \times (a \times PLR^3 + b \times PLR^2 + c \times PLR + d) \tag{4.12}$$

$$T_{con,in} = T_{wb,in} + 5 \tag{4.13}$$

Pump model: The cooling water pumps are constant speed pumps and they are assumed to work at rated power. The chilled water pumps are variable speed pumps. Their electricity consumption depends on the pressure drop (Δp_{cwp}), the water flow rate (m_w) and pump efficiency (η_{cwp}) as shown by Equation (4.14). The pressure drop of the chilled water loop (equal to the pressure head of pumps) in the building is assumed to be linear to the water flow rate (m_w) as shown in Figure 4.2 and Equation (4.15). It presents the case where some effective (but not optimal) differential pressure set-point reset strategy (pressure set-point is simply set to be linear to the water flow rate) is implemented, representing the operation at medium level energy efficiency in practice. Merging Equation (4.14) and Equation (4.15), Equation (4.16) is obtained. Two important parameters need to be identified to calculate the electricity consumption. Therefore, two conditions based on the on-site data analysis are used to

identify the two parameters. The chilled water flow rate in the building is assumed to be linear to cooling load (assuming constant differential temperature of chilled water) and the minimum water flow rate is assumed to be 20% of design flow rate. The rated power of each chilled water pump is 9 kW at the design flow rate, while the power consumption is assumed to 2 kW at the minimum water flow rate (20% of design flow rate). Finally, energy consumption model of chilled water pumps can be obtained as Equation (4.17).

$$W_{cwp} = \frac{\Delta p_{cwp} \times m_{wa}}{\eta_{cwp}} \tag{4.14}$$

$$\Delta p_{cwp} = \Delta p_{cwp,min} + \alpha' \times \frac{m_{wa}}{m_{wa,design}} \tag{4.15}$$

$$W_{cwp} = \alpha_{cwp} \times \frac{m_{wa}}{m_{wa,design}} + \beta_{cwp} \times \left(\frac{m_{wa}}{m_{wa,design}}\right)^2 \tag{4.16}$$

$$W_{cwp} = 10 \times \frac{m_{wa}}{m_{wa,design}} - 1 \times \left(\frac{m_{wa}}{m_{wa,design}}\right)^2 \tag{4.17}$$

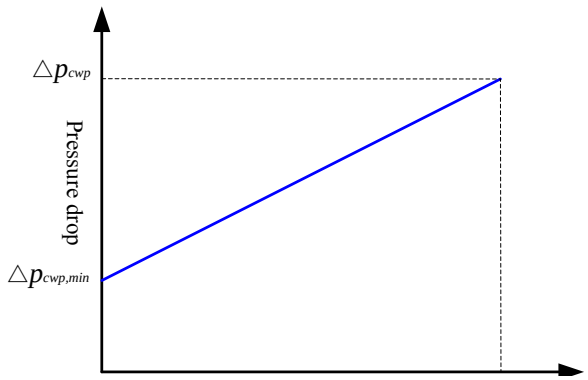

Figure 4.2 Pressure drop vs water flow rate in chilled water loop

Cooling tower model: For a cooling tower with constant flow resistance, the air flow rate (m_a) is proximately proportional to the fan speed (n). The cooling tower cooling capacity (Q_{ct}) also varies proximately in direct proportion to the fan speed. Full fan speed can provide 100% of cooling capacity and half fan speed can provide 50% of cooling capacity. Therefore, the correlations between air flow rate and the fan speed as well as the cooling capacity and air flow rate are obtained as shown in Equation (4.18) and Equation (4.19). The relationship between the air flow rate and the corresponding fan power consumption can be represented by Equation (4.20). Where, A' and k are constant parameters depending on the tower size. The fan power consumption varies with the cube of the speed ratio ideally (k=3) as shown in Equation (4.21). The fan energy consumption of the cooling tower is finally calculated using Equation (4.22). In this study, k is selected as 1.5 which is determined on the basis of practical in-situ operation data. In fact, it is impossible for cooling towers to achieve the ideal performance (k=3) in practical operations.

$$\frac{m_a}{m_{a,design}} = \frac{N}{N_{a,design}} \tag{4.18}$$

$$\frac{Q_a}{Q_{a,design}} = \frac{m_a}{m_{a,design}} \tag{4.19}$$

$$W_{ct} = A' \times {m_a}^k \tag{4.20}$$

$$\frac{W_{ct}}{W_{ct,design}} = (\frac{Q_{ct}}{Q_{ct,design}})^k \tag{4.21}$$

$$W_{ct} = W_{ct,design} \times (\frac{Q_{ct}}{Q_{ct,design}})^k \tag{4.22}$$

AHU fan model: The power consumed by a fan (W_{fan}) is calculated based on the pressure head of the fan (Δp_{fan}), the air flow rate (v_a) and the fan efficiency (η_{fan}) as shown in Equation (4.23). The design air flow rate is about 13 m^3/s, and the fan efficiency is assumed to be 0.4. The pressure head of the fan (Δp_{fan}) is 615 Pa, and the rated power consumption is 20 kW. The total system pressure drop (fan pressure head) (Δp_{fan}) consists of the pressure drop after the pressure sensor point (VAV box etc.) (Δp_{sen}) and pressure drop in other parts of the air system (Δp_{oth}) such as supply duct, cooling coil and main return duct etc. as shown in Equation (4.24). Thus, the fan power consumption can be given by Equation (4.25). Assuming $\Delta p_{sen}=0.4\times\Delta p_{fan}$, an empirical fan power model is finally obtained as Equation (4.26). In addition, a simple empirical relation between total air flow rate of all AHUs and the building cooling load, as shown in Figure 4.3, is assumed based on the case while a medium level and simple optimal control strategy is implemented. The percentage of the air flow rate is equal to percentage of the cooling load when the cooling load is between 60% and 100% where the AHU supply air temperature is set as constant. When the cooling load is 20% or below, the air flow rate is 40% of the design flow rate as the minimum air flow rate, while the AHU supply air temperature set-point is reset (increased) to maintain such minimum air flow rate as required in building concerning various issues, such as air distribution and ventilation. When the cooling load is between 20% and 60%, the air flow rate (i.e. between 40% and 60% of design flow rate) is proportional to the cooling load, which can be also controlled by resetting the AHU supply air temperature set-point.

$$W_{fan} = \frac{\Delta p_{fan} \times v_a}{\eta_{fan}} \tag{4.23}$$

$$\Delta p_{fan} = \Delta p_{sen} + \Delta p_{oth} \tag{4.24}$$

$$W_{fan} = \frac{\Delta p_{sen} \times v_{a,design}}{\eta_{fan}} \times \frac{v_a}{v_{a,design}} + \frac{\chi \times v_{a,design}{}^3}{\eta_{fan}} \times (\frac{v_a}{v_{a,design}})^3 \tag{4.25}$$

$$W_{fan} = 8 \times \frac{v_a}{v_{a,design}} + 12 \times (\frac{v_a}{v_{a,design}})^3 \tag{4.26}$$

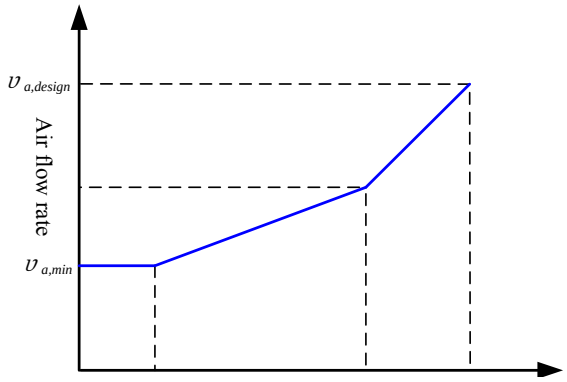

Figure 4.3 Air flow rate vs cooling load

Absorption chiller: The absorption chiller is driven by the recovered heat from the BDG. The cooling generated by the absorption chiller depends on the exhaust heat from the BDG, as shown in Equation (4.27). Where, η_{hrs} is the heat recovery system efficiency, COP_{ac} is coefficient of performance of the absorption chiller.

$$Q_{ac} = \eta_{BDG} \times (1 - \eta_{BDG}) \times c_{p,oil} \times F_{oil} \times COP_{ac} \tag{4.27}$$

Thermal storage tank model

A thermal storage tank is used in the optimal scheduling strategies presented in Chapter 7 and 8. The chilled water in the thermal energy storage tank is stratified with warm water at the upper part and the cool water at the lower part. The cool water

($T_{TES,cold}$) charged to the tank is assumed to have the same temperature as the supply chilled water. When the tank discharges, the cool water stored in the bottom of the tank will be supplied to the HVAC system as supply chilled water. Meanwhile, the same amount of chilled water from the HVAC system will also be returned to the tank on the top as warm water.

$$Q^t_{TES,cold} = m^t_{TES,cold} c_{p,w} \left(T_{TES,warm} - T_{TES,cold}\right) - \eta^t_{TES} Q_{TES,cold,max} \quad (4.28)$$

The amount of cold energy ($Q^t_{TES,cold}$) stored in the thermal storage tank at time *t* is estimated by Equation (4.28). Where, $m^t_{TES,cold}$ is the amount of cold water stored in the tank. η^t_{TES} is the cold loss coefficient and assumed to be 0.5% of the storage capacity per hour. The delay effects of charging and discharging are ignored in this study.

4.3 Renewable Energy System Models

PV model: The PV power generation can be computed by Equation (4.29) (Skoplaki and Palyvos 2009; Kusakan and Vermaak 2014). Where, A_{PV} is the total area of PV (m^2). η_m is the PV module efficiency. P_f is the packing factor. η_{PC} is the power conditioning efficiency. I_{irra} is the hourly irradiance (kWh/m^2).

$$W_{PV} = A_{PV} \times \eta_m \times P_f \times \eta_{PC} \times I_{irra} \quad (4.29)$$

Wind turbine model: Power generation from the wind turbine can be computed by Equation (4.30) (Kusakan and Vermaak 2014; Ghedamsi and Aouzellag 2010). Where, ρ_a is the air density (kg/m^3), $c_{p,w}$ is the coefficient of the wind turbine performance,

η_{WT} is the combined efficiency of the generator and wind turbine, A_{WT} is the area of blade, v_{wind} is the wind velocity.

$$W_{WT} = 0.5 \times \rho_a \times A_{WT} \times v_{wind}^3 \times c_{p,w} \times \eta_{WT} \quad (4.30)$$

Bio-diesel generator model: The fuel consumption of the bio-diesel generator in operation is estimated by Equation (4.31) (Ismail et al. 2012). In this study, the power generation is controlled to match the heating need of the absorption chiller, as shown by Equation (4.32) (Mago and Hueffed 2010). Where, W_{BDG} and $W_{rated,BDG}$ are the actual power output and the rated power of the BDG respectively. A_G and B_G are the coefficients of the consumption curve and the values.

$$F_{bio} = A_G \times W_{BDG} + B_G \times W_{rated,BDG} \quad (4.31)$$

$$W_{BDG} = \frac{Q_r}{(1-\eta_{BDG})\times\eta_{hrs}} \times \eta_{BDG} \quad (4.32)$$

4.4 Validation of Models

The parameters of the above energy system models are determined and identified using the specifications and/or operation data of the energy systems in the ZCB. Before used for the optimization study on the renewable energy systems, the energy system models are validated using the in-situ data from the ZCB. Figure 4.4-4.7 present the comparisons between the actual measurements (collected by building management system) and outputs of some models in a week of October 2013. The peak value of solar radiation is about 865 W/m^2. The peak cooling demand is 143kW in this week. The measured solar radiation (i.e. hourly irradiance) is used as the input

of the PV model. It can be found that the PV power generation predicted by the model matches well with the measured value (Figure 4.4). The measured heat output is used as the input of the bio-diesel model to predict the power generation and fuel consumption. It can be found that the power generation predicted by the bio-diesel generator model matches well with the measurement (Figure 4.5). The measured power consumption of the chillers is collected by BMS in which electricity consumption of each device is collected and stored. The measured cooling load of the electric chillers (converted into PLR), the chilled water temperature and the ambient air wet-bulb temperature are used as the input of the electric chiller model. The chillers power consumption in the chiller model output is calculated based on the COP model. The COP model is built based on fitting the in-situ data. In fact, the measured power consumption of the chillers is slightly larger than the model output (Figure 4.6). The measured total building cooling load is used as the input of the fan and pump models. The total power consumption of the pumps and fans (sum of pump and fan model outputs) is compared with the measurement (Figure 4.7). It can be found that the difference between the model output and measurement is obviously larger than that of the other models. It is due to the fact that the energy consumption of the fans and pumps are affected by their control strategies and simple semi-optimal control strategies are assumed in developing the empirical models. However, the accuracy is acceptable for such processes involving many operation uncertainties.

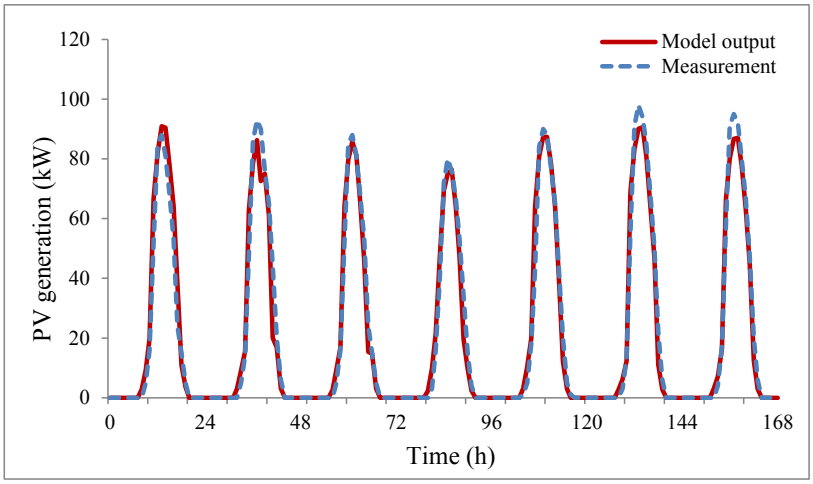

Figure 4.4 Model output vs actual measurement of PV generation

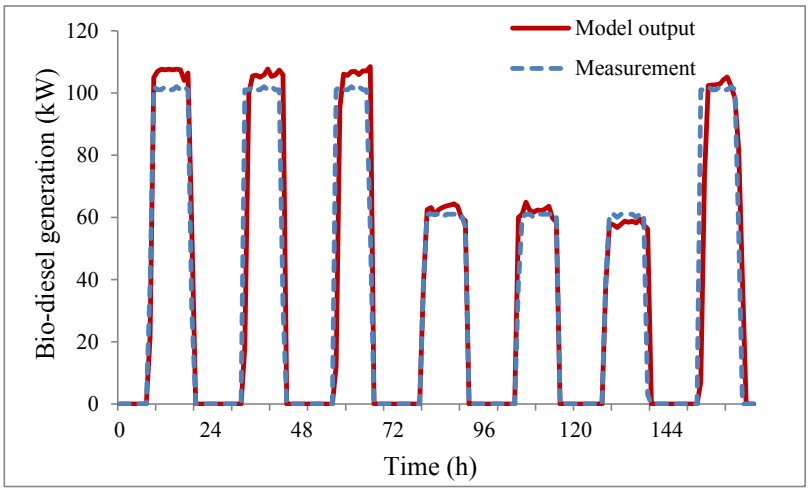

Figure 4.5 Model output vs actual measurement of bio-diesel generator

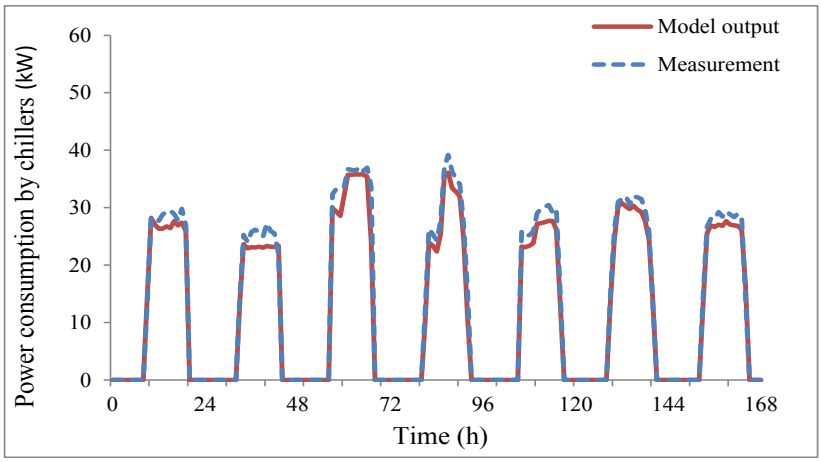

Figure 4.6 Model output vs actual measurement of power consumption by chillers

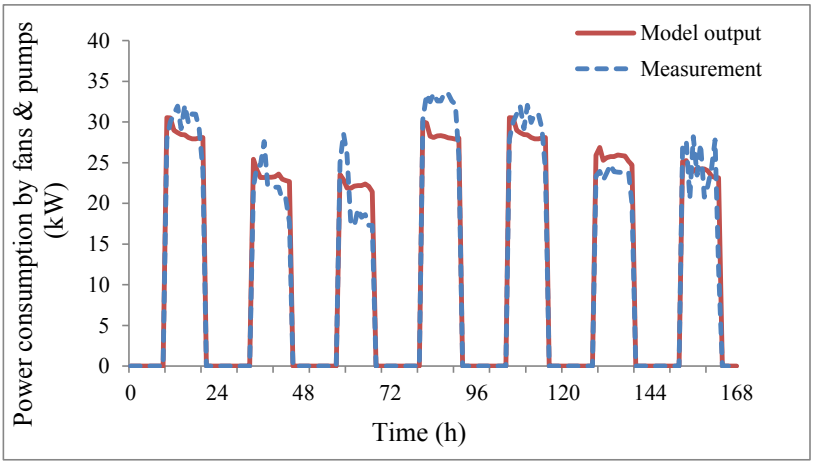

Figure 4.7 Model output vs actual measurement of power consumption by fans & pumps

4.5 Summary

This Chapter presents the specifications of the reference building and their energy systems as well as the energy system models, which are used for the design and control studies on the energy systems in nZEBs in the following chapters.

The electricity consumption/demand of the reference building comes from two sub-systems: HVAC system (including the electric chillers, pumps, cooling tower fans and AHU fans) and other appliances (including lighting, socket outlet, fuse spur, etc.). The HVAC component models are developed based on the actual design and operation performance of the ZCB. The energy consumption of the other appliances is obtained from the in-situ measurements and assumed to be fixed pattern in every day. The PV panel, wind turbine and bio-diesel generator are used as the electricity providers while the power grid is assumed as the energy storage to store surplus electricity and to cover the power shortage.

The parameters of the energy system models are determined and identified using the specifications and operation data of the energy systems in the ZCB. It was found that PV power generation and the BDG power generation predicted by their models match well with the corresponding measurements. The measured power consumption of the chillers is slightly larger than the model output. For the total power consumption of the pumps and fans, the difference between the model output and measurement is a little larger than that of the other models. In general, the accuracy is acceptable for such processes involving many operation uncertainties.

CHAPTER 5 DESIGN OPTIMIZATION OF RENEWABLE ENERGY SYSTEMS IN nZEBs

The performances of nZEBs depend largely on the design of their renewable energy systems. Existing design software tools available are not suitable to optimize the design of renewable energy systems that affect the building energy consumption. Furthermore, only limited studies on the design optimization of nZEBs consider the stress of the buildings on the grid. This chapter presents a comparison study on two design optimization methods, i.e. single objective method and multi-objective optimization method, for the design of renewable energy systems in nZEBs.

Section 5.1 presents a brief introduction on the selection of optimization methods used for optimizing the design of energy systems. *Section 5.2* presents the procedure of the single-objective and multi-objective optimization methods applied in the renewable energy system design. Three objective functions, i.e. total cost (TC), carbon dioxide emissions (CDE) and grid interaction index (GII), are used to evaluate the building performance. *Section 5.3* presents two case studies to investigate the impacts of different combinations of renewable energy systems on the building performance and to evaluate the capability as well as the effectiveness of the two optimization methods. A summary of this chapter is given in *section 5.4*.

5.1 Selection of Design Optimization Methods

Effective optimization methods are essential for the optimal design of buildings and their energy systems. Over 50% of previous research efforts on building optimization were concerned with single objective problems and, around 40% of the efforts addressed multi-objective problems, while a few efforts applied a weighted-sum approach to transform multiple objectives into single objective problems (Evins 2013).

Multi-objective optimization method can be used to address the mathematical optimization problems involving more than one objective function to be optimized simultaneously. A representative set of Pareto optimal solutions are provided for decision makers in the present of trade-offs between two or more conflicting objectives. An example of applications can be found in the study of Wang et al. (2005). Where, a multi-objective genetic algorithm was employed to examine the trade-off between economical and the environmental performances for green building design.

The weighted-sum approach is a simple method to convert multi-objectives into one objective but the disadvantage is that only one set of optimal values can be obtained for each weighting set. An example application can be found in another study of Wang et al. (2003), where structured genetic algorithms was used to address the economical and the environmental objectives by the weighted-sum technique.

Evolutionary algorithms are regarded as a common meta-heuristic optimization algorithm and widely used for optimizations in different fields. GA (Genetic Algorithm), as one type of evolutionary algorithms, is based on the principles of selection and evolution to produce several solutions to a given problem. It is able to

create a high quality solution for optimization problems. Non-dominated sorting Genetic Algorithm (NSGA) is an extension of the GA for settling the multi-objective optimization problems. There are two versions of the algorithm, the classical NSGA and the modified form (NSGA-Ⅱ). NSGA-Ⅱ, which has a better sorting algorithm, incorporates elitism and needs no sharing parameter to be chosen *a priori*, is widely implemented for multi-objective optimization problems. An example of application of GA and NSGA-Ⅱ can be found in the optimization study of Palonen et al (2009). A genetic algorithm, developed based on NSGA-Ⅱ, was used for both single and multi-objective optimization problems in selecting the optimal building design parameters.

In the design of renewable energy systems in nZEBs, the indices such as the cost and/or CO_2 emissions and/or grid interaction index may be of great importance for different designers. In this study, GA and NSGA-Ⅱ are employed as the optimization methods to study the single and multi-objective optimization problems in the optimal design of renewable energy systems in nZEBs.

5.2 Formulation of Design Optimization Problem

5.2.1 Single-objective Design Optimization using GA

Figure 5.1 shows the schematic diagram of the single-objective optimization procedure. The typical meteorological year in Hong Kong (i.e. 1987) is selected for annual building cooling load simulation and the simulation time step used is one hour. The weather data & occupancy/equipment schedules, parameters of energy systems and the ranges of renewable energy system sizes (PV, wind turbine, bio-diesel

generator) are set as the input parameters for building model, energy system models and GA optimizer respectively. In the optimization step, weighted-sum objective function (Equation 5.7d) combining the three objective functions is minimized. GA, a widely used optimization method using techniques inspired by natural evolution, is implemented to obtain the optimal renewable energy system sizes in the LEB and nZEB in Matlab 2006. The building model is firstly modeled in a building energy simulation program - TRNSYS. The specifications of the building, weather, PV, wind turbine and bio-diesel generator are provided for the building model and renewable energy system models. Occupancy schedule, lighting schedule as well as other equipment are set the same as that in the reference building (i.e. Hong Kong ZCB). Secondly, the building cooling load generated from simulation on TRNSYS is provided as the inputs to the energy system models developed on Matlab. Then building electricity demand and electricity generation are computed using the energy system models. Finally the objective function is evaluated and minimized by the GA optimizer based on trial values of renewable energy system sizes (PV, wind turbine and bio-diesel generator).

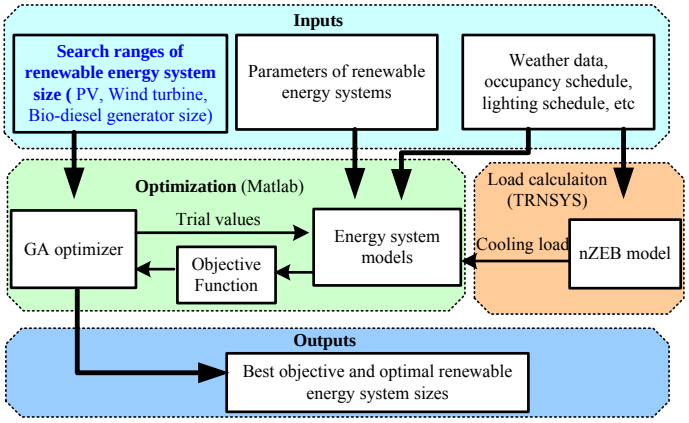

Figure 5.1 Single-objective design optimization using GA

5.2.2 Multi-objective Design Optimization using NSGA-Ⅱ

Figure 5.2 shows the schematic diagram of the multi-objective optimization procedure. The input parameters of the building model, energy system models and optimizer are the same as that in the single-objective optimization. Three objective functions (Equation 5.1, 5.2 and 5.5) are assessed and minimized. Different trial values are searched and further applied for finding the optimal results. NSGA-Ⅱ provided in Matlab 2006 is used to obtain pareto-front sets for different solutions. For most problems, NSGA-Ⅱ is able to find a much better spread of solutions and better convergence near the true Pareto-optimal front compared with other two elitist multi-objective evolutionary algorithms (i.e. Pareto-archived evolution strategy and strength-Pareto evolutionary algorithm) (Deb 2002). Figure 5.2 shows the procedure of multi-objective design optimization using NSGA-Ⅱ.

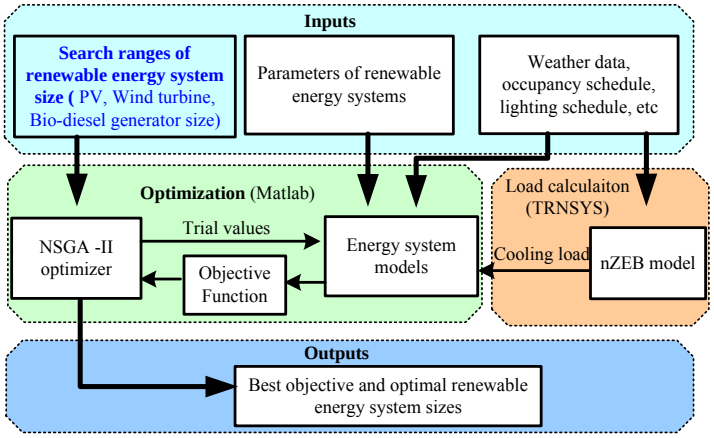

Figure 5.2 Multi-objective design optimization using NSGA-Ⅱ

5.2.3 Objective Functions

In order to evaluate the performance of buildings with renewable energy systems of different combinations, three objective functions are considered: total cost (TC), carbon dioxide emissions (CDE) and grid interaction index (GII).

Minimization of the total cost (TC) in a year is presented by Equation (5.1). The total cost is the sum of annual building operational cost ($Cost_{operation}$) and annual renewable energy systems investment cost ($Cost_{resi}$). Minimization of the total carbon dioxide emissions (CDE), which come from electricity generation and bio-diesel generator, is presented by Equation (5.2). The carbon dioxide emissions from delivered electricity are calculated using Equation (5.3). W_{im} and W_{ex} are the imported and exported powers from/to grid respectively. The carbon dioxide emissions from bio-diesel are calculated using Equation (5.4).

$$Min\ TC = Cost_{resi} + Cost_{operation} \tag{5.1}$$

$$Min\ CDE = CDE_{ele} + CDE_{BDG} \tag{5.2}$$

$$CDE_{ele} = (W_{im} - W_{ex}) \times cde_{ele} \tag{5.3}$$

$$CDE_{BDG} = F_{bio} \times cde_{bio} \tag{5.4}$$

The building-grid interaction, described in Equation 5.6, is based on the ratio between net exported energy (i.e. the difference between the exported energy, W_{ex}, and imported energy, W_{im}) and the average energy demand in the building during a given period. Grid interaction index (GII) is defined as the standard deviation of the

building-grid interaction over the year as shown in Equation 5.5. It is used to estimate the average stress of building on the grid and a low standard deviation is preferred.

$$Min\ GII = STD(f'_{grid,i,T}) \tag{5.5}$$

$$f'_{grid,i,T} = \frac{W_{ex,i} - W_{im,i}}{\int_{t1}^{t2} E_i\, dt/T} \tag{5.6}$$

Multi-objective optimization problems can be simplified into single-objective optimization by using weighted-sum of the three objectives, as shown in Equation 5.7d. The combined objective (f) is used to evaluate the performance of the building energy systems. The sum of w_1, w_2 and w_3 is 1. The same building configuration after deleting all renewable energy systems is chosen as the "benchmark building" (BB) for normalizing objectives. Where, TC_{BB}, CDE_{BB} and $f_{grid,i,T,BB}$ are the total cost, carbon dioxide emission and grid interaction index of "benchmark building" respectively. TC_n, CDE_n and $f_{grid,i,T,n}$ are the normalized total cost, normalized carbon dioxide emission and normalized grid interaction index. A smaller combined objective represents a better performance of building energy systems.

$$TC_n = TC/TC_{BB} \tag{5.7a}$$

$$CDE_n = CDE/CDE_{BB} \tag{5.7b}$$

$$f_{grid,i,T,n} = f_{grid,i,T}/f_{grid,i,T,BB} \tag{5.7c}$$

$$f = w_1 \times TC_n + w_2 \times CDE_n + w_3 \times f_{grid,i,T,n} \tag{5.7d}$$

5.3 Case Study: Application on Hong Kong Zero Carbon Building

The following two case studies were conducted to investigate and compare the effectiveness of the single objective optimization using GA and multi-objective optimization using NSGA-Ⅱ on the sizing of the renewable energy systems. *Case 1*: Optimal design of renewable energy systems for two types of buildings (LEB and nZEB) using single objective optimization approach; *Case 2*: Optimal design of renewable energy systems for the same buildings using multi-objective optimization approach. It should be note, case study is conducted on two types of buildings (LEB and nZEB), which is intent to evaluate the effect of the constraint of annual energy balance on the design solution for buildings.

5.3.1 Description of Building System Configuration

The building energy systems used in this optimization study are proposed on the basis of the energy systems in the Hong Kong ZCB, shown in Figure 5.3. The main parameters of the energy systems are listed in Table 5.1. It should be note, the energy system parameters (i.e. unit price, lifetime) are selected at a medium level, and most values are obtained from the previous references. The daily peak values of the solar radiation and wind velocity in the typical year are shown in Figure 5.4. The highest values in the year are 1017 W/m^2 and 15 m/s respectively.

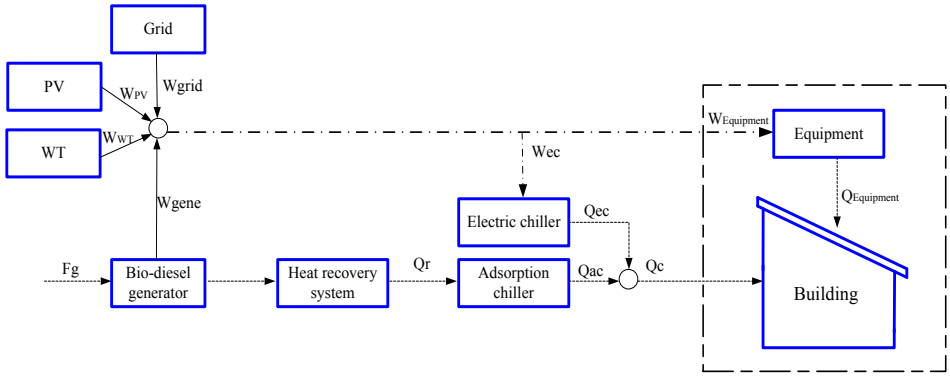

Figure 5.3 Energy flows among the energy systems

The electricity consumption and generation in one week in August are shown in Figure 5.5. Both peak electricity generations of the bio-diesel generator and PV were about 100 kW. The peak electricity consumption of the HVAC system in office hour was between 60 and 70 kW. Other load was below 10 kW in non-office hour and around 30 kW in office hour.

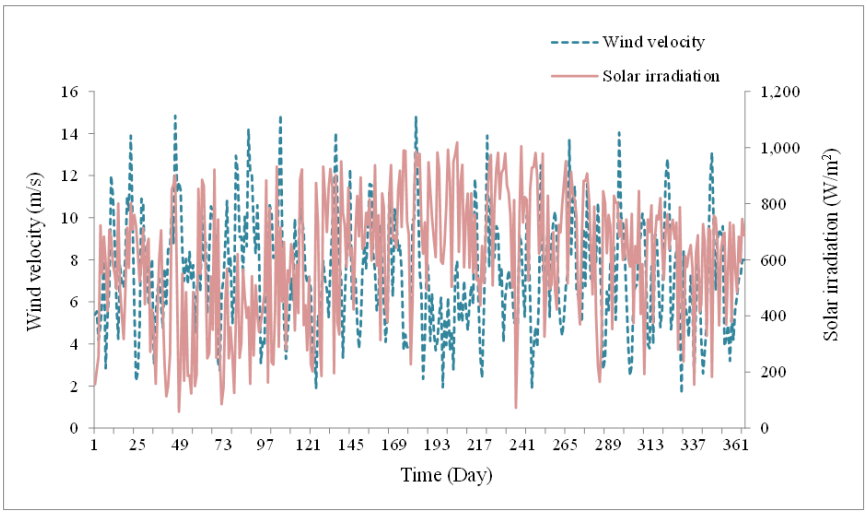

Figure 5.4 Daily peak values of solar radiation and wind velocity in typical year

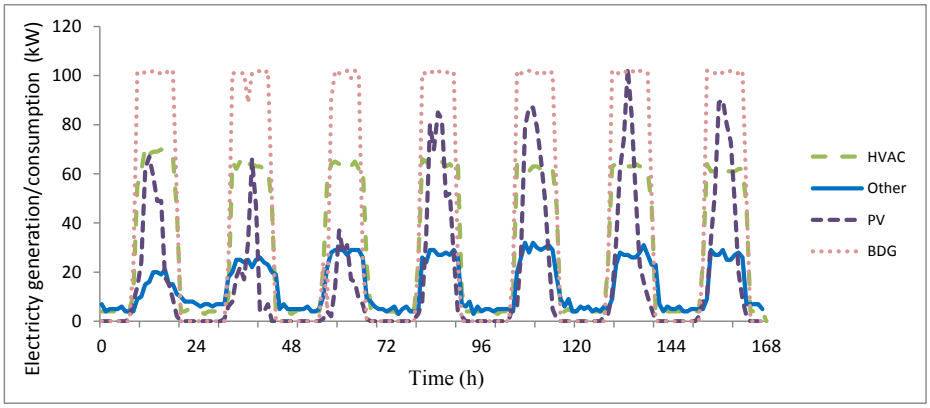

Figure 5.5 Energy consumption and generation in one week in August

Table 5.1 Basic information and energy system parameters

Parameters	Value
Heat recovery system efficiency	0.8 (Liu et al. 2012)
Bio-diesel generator efficiency	0.3 (Mago and Hueffed 2010)
Coefficient of performance of absorption chiller	0.7 (Liu et al. 2012)
Unit price of bio-diesel generator (USD/kW)	205.53 (Mago and Hueffed 2010)
Unit price for photovoltaic (USD/m^2)	378.17
Unit price for wind turbine (USD/kW)	288.86
Oil price (USD/l)	1.3 (bio-diesel price 2015)
Delivered electricity price (USD/kWh)	0.13
Exported electricity price (USD/kWh)	0.065
Lifetime for bio-diesel generator (hour)	40,000 (Bekele and Tadesse 2012)
Lifetime for photovoltaic (year)	20 (Bekele and Tadesse 2012)
Lifetime for wind turbine (year)	20 (Bekele and Tadesse 2012)
Coefficient, A_G (l/kWh)	0.246 (Ghedamsi et al. 2010)
Coefficient, B_G (l/kWh)	0.08145 (Ghedamsi et al. 2010)
Emission factors of electricity from the grid	0.608 (CO_2 emission factors 2010)

Emission factors of bio-diesel combustion	0.552 (CO_2 emission factors 2010)

5.3.2 Results of Case 1 - Using Single Objective Optimization Approach

In the ZCB, the PV with an area of 1015 m^2 and the bio-diesel generator with a rated power of 100 kW are installed on site. The average energy consumption in this building is about 25 kW. Referring these actual sizes of the energy systems and the actual energy consumption of the building, the searching ranges for LEB are set between 0 and 40 kW, between 50 and 150 kW, and between 500 and 1500 m^2 for WT size, BDG capacity and PV area respectively. The searching ranges for the nZEB are set between 0 and 40 kW and between 50 and 150 kW for the WT size and BDG capacity respectively, while the PV area is a dependent variable determined by the annual energy balance of the building. The results of the optimal renewable energy system sizes for the LEB and nZEB using single objective optimization are summarized in Table 5.2. The ZCB after deleting all renewable energy systems is used as the "benchmark building" (BB) in this study. The annual total cost, CO_2 emissions and grid interaction index of the benchmark building were 35,274 USD, 164,974 kg and 1.1386 respectively. Different weighting factors could be selected for different situations and usually determined by the users according to their preference. In this case study, four scenarios (A, B, C, D) based on different weighting factors are investigated and compared. In Scenario A, the three objectives are treated equally. In other three scenarios, only one of three objectives is concerned. The results show that the minimum values (0.82, 0.82) of the objective functions were less than 1 in Scenario A for both buildings. It means that the performance of optimized energy systems in both LEB (WT=33.9 kW, BDG=50 kW and PV=500.2 m^2) and nZEB (WT=40 kW, BDG=50.1 kW and PV=458.3 m^2) were better than that of the benchmark building. It

is worth noticing that the obtained optimal sizes of BDG and PV reach their lower limits in this case, and total capacity of the LEB and nZEB is nearly the same due to these searching ranges set in this study. When only the total cost was concerned in Scenario B, minimum values (1.9, 1.83) of the objective functions were close to 2 due to the high investment cost of renewable energy systems. Therefore, the minimum total costs of energy systems in LEB and nZEB were nearly twice of the energy systems in the benchmark building. However, the performances of LEB and nZEB in Scenario C and D were better than that of the benchmark building when priority was put on reducing CO_2 emissions or grid interaction index. It is worth noticing that the minimum value of the objective function of LEB was negative (-0.46) in Scenario C. It means that, in a comprehensive view, CO_2 emissions from power imported from grid and bio-diesel generator was offset by the contribution of the surplus power generation in the building exported to the grid.

Table 5.2 Optimal RES sizes for buildings using GA approach

Scenario No.	Weighting factors w_1, w_2, w_3	LEB				nZEB			
		WT (kW)	BDG (kW)	PV (m^2)	Minimum objective value	WT (kW)	BDG (kW)	PV (m^2)	Minimum objective value
A	1/3, 1/3, 1/3	33.9	50.0	500.2	0.82	40.0	50.1	458.3	0.82
B	1, 0, 0	20.8	50.0	500.0	1.90	40.0	50.0	462.7	1.83
C	0, 1, 0	40.0	97.6	1,493.9	-0.46	0.8	50.0	1,237.6	0.13
D	0, 0, 1	0.0	50.0	500.0	0.32	23.4	52.1	699.7	0.45

Figure 5.6 presents a comparison between the total cost, CO_2 emissions and grid interaction index of the three buildings (BB, LEB and nZEB) in four scenarios. As shown in Figure 5.6A, the total annual costs of both LEB and nZEB in all scenarios

were much higher than the cost of the benchmark building. Particularly in Scenario C, the total cost of LEB was nearly 3 times of that of the benchmark building. In Figure 5.6B, CO_2 emissions of both LEB and nZEB decreased dramatically compared with that of the benchmark building and even became negative (i.e., LEB in Scenario C). This means that the total CO_2 emissions coming from the bio-diesel generator and the power imported from the grid were less than the CO_2 emissions reduction due to the power exported to grid. In another word, the renewable energy system generated more electricity than that demanded by the building. Figure 5.6C shows that the grid interaction index (GII) of both LEB and nZEB were much smaller than that of the benchmark building in most scenarios (A, B and D) while the grid interaction index of LEB was higher than that for the benchmark building in Scenario C. For LEB, the higher cost resulted in lower CO_2 emissions but higher grid interaction index. For nZEB, the cost, CO_2 emissions and grid interaction index had less fluctuation in different scenarios.

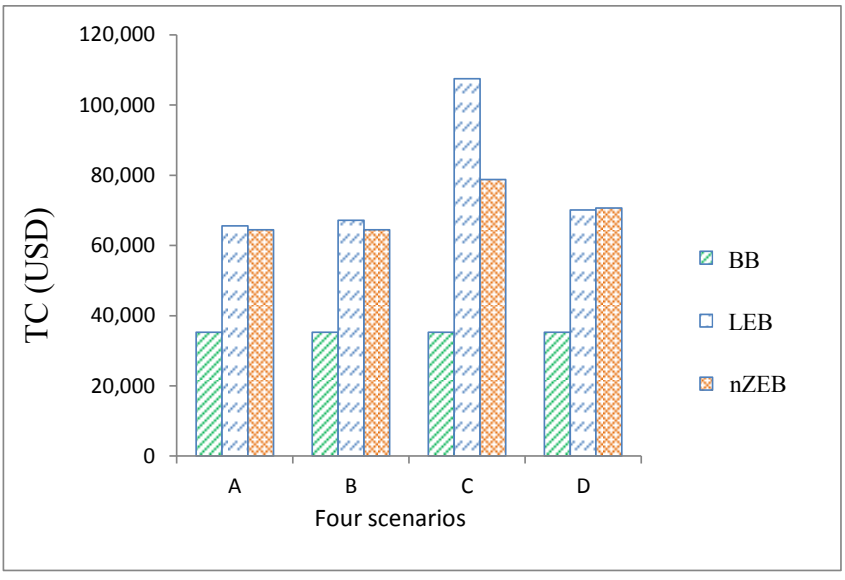

A: Total cost (TC) of different buildings

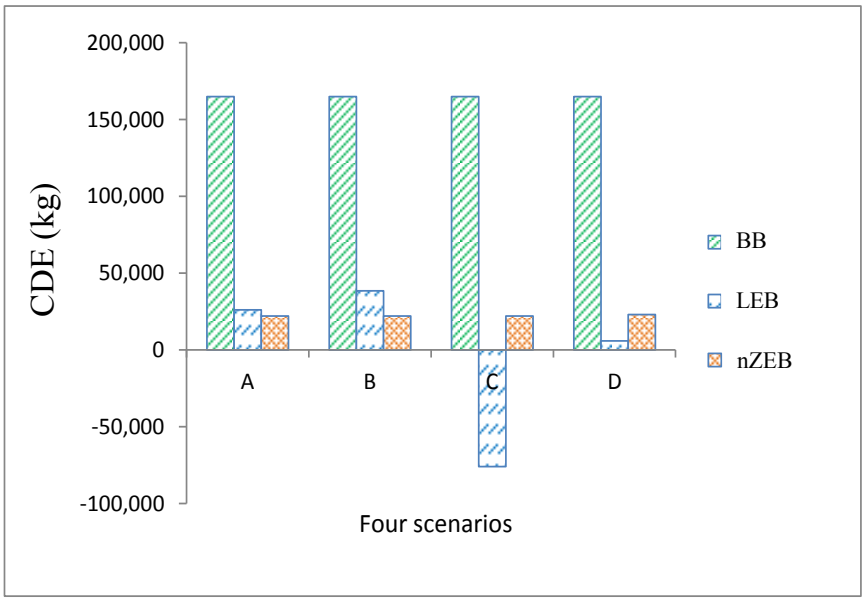

B: CO_2 emission (CDE) of different buildings

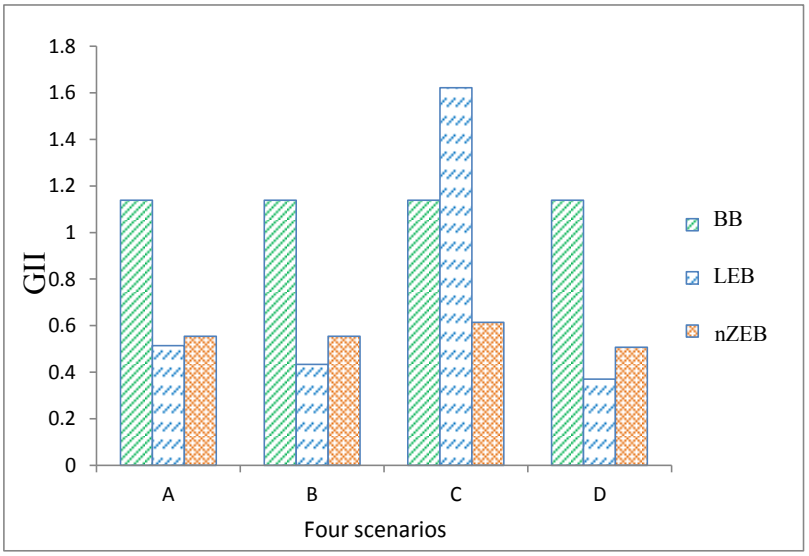

C: Grid interaction index (GII) of different buildings

Figure 5.6 Total cost (TC) , CO2 emissions (CDE) and Grid interaction index (GII) of three buildings in different scenarios

5.3.3 Results of Case 2 - Using Multi-objective Optimization Approach

The multi-objective optimization approach was also applied to optimize the sizes of renewable energy systems in the LEB and nZEB respectively. The searching ranges were set to be the same as that in the previous case study. The best pareto-front sets obtained are shown in Figure 5.7. This figure also illustrates the diversity features of NSGA-II in comparison with the optimal results in Case 1. The marks, GA-A, GA-B, GA-C and GA-D, stand for the results of GA optimization (Case 1) in Scenario A, B, C and D respectively. With regards to the LEB, minimization of the total cost naturally requires reduced investment of renewable energy systems. Because of the reduction in the renewable energy system investment, the corresponding electricity imported from the grid increased, resulting increased CO_2 emissions dramatically. It is obvious that the two objectives (i.e. total cost and CO_2 emissions) are contradicting with each other (see Figure 5.7A). The reduction of renewable energy system investment results in less electricity flow between the building and the grid, therefore lower grid interaction index is obtained (see Figure 5.7). When there was no investment on renewable energy system (i.e., benchmark building), the GII was high (GII=1.1386). With the increase of renewable energy system investment, the grid interaction index reduced until it reached below 0.4 (corresponding cost was around 6×10^4 USD), due to less electricity imported from the grid. When the investment increased further, the grid interaction index changed in the adverse direction and increased even higher than that of the benchmark building, due to increased surplus electricity exported to the grid. It is obvious that a lower CDE can be achieved at the expense of a higher cost and higher GII in the searching range of the design variables. It well agrees with the GA optimization results in Scenario C (i.e. CDE=-76,074 kg, Cost=107,490 USD and

GII= 1.622) where only minimizing CO_2 is of concern. Note, three "additional" points calculated outside the used searching range of the design variables are added in Figure 5.7B and 5.7C respectively to show the trend of GII. The pareto-front sets obtained can provide the relationship/trend among/of the three objectives (i.e. total cost, CDE and GII) in different design options. This is very meaningful for design makers, facilitating them to select one or more appropriate compromised solutions based on their requirements (e.g. an example is given in Table 5.3).

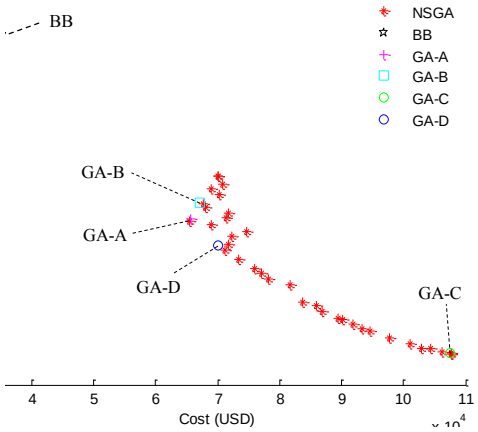

(5.7A)

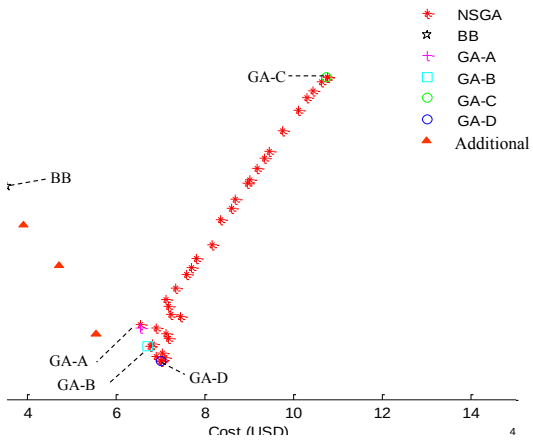

(5.7B)

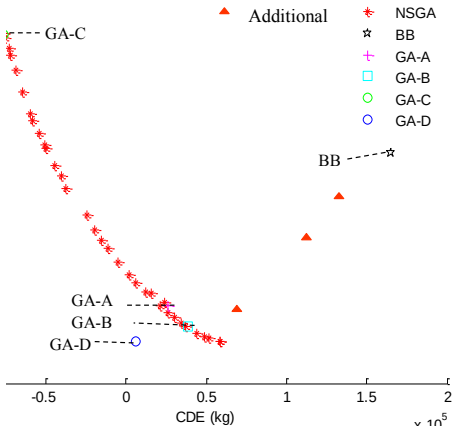

(5.7C)

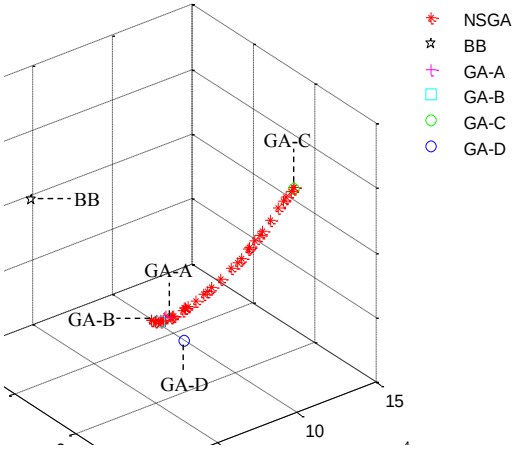

(5.7D)

Figure 5.7 The pareto-optimal sets (35 solutions) in two-dimensional and three-dimensional objective spaces for LEB

For the nZEB, as shown in Figure 5.8A, it is observed that the minimization of total cost resulted in less variations in CO_2 emission, showing a different trend compared with that of the LEB. The total cost, CDE and GII for nZEB show little variations within different design options, which may be due to the constraint of zero energy

balance between the building and the grid. For CO_2 emissions in nZEB, it comes from fuel consumption in BDG since the electricity from/to grid is balanced anually in the case of nZEB. However, among the 35 pareto-optimal sets obtained, BDG size was found to be varid within a small range, i.e. between 50 and 52 kW. Therefore, CO_2 emissions had less variation in the case of nZEB. The performance of the benchmark building and the nZEB in four scenarios given by the GA optimization are also marked in Figure 5.8. The costs of the systems designed in Scenario GA-A (64,507 USD) and GA-B (64,484 USD) were much lower than that in Scenario GA-C (78,793 USD) and GA-D (70,713 USD) while the CDE values in the four scenarios were almost the same (about 22,500±500 kg) as shown in Figure 5.8A. It is therefore obvious that systems in Scenario GA-A and GA-B are better choices concerning the cost and CDE. The system in Scenario GA-C is not a good choice since it costed higher (Cost=78,793 USD) with a higher grid interaction index (GII=0.6137) but offered less CO_2 emissions reduction (CDE=22,043 kg) as shown in Figure 5.8B.

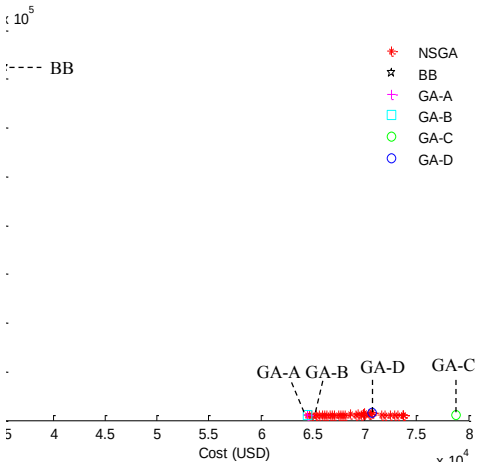

(5.8A)

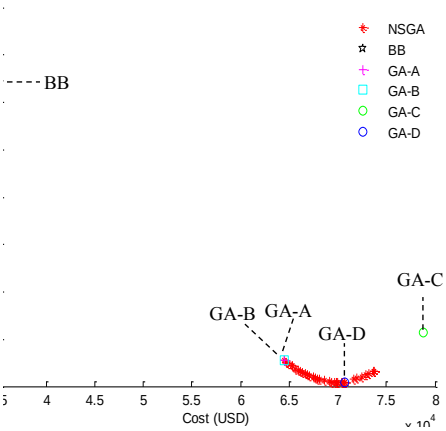

(5.8B)

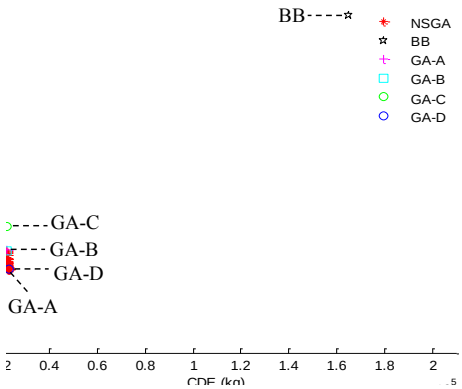

(5.8C)

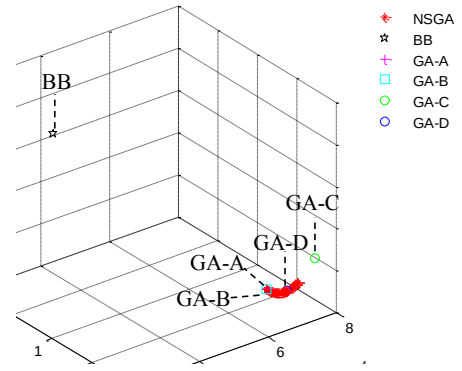

(5.8D)

Figure 5.8 The pareto-optimal sets (35 solutions) in two-dimensional and three-dimensional objective spaces for nZEB

For more detailed investigation, a subset of pareto-optimal solutions given by NSGA-II (generation=1000 and paretofraction=0.7) is listed in Table 5.3. The ranges of the total cost, CO_2 emissions, grid interaction index in LEB were between 65,410 USD and 107,640 USD, between -76,359 kg and 58,313 kg, and between 0.37 and 1.63 respectively. The ranges of the total cost, CO_2 emissions and grid interaction index in LEB were between 64,484 USD and 73,680 USD, between 22,043 kg and 22,963 kg, and between 0.51 and 0.55 respectively. Based on this table, decision makers can select the suitable solution(s) according to their requirements. Taking the LEB for example, if a designer expects that the total cost (TC) is below 90,000 USD, solutions 1-24 are satisfactory. If an additional requirement of CO_2 emissions (CDE) below zero is introduced, solutions 15 and 17-24 are acceptable. If a further criterion of the grid interaction index (GII) below 1 is added, only the solutions 15 and 17-21 are left for the consideration of the decision maker.

5.3.4 Comparison between Single and Multi-objective Optimization Methods

For GA optimization, the generation number is one of the important parameters that affect the results of best fitness values. The fitness value of an individual (any point to which one can apply the fitness function) is the value of the fitness function (the objective function) for that individual. The best fitness value for a population (an array of individuals) is the minimum value of the objective function for the population.

Table 5.3 Pareto-optimal solutions for buildings using NSGA-II approach

Solutions	LEB						nZEB					
	TC (USD)	CDE(kg)	GII	WT(kW)	BDG(kW)	PV(m^2)	TC(USD)	CDE(kg)	GII	WT(kW)	BDG(kW)	PV(m^2)
1	65,410.2	23,918.8	0.53	36.0	50.0	502.7	64,484.0	22,042.8	0.55	40.0	50.0	462.7
2	67,700.8	37,538.0	0.43	20.1	50.2	528.9	64,711.1	22,042.9	0.55	39.3	50.0	476.5
3	68,152.5	34,360.9	0.45	20.9	50.2	576.7	64,933.1	22,062.6	0.55	38.7	50.0	488.4
4	68,982.9	21,373.5	0.52	28.1	50.7	687.1	65,373.7	22,244.9	0.54	37.7	50.5	486.4
5	69,037.6	48,733.5	0.39	9.0	50.3	510.8	65,373.7	22,244.9	0.54	37.7	50.5	486.4
6	70,137.2	58,312.6	0.37	0.0	50.0	500.0	65,683.4	22,063.6	0.54	36.5	50.0	531.9
7	70,137.2	58,312.6	0.37	0.0	50.0	500.0	65,927.2	22,103.4	0.53	35.8	50.1	541.4
8	70,367.8	44,245.7	0.40	8.4	50.5	610.0	66,141.7	22,200.3	0.53	35.4	50.4	536.2
9	70,877.1	51,948.4	0.39	2.7	51.1	541.0	66,336.0	22,123.4	0.53	34.7	50.2	558.8
10	71,250.0	1,959.1	0.64	36.8	51.8	882.8	66,708.9	22,267.7	0.53	33.8	50.5	563.5
11	71,355.5	26,416.7	0.49	18.0	50.8	777.5	66,849.0	22,078.9	0.52	33.1	50.1	594.7
12	71,776.8	6,436.4	0.61	31.1	50.8	936.4	67,105.2	22,218.8	0.52	32.6	50.4	591.6
13	71,803.9	30,581.0	0.47	13.5	50.4	794.5	67,459.5	22,229.0	0.52	31.6	50.4	611.4
14	72,254.6	12,492.5	0.57	25.3	50.6	930.3	67,731.3	22,117.3	0.52	30.6	50.2	639.8
15	73,405.2	-4,654.0	0.69	36.9	53.1	973.2	67,900.8	22,058.7	0.52	30.1	50.0	658.4
16	74,614.3	15,842.5	0.57	20.2	54.7	822.7	68,126.0	22,168.4	0.51	29.6	50.3	655.2

17	75,912.2	-11,452.9	0.75	36.9	55.0	1,048.9	68,638.4	22,474.3	0.51	28.6	51.0	644.6
18	77,048.1	-15,043.6	0.78	36.2	54.7	1,145.8	69,198.8	22,301.9	0.51	26.7	50.6	699.5
19	78,196.0	-19,685.4	0.82	38.5	56.7	1,130.8	69,343.0	22,421.1	0.51	26.5	50.9	690.5
20	81,691.5	-24,286.8	0.89	33.9	58.2	1,269.0	69,653.9	22,297.9	0.51	25.4	50.6	725.2
21	83,644.5	-37,168.4	0.99	39.2	59.2	1,401.0	69,846.6	22,753.5	0.51	25.5	51.6	679.9
22	85,986.1	-40,225.0	1.04	36.8	60.8	1,461.1	69,895.0	22,540.4	0.51	25.1	51.1	709.5
23	86,941.2	-44,612.8	1.08	39.4	62.7	1,442.2	69,945.9	22,852.1	0.51	25.4	51.8	673.2
24	89,511.0	-49,781.0	1.15	39.4	65.9	1,458.9	70,413.3	22,608.5	0.51	23.7	51.3	706.8
25	90,172.0	-50,348.2	1.17	39.7	67.6	1,415.5	70,526.7	22,720.2	0.51	23.6	51.5	721.8
26	91,812.7	-54,213.3	1.22	39.5	68.9	1,466.9	70,706.5	22,962.6	0.51	23.4	52.1	699.7
27	93,294.2	-57,892.7	1.27	39.9	70.6	1,487.8	70,712.7	22,961.4	0.51	23.4	52.1	699.7
28	94,545.4	-59,252.6	1.30	39.1	72.2	1,493.7	71,616.1	22,042.8	0.51	19.6	50.0	865.9
29	97,656.9	-64,153.7	1.38	39.8	77.8	1,454.1	71,996.2	22,042.8	0.52	18.6	50.0	885.7
30	100,980.1	-68,849.9	1.48	38.9	82.6	1,481.9	72,485.2	22,042.8	0.52	17.3	50.0	911.4
31	102,966.1	-72,131.8	1.53	39.4	86.3	1,484.8	72,848.5	22,042.8	0.52	16.3	50.0	931.2
32	104,392.7	-72,727.3	1.56	39.0	89.6	1,471.3	73,160.7	22,042.8	0.53	15.4	50.0	949.0
33	106,267.1	-75,302.1	1.61	39.5	93.8	1,492.8	73,679.8	22,042.8	0.53	14.0	50.0	976.6
34	107,617.8	-76,359.3	1.63	40.0	97.8	1,500.0	73,680.1	22,042.8	0.53	14.0	50.0	976.6
35	107,640.3	-76,241.8	1.62	39.9	97.8	1,500.0	73,680.1	22,042.8	0.53	14.0	50.0	976.6

Figure 5.9 presents the best fitness values of Scenario A for LEB and nZEB under the following settings: crossover fraction=0.8, migration fraction=0.2, population size=50, StallGenLimit=200, function tolerance=1.0×10^{-10}. For both of LEB and nZEB, the fitness values approached stable values at about 100^{th} generation. The execution times and fitness values at different generations for nZEB and LEB are further analyzed as shown in Figure 5.10. The execution times for both of LEB and nZEB increased with the increase of generation number. At 10^{th} generation, the execution time is approximately 500 seconds while about 4000 seconds are needed at 100^{th} generation.

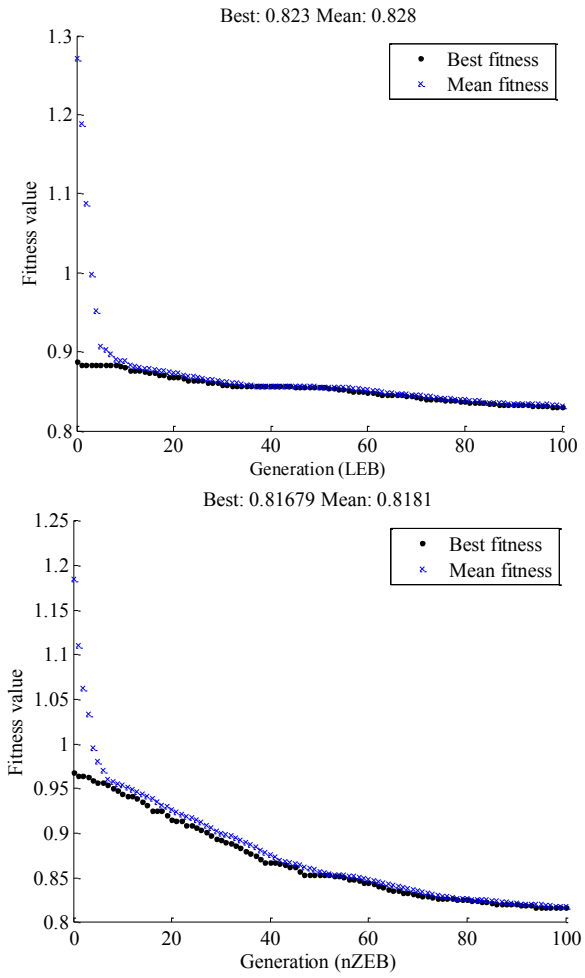

Figure 5.9 Fitness values for LEB and nZEB at the generation 100 (Scenario A-GA)

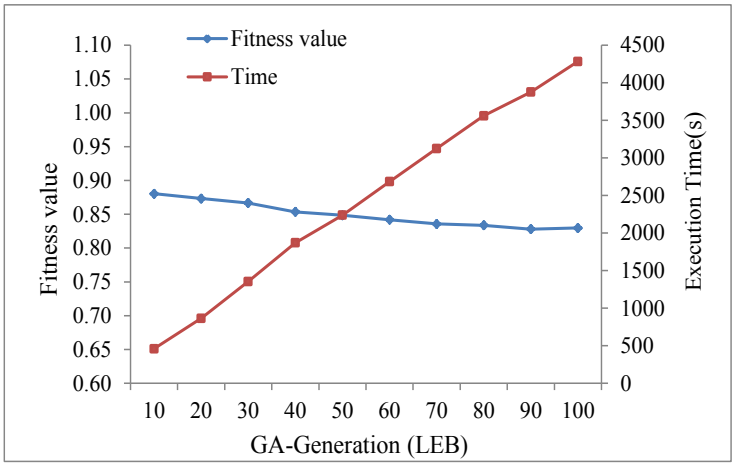

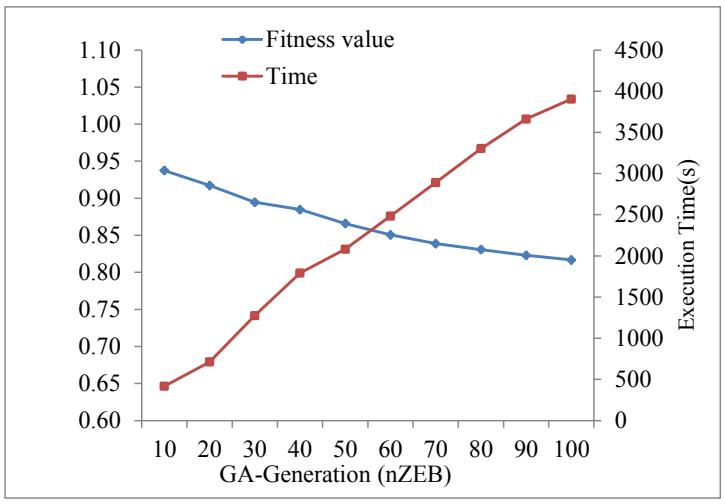

Figure 5.10 Effect of different generations on fitness values and execution times (Scenario A-GA)

For the implementation of NSGA-II, the effects of generation number on the execution time and searched ranges of pareto-optimal sets were also significant as showing in Table 5.4. Where, the following parameters are specified: paretofraction=0.7, crossover fraction=0.8, migration fraction=0.2, population size=50, StallGenLimit=200, function tolerance=1.0×10^{-10}. The generation number was set as 100, 200, 400, 600, 800, and 1000 respectively. For the LEB, the execution time increased from 4,644 seconds (generation=100) to 46,523 seconds (generation=1,000),

corresponding to the obtained best total cost from 69,886 USD to 65,410 USD and the best CO_2 emissions from -40,685 kg to -76,359 kg. The best grid interaction index remained stable at the above generation numbers. For the case of nZEB, no improvement can be found on the obtained best CO_2 emissions and the best grid interaction index when the generation number increased beyond 100. The obtained best cost reduced from 77,597 USD (generation=100) to 64,484 USD (generation=1000).

Table 5.4 Effect of generation number on ranges of objectives searched by NSGA-II method

LEB				
Generation	Execution time(s)	TC (USD)	CDE (kg)	GII
100	4644	[69,886, 109,962]	[-40,685, 58,257]	[0.37, 1.50]
200	8369	[69,060, 110,258]	[-46,024, 58,315]	[0.37, 1.52]
400	18344	[67,239, 110,021]	[-62,947, 58,305]	[0.37, 1.58]
600	24351	[66,265, 107,487]	[-66,903, 58,298]	[0.37, 1.56]
800	36251	[66,620, 107,350]	[-69,116, 58,315]	[0.37, 1.57]
1000	46523	[65,410, 107,640]	[-76,359, 58,313]	[0.37, 1.63]
nZEB				
Generation	Execution time(s)	TC (USD)	CDE (kg)	GII

100	4341	[77,597, 78,961]	[22,043, 23,984]	[0.57, 0.62]
200	9629	[69,585, 74,648]	[22,043, 23,020]	[0.51, 0.54]
400	17957	[67,920, 75,310]	[22,043, 23,088]	[0.51, 0.55]
600	26933	[67,943, 75,198]	[22,043, 22,977]	[0.51, 0.55]
800	35779	[64,758, 74,586]	[22,043, 22,961]	[0.51, 0.55]
1000	44382	[64,484, 73,680]	[22,043, 22,963]	[0.51, 0.55]

The minimum objectives given by two optimization methods are compared in Table 5.5. Fewer generation number, requested less execution time, was needed for GA to get one best result each time (for a set of weighting factors), while ten times of generation number and execution time were needed for NSGA-II but to get a large range of pareto-optimal sets.

Table 5.5 Comparison between the effects of GA and NSGA-II on minimum objectives obtained

		LEB					
Methods	Generation	Min (TC)	Difference (%)	Min (CDE)	Difference (%)	Min (GII)	Difference (%)
GA	100	67,158	-	-76,074	-	0.37	-
NSGA-II	1,000	65,410	2.672%	-76,359	0.374%	0.37	0.00%
		nZEB					
Methods	Generation	Min (TC)	Difference (%)	Min (CDE)	Difference (%)	Min (GII)	Difference (%)
GA	100	64,486	-	22,043	-	0.51	-

NSGA-II	1,000	64,484	0.002%	22,043	0.00%	0.51	0.00%

5.3.5 Findings and Limitations

The results of the single objective optimization show that the optimal results obtained when minimizing the combined objective (objective=0.82/0.82, for LEB and nZEB respectively), minimizing CO_2 emissions only (objective=-0.46/0.13) and minimizing the grid interaction index only (objective=0.32/0.45) for both LEB and nZEB are much better than the corresponding performance (objective=1.0) in the benchmark building. When only the total cost is concerned in optimization, the total cost of LEB and nZEB (objective=1.9/1.83) was about 2 times of that for the benchmark building. When using multi-objective optimization, three objectives (i.e. total cost, CO_2 emissions and grid interaction index) are considered in parallel and a subset of pareto-optimal solutions is identified in a single run. For the low energy building, the reduction in the renewable energy system investment results in a dramatic increase of CO_2 emissions and lower grid interaction index. However, the cost, CO_2 emissions and grid integration index for the nZEB have little variations when different design options are selected, due to the constraint of zero annual energy balance. By comparing these optimal design solutions of renewable energy system, decision makers could understand the trade-off relationship among the three objectives and the effects of the design parameters on the objectives.

The generation numbers set in optimization algorithm may cause potential numerical errors on the optimal results obtained. Thus, the effects of generation numbers on the results and execution times of GA and NSGA-II optimization are investigated. In GA

optimization, fewer generations (100) and less execution time (less than 5000 seconds) are needed to get one set of best design parameters. However, in NSGA-II optimization, ten times of generations (1000) and more execution time (more than 40000 seconds) are needed for searching a large range of pareto-optimal sets. The time-consuming optimization calculations (more than 1 hour for GA and more than 10 hours for NSGA-II optimization) mainly derive from the building energy system models used. In order to obtain the accurate and robust design results, more accurate nonlinear building energy system models are developed and used, although they are simplified models and not complex. Less execution time and generation number will be required for optimization when simpler linear building energy system models are employed.

The design optimization in this study focuses on finding the optimal options and combinations of renewable energy system sizes only. Similar design studies can be found also in Khatib et al. (2011) and Zhou et al. (2013). In their studies, the optimization design of renewable energy systems was conducted concerning the total annual cost only. The embodied energy is not considered in this study. As stated by Stephan et al (2013), the embodied energy is usually higher than that in normal buildings. In a low energy building, the embodied energy may represent more than 70% of the total embodied and operational enegry over 100 years. Blengini and Di Carlo (2010) also demonstrated that as operational energy decreases due to energy efficiency, the significance of the embodied energy will increase. Therefore, more parameters need to be considered in the design optimization if the scope is extended to cover the embodied energy and the effects of operation strategies used in future studies.

Additionally, the uncertainty of the renewable energy generation, building loads and energy tariffs should be considered to obtain more robust design results.

5.4 Summary

In this chapter, the study on the design optimization of renewable energy systems in the LEB and nZEB is presented. With properly sized renewable energy systems, cost-saving, environment-friendly and even low impact of the building on the grid can be achieved in the development of nZEB.

Genetic Algorithm (GA) method and non-dominated sorting Genetic Algorithm-Ⅱ (NSGA-Ⅱ) approach are applied to choose the optimal sizes of renewable energy systems for two types of buildings in Hong Kong, i.e. LEB and nZEB. Simulation-based optimization is applied in this study to optimize the renewable energy system sizes of the buildings using GA and NSGA-Ⅱ approach for single objective optimization and multi-objectives optimization respectively. The total cost, CO_2 emissions and grid interaction index are considered as the three objectives for the design optimization.

The results show that when the emphasis is put on CO_2 emissions only, grid interaction index only, or the combined objective concerning the total cost, CO_2 emissions and grid interaction index equally in the single objective optimization, the performances of both LEB and nZEB are better than the corresponding performance of the benchmark building. However, when the total cost is the only objective to be minimized, a reverse trend is obtained. Using the multi-objective optimization, a

subset of pareto-optimal solutions is obtained and the relationship among the three objectives is identified.

Comparing the results given by the two methods, the single objective optimization, by lumping the three objectives into one, can obtain the "best" solution directly. But the designers are not given any information on the effects of the parameters to be optimized on the different design objectives. The multi-objective optimization, by considering the total cost, CO_2 emissions and grid interaction index in parallel, provides rich and valuable information on these effects to decision makers, allowing them to find one or more appropriate compromised solutions from the sets of pareto-solutions obtained.

CHAPTER 6 IMPACT OF OPERATION VARIABLES ON THE PERFORMANCE ROBUSTNESS OF nZEBs

In Chapter 5, optimal design of renewable energy system sizes for nZEBs is presented. However, the sensitivity of energy performance of nZEBs to the discrepancies between the real and design operation conditions (e.g. weather condition and demand load) are not yet clear. Sensitivity analysis, a valuable tool for decision-makers, can be used to explore the impacts of the changes in input variables on model outputs.

This chapter presents an investigation on the impact of operation variables on the performance robustness of nZEBs. *Section 6.1* presents an overview of different sensitivity analysis methods used to assess the effect of input variables. In *Section 6.2*, the approach and steps of sensitivity analysis in this study are provided. In *Section 6.3*, the optimal sized renewable energy systems and the correspondingly performance are provided based on the optimization methods introduced in Chapter 5. *Section 6.4* presents the study on one-way sensitivity analysis, two-way sensitivity analysis and multiway sensitivity analysis for PV/WT/BDG system to identify the significant factors that affect the building performance. *Section 6.5* presents the comparison study on performance robustness of four design options by using multiway sensitivity analysis. A summary of this chapter is given in *Section 6.6*.

6.1 An Overview of Sensitivity Analysis Methods

Sensitivity analysis is a valuable tool to study how the uncertainty in the output of a building energy system can be apportioned to different sources of uncertainty in its inputs. The sensitivity analysis methods could be classified into several categories, including: (1) mathematical; (2) statistical; and (3) graphical (Frey and Patil 2002; El-Temtamy and Gendy 2014). Other classifications mainly focus on the capability of a specific technique, rather than the methodology (Saltelli et al. 2000). Mathematical methods typically involve the calculation of the output for a few input values that represent the possible range of the input (Salehi et al. 2000), which includes nominal range sensitivity analysis, breakeven analysis, automatic differentiation and difference in log odds ratio. Statistical methods assess the effects of input variables, which are assigned as probability distributions, on the output distribution. It could be used to identify the effect of interactions among multiple inputs. The methods include analysis of variance, response surface method, regression analysis, etc. Graphical methods allow users to evaluate the sensitivity in the form of graphs, surfaces or charts, which could give a visual indication of how the outputs are affected by the input variables. The typical techniques include tornado graphs, radar plots, scatter plots, cobweb pots, etc. Generally, graphical methods could be used for better representation of the results combined with the mathematical and/or statistical methods.

The aim of sensitivity analysis performed in this study is to identify the significant factors that affect the nZEB performance and to rank the robust performance of different design options. The combination of one-way/two-way/multiway sensitivity analysis can be used to achieve such a goal. This study could help decision makers in

making selections with visualized relationships between the output and input factors. It is true that sensitivity study using Monto-Carlo simulation can reflect more information such as the probability distributions of parameters uncertainty, and a further study will be conducted to quantify the uncertainty of parameters on results.

6.2 Approach and Steps of Sensitivity Analysis

Figure 6.1 shows the approach and steps of the sensitivity analysis to evaluate the performance of nZEBs with different energy system design options. At the first step (I), an optimization software tool based on genetic algorithm (GA) is implemented to obtain the optimal sizes of renewable energy systems and the corresponding building performance. GA is one of the most preferable and widespread searching algorithms for optimization problems. It is easy to be transferred in existing simulations and models. The values of weather data and occupancy/equipment schedules, the parameters of energy systems and renewable energy systems are set as the inputs and parameters for building model (developed in the building energy simulation program, TRNSYS) and the system models (developed in Matlab 2006). The size ranges of renewable energy systems are set as the constraints for the GA optimizer (included in Matlab 2006). The objective function, combining the total annualized cost (TC), CO_2 emissions (CDE) and the grid interaction index (GII) using weighting factors shown in Equation 6.1, is evaluated and minimized by the GA optimizer.

At the second step (II), the comprehensive performance of the building, when the input variables vary over certain arranges, is computed using the objective function and the same building energy and renewable energy system models. Four most important

input variables representing the working condition of buildings are selected and each of them is assigned with a variation range. In this study, the input variables concerned include wind velocity, solar radiation, building cooling load and other load. The building cooling load refers to the total cooling needed from the chiller plant. The other load refers to the total other load of all electricity appliances in the building except the air-conditioning system.

At the third step (III), the one-way sensitivity analysis, two-way sensitivity analysis and multi-way sensitivity analysis are performed on the optimized PV/WT/BDG system. The input variables that have significant impacts on the building performance are identified. Multiway sensitivity analysis is also performed on the other three design options. By comparing the performances of the four design options considering variations in input variables, the performance robustness of the four design options are assessed and ranked.

In this study, the renewable energy systems concerned are photovoltaic (PV), wind turbine (WT) and bio-diesel generator (BDG). Four most commonly used system combinations or design options (i.e., PV/WT/BDG, PV/WT, PV/BDG and WT/BDG) are considered. The typical meteorological year in Hong Kong (i.e. 1987) is selected as the weather condition for building energy systems simulation, which is commonly used as the representative year in the building field in Hong Kong. Detailed energy system models used can be found in the Chapter 4.

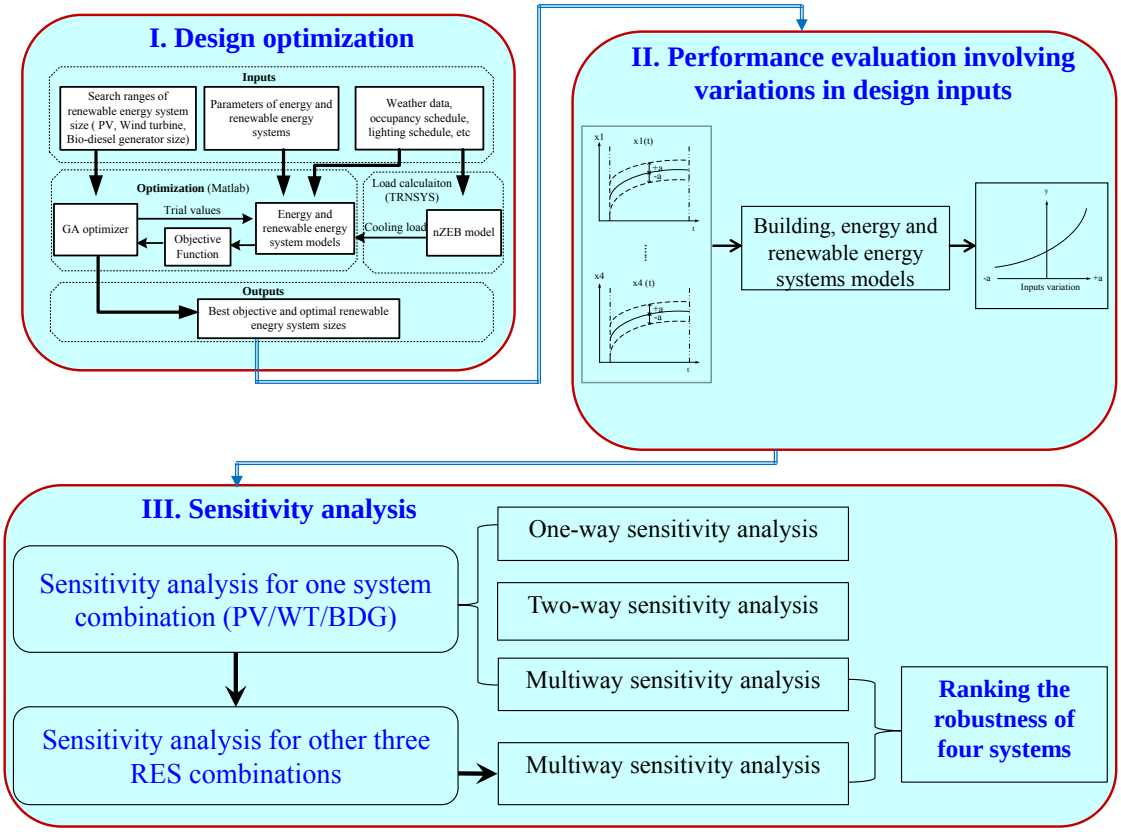

Figure 6.1 Approach and steps of sensitivity analysis

Objective function: In order to conduct a comprehensive evaluation on the building performance, a combined objective (*f*) is used. It considers the performance indices of the total annualized cost (TC), CO_2 emissions (CDE) and the grid interaction index (GII) using weighting factors as shown in Equation (6.1). Where, TC_n , CDE_n and GII_n are the dimensionless values of the above three indices. TC_n, CDE_n and GII_n are the values of the three indices divided by their corresponding indices of the benchmark building. As in nZEBs, it is required that the energy generated is equal to the building energy demand over a year. w_1, w_2, w_3 are assigned to indicate the relative importance of the three objectives (i.e. TC_n , CDE_n and GII_n). The sum of weighting factors w_1, w_2 and w_3 is 1. They can be tuned according to the preferences of the decision makers. In this study, the three objectives are assumed to be equally important, that is $w_1 = w_2 =$

$w_3 = 1/3$. The benchmark building (BB) refers to the ZCB after deleting all renewable energy systems. Equation (6.1a), from reference (Maheri 2014), is used to estimate the total annualized cost (TC). The CO_2 emissions come from electricity generation (CDE_{ele}) and bio-diesel generator (CDE_{BDG}) as shown in Equation (6.1b). Grid interaction index (GII), as shown in Equation (6.1c), is used to estimate the average stress of a building on the grid. It is defined as the standard deviation of the building-grid interaction ($f_{grid,i,T}$) over a year. A smaller combined objective represents a better performance of the building system design option and is therefore preferred.

$$\min f = w_1 \times TC_n + w_2 \times CDE_n + w_3 \times GII_n \quad (6.1)$$

$$\text{s.t. } \varphi(x_1, x_2, x_3) = 0$$

$$TC = C_t \times UCRF \quad (6.1a)$$

$$CDE = CDE_{ele} + CDE_{BDG} \quad (6.1b)$$

$$GII = STD(f_{gird,i,T}) \quad (6.1c)$$

where, C_t and $UCRF$ are the total life-span cost and uniform capital recovery factor respectively. C_t, $UCRF$ and $f_{grid,i,T}$ can be calculated using Equation (6.2), (6.3) and (6.4) respectively. C_j is the cost including capital cost, operation cost and maintenance cost in the year, j. The parameter d represents the annual discount rate and N_s is the life-span of the energy system in years. W_{ex}, W_{ex} and E_i represent the exported energy, imported energy and the average energy demand of the building during a given period, respectively.

$$C_t = \sum_{j=0}^{N_S} \frac{C_j}{(1+d)^j} \tag{6.2}$$

$$UCRF = \frac{d \times (1+d)^{N_S}}{(1+d)^{N_S} - 1} \tag{6.3}$$

$$f_{gird,i,T} = \frac{W_{ex,i} - W_{im,i}}{\int_{t1}^{t2} E_i \, dt / T} \tag{6.4}$$

6.3 Operation Variables and Their Impacts on Building Performance

The sizes of four design options (i.e. PV/WT/BDG, PV/WT, PV/BDG and WT/BDG) are determined using GA method, as shown in Table 6.1. The combined objective of the benchmark building (BB) is equal to 1 according to the definition of the objective function in this study. It is observed that the combined objectives of the building under three design options are less than 1, including PV/WT/BDG (f=0.91), PV/WT (f=0.85) and WT/BDG (f=0.93). This means that the comprehensive performances of these three design options are better than that of the benchmark building. However, the comprehensive performance of the building with PV/BDG system (f=1.26) is worse than that of the benchmark building.

In practical operation, the weather conditions and building loads usually deviate from that used at the design stage. In this study, four design input variables considered are shown in Table 6.2 and the maximum ranges of their variations are assigned to be ±20%.

Table 6.1 Optimal sizes of renewable energy systems and corresponding performances

Design options	PV (m^2)	WT (kW)	BDG (kW)	f	TC (USD)	CDE (kg/kWh)	GII
- (BB)	0.0	0.0	0.0	1.00	30,893.6	144,487.2	1.13
PV/WT/BDG (nZEB)	256.4	50.0	49.5	0.91	62,149.2	18,486.8	0.68
PV/WT (nZEB)	762.3	100.0	0.0	0.85	43,827.4	14.4	1.28
PV/BDG (nZEB)	767.5	0.0	60.2	1.26	92,274.5	22,011.0	0.74
WT/BDG (nZEB)	0.0	50.0	61.8	0.93	61,023.2	22,516.9	0.74

Table 6.2 Input variables investigated in sensitivity analysis

Variables	Maximum range of change (%)
Wind velocity	-20 to +20
Other load	-20 to +20
Cooling load	-20 to +20
Solar radiation	-20 to +20

In order to evaluate the impact of the four operation variables on the building performances collectively, the minimum and maximum values of the combined objective (comprehensive performance) associated to different magnitudes of variations in the four variables are presented in Figure 6.2. The minimum and maximum values of the combined objective are 0.852 and 1.09 respectively. With 20% variations in the four input variables, the maximum variation of the combined objective is about 26.2%. It is important to notice that the variations in the four variables have different impacts on the combined objective in terms of direction and the magnitude. Each point on the curve represents a case when the combination of

signs of the variations results in the lowest (left side) or highest (right side) combined objective at certain magnitude (X-axis) of variations in all input variables. It is also worth noticing that the combined objective of the PV/WT/BDG system without introducing variations to the input variables is 0.91 (also see Table 6.1).

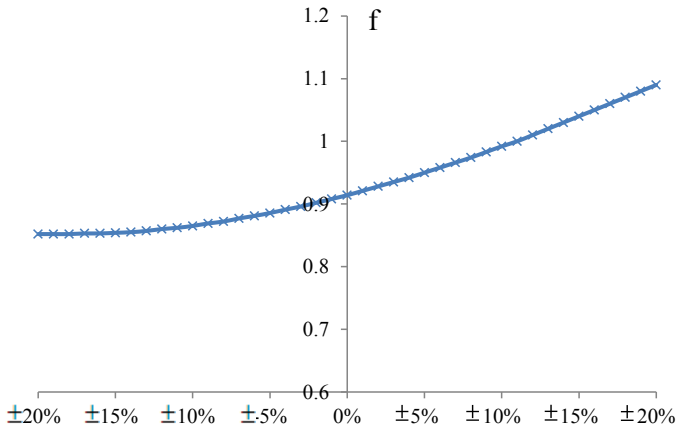

Figure 6.2 Maximum impacts of variations in input variables on the combined objective

6.4 Sensitivity Analysis of PV/WT/BDG System

6.4.1 One-way Sensitivity Analysis of PV/WT/BDG System

One-way sensitivity analysis allows a user to assess the impacts of changes in certain input parameters on the conclusions of a model (Frey and Patil 2002). For each change of a variable, the impact on the outputs of the model could be recorded while all the other variables are kept at their baseline values. The sensitivity analysis results of the PV/WT/BDG system are shown in Table 6.3-6.6. The low and high values of the operation cost, CO_2 emissions, grid interaction index and combined objective, their swing values and the corresponding input values are shown in these tables. The outputs

are also presented as tornado charts (shown in Figure 6.3) and arranged downward from largest variance to smallest variance.

From the one-way analysis, it can be seen that, for the outputs except the combined objective, the input variable associated with largest output variance is the wind velocity, followed by the other load and cooling load. The variation of the solar radiation has a weak impact on these outputs. With respect to the operation cost (see Table 6.3), CO_2 emissions (see Table 6.4) and the grid interaction index (see Table 6.5), the variances caused by the variation of the wind velocity account for 49.8%, 71% and 93.13% respectively. It is followed by the other load, with the variances of 25.08%, 19.54%, and 4.97% respectively. It is worth noticing that the variances caused by the solar radiation are all less than 1%. It could be concluded that wind velocity is the most influential input variable to the above three outputs, which may be due to that the wind power is proportional to the cube of the wind velocity and thus the variation of the wind velocity could affect the outputs significantly.

However, it is interesting to note that the combined objective (see Table 6.6) is not most sensitive to the wind velocity (17.8%), but to the other load (variance=44.4%) and followed by cooling load (variance=34.2%). This is because that the operation cost, CO_2 emissions and the grid interaction index are all most sensitive to the wind velocity, but the directions of their impacts are not the same. In other words, the increase of the wind velocity could greatly reduce the operation cost and CO_2 emissions, but has a dramatic and negative effect on the grid interaction index. Therefore the combined objective concerning the three outputs equally is not influenced greatly by the wind velocity. The results indicate that when the operation

cost (or total annualized cost) and/or CO_2 emissions are concerned, the accuracy of the wind velocity prediction should be of the priority to be concerned during the design stage. In the meanwhile, more attention should be paid to the accuracy of building loads prediction regarding the comprehensive objective.

For the variation of wind velocity, the lowest outputs of operation cost (42,291.6 USD) and CO_2 emissions (-16,208.2 kg/kWh) occurred at the maximum wind velocity ($1.2*V_d$). It is obvious that an increase in wind velocity could result in a lower electricity demand from grid thus a lower operation cost and CO_2 emissions will be achieved. However, a low grid interaction index (0.492) is obtained at the minimum wind velocity ($0.8*V_d$).

Table 6.3 Operation cost of PV/WT/BDG system - single-factor sensitivity analysis

Variable	Output - Operation cost				Corresponding input variable	
	Low (USD)	High (USD)	Swing (USD)	Variance	Low output	High output
Wind velocity	42,291.6	49,873.1	7,581.5	49.83%	$1.2*V_d$	$0.8*V_d$
Other load	44,016.0	49,394.7	5,378.7	25.08%	$0.8*W_d$	$1.2*W_d$
Cooling load	44,063.2	49,327.9	5,264.7	24.03%	$0.8*Q_d$	$1.2*Q_d$
Solar radiation	46,098.3	47,203.1	1,104.8	1.06%	$1.2*R_d$	$0.8*W_d$

Table 6.4 CO_2 emissions of PV/WT/BDG system - single-factor sensitivity analysis

Variable	Output - CO_2 emissions (CDE)				Corresponding input variable	
	Low (kg/kWh)	High (kg/kWh)	Swing (kg/kWh)	Variance	Low output	High output
Wind velocity	-16,208.2	41,656.0	57,864.2	71.00%	$1.2*V_d$	$0.8*V_d$
Other load	3,254.9	33,613.5	30,358.7	19.54%	$0.8*W_d$	$1.2*W_d$
Cooling load	9,177.9	29,229.0	20,051.1	8.53%	$0.8*Q_d$	$1.2*Q_d$
Solar radiation	15,117.5	21,750.9	6,633.4	0.93%	$1.2*R_d$	$0.8*W_d$

Table 6.5 Grid interaction index of PV/WT/BDG system - single-factor sensitivity analysis

Variable	Output - Grid interaction index(GII)				Corresponding input variable	
	Low	High	Swing	Variance	Low output	High output
Wind velocity	0.492	1.024	0.532	93.13%	$0.8*V_d$	$1.2*V_d$
Other load	0.630	0.753	0.123	4.97%	$1.2*W_d$	$0.8*W_d$
Cooling load	0.665	0.741	0.076	1.90%	$1.2*Q_d$	$0.8*Q_d$
Solar radiation	0.678	0.682	0.004	0.00%	$0.8*R_d$	$1.2*W_d$

Table 6.6 Combined objective of PV/WT/BDG system - single-factor sensitivity analysis

Variable	Output – Combined objective (f)				Corresponding input variable	
	Low	High	Swing	Variance	Low output	High output
Wind velocity	0.889	0.947	0.058	17.8%	$1.2*V_d$	$0.8*V_d$
Other load	0.873	0.964	0.092	44.4%	$0.8*W_d$	$1.2*W_d$
Cooling load	0.883	0.964	0.081	34.2%	$0.8*Q_d$	$1.2*Q_d$
Solar radiation	0.902	0.928	0.026	3.6%	$1.2*R_d$	$0.8*W_d$

A more complete view on the relationships between each input variable and the performance is provided in Figure 6.4. It shows how a model output is affected by the percentage of change in each of the input variables. The *x*-axis is the change range of input variables represented as the percentage of their corresponding baseline values, while *y*-axis is the associated model output. The center of the plot is the output obtained when all the input variables are set at their baseline values.

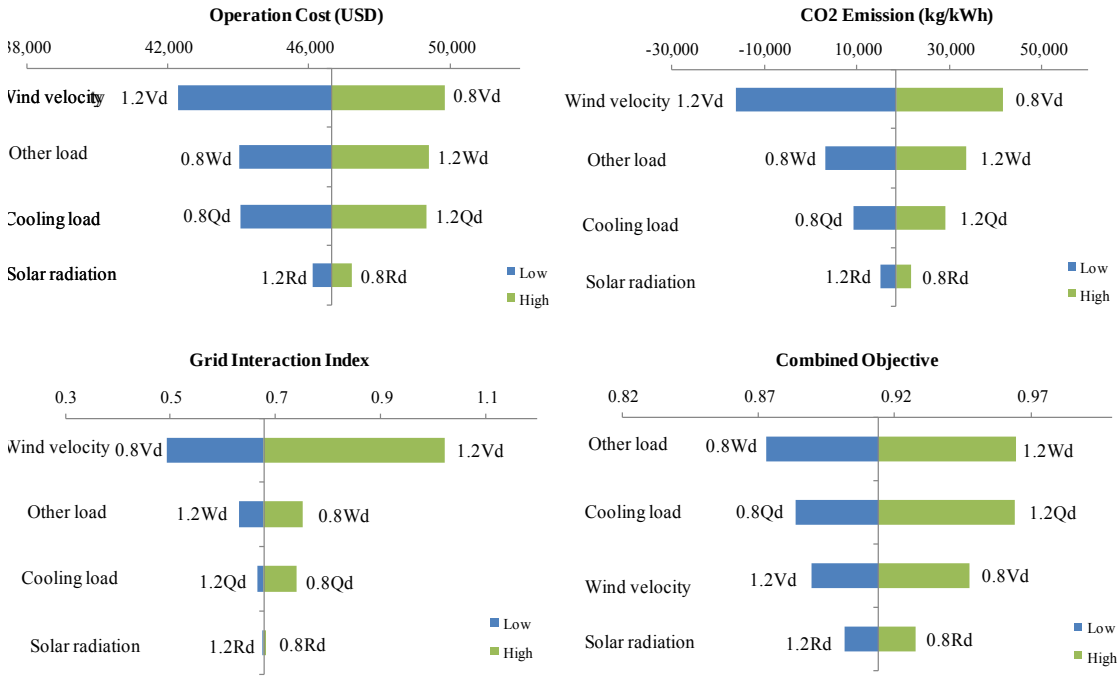

Figure 6.3 Single-factor tornado diagrams for outputs sorted by variance

Near-linear relationships can be observed for the operation cost *vs* the input variables except the wind velocity. The CO_2 emissions are linear with the solar radiation and the other load only. However, the grid interaction index is nonlinear with all the input variables except the solar radiation. The combined objective is near-linear with solar radiation, nonlinear with wind velocity, other load and cooling load. The results also reveal that the increase of wind velocity has strong positive effect on both operation

cost saving and CO_2 emissions reduction. While both the increases of other load and cooling load have negative effects on the two outputs. However, the increase of wind velocity has a significant and negative effect on the grid interaction index. Thus, the effect of wind velocity on the combined objective is alleviated because the directions of its effects on the three outputs are different. In addition, a notable positive effect on the combined objective is obtained by reducing the other load or building cooling load.

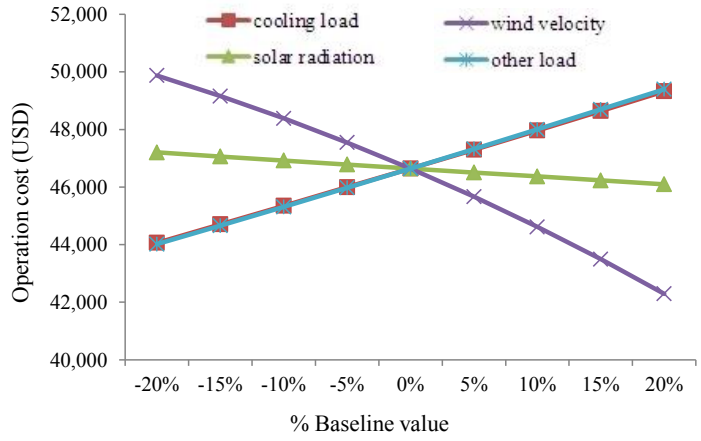

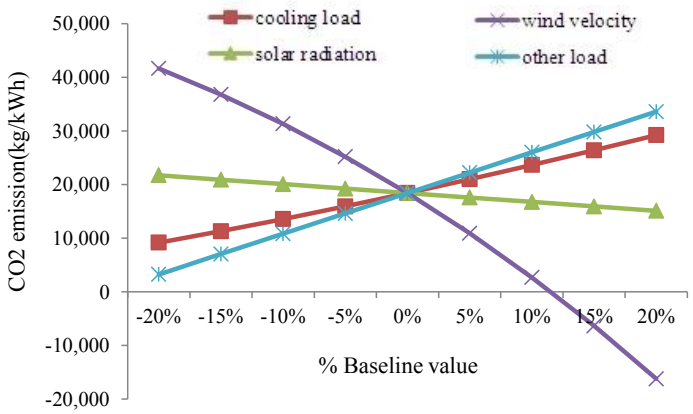

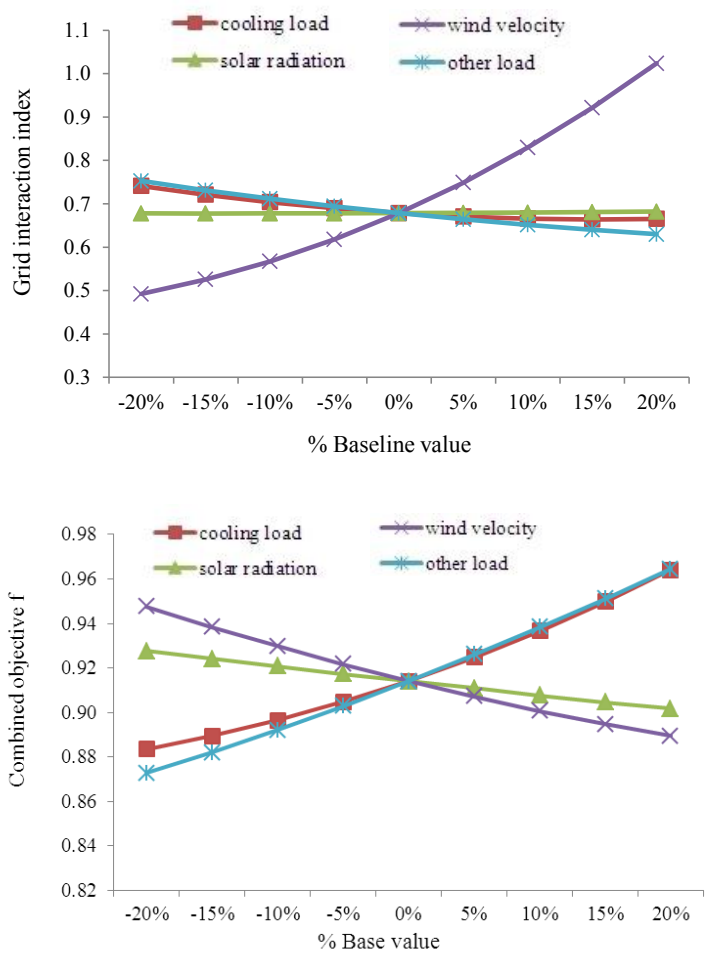

Figure 6.4 Outputs (performances) vs design input variables (operation variables)

6.4.2 Two-way Sensitivity Analysis of PV/WT/BDG System

The effects of simultaneous changes in any two input variables on the outputs are also studied by two-way (or two-factor) sensitivity analysis. Since there are four input variables, six pairs (i.e., 4 × (4-1)/2) should be evaluated to investigate the impact of each possible combination. The outputs are calculated for each pair when the variables of the pair are changed to their low/high extreme values simultaneously and other input variables are kept at their baseline values.

Table 6.7 Operation cost of PV/WT/BDG system – two- way sensitivity analysis

Variable	**Output - Operation cost**				**Corresponding input variable**	
	Low (USD)	High (USD)	Swing (USD)	Variance	Low output	High output
Wind velocity& Other load	39,842.7	52,792.9	12,950.3	27.83%	$1.2*V_d$, $0.8*W_d$	$0.8*V_d$, $1.2*W_d$
Cooling load & Wind velocity	39,796.7	52,648.4	12,851.7	27.40%	$0.8*Q_d$, $1.2*V_d$	$1.2*Q_d$, $0.8*V_d$
Cooling load & Other load	41,574.6	52,158.2	10,583.6	18.59%	$0.8*Q_d$, $0.8*W_d$	$1.2*Q_d$, $1.2*W_d$
Solar radiation & Wind velocity	41,781.0	50,469.3	8,688.3	12.52%	$1.2*R_d$, $1.2*W_d$	$0.8*R_d$, $0.8*W_d$
Solar radiation & Other load	43,517.0	49,990.7	6,473.7	6.95%	$1.2*R_d$, $0.8*W_d$	$0.8*R_d$, $1.2*W_d$
Cooling load & Solar radiation	43,567.0	49,924.0	6,357.1	6.71%	$0.8*Q_d$, $1.2*R_d$	$1.2*Q_d$, $0.8*R_d$

Table 6.8 CO_2 emissions of PV/WT/BDG system – two- way sensitivity analysis

Variable	**Output - CO_2 emissions**				**Corresponding input variable**	
	Low (kg/kWh)	High (kg/kWh)	Swing (kg/kWh)	Variance	Low output	High output
Wind velocity & Other load	-31,387.5	56,835.4	88,222.9	34.39%	$1.2*V_d$,$0.8*W_d$	$0.8*V_d$,$1.2*W_d$
Cooling load& Wind velocity	-25,464.5	52,450.8	77,915.3	26.82%	$0.8*Q_d$,$1.2*V_d$	$1.2*Q_d$,$0.8*V_d$
Solar radiation & Wind velocity	-19,524.9	44,972.7	64,497.6	18.38%	$1.2*R_d$,$1.2*V_d$	$0.8*R_d$,$0.8*V_d$
Cooling load & Other load	-6,001.5	44,408.3	50,409.8	11.23%	$1.2*R_d$,$0.8*W_d$	$0.8*R_d$,$1.2*W_d$
Solar radiation & Other load	-61.8	36,930.2	36,992.1	6.05%	$1.2*R_d$,$0.8*W_d$	$0.8*R_d$,$1.2*W_d$
Cooling load & Solar radiation	5,861.2	32,545.7	26,684.5	3.15%	$0.8*Q_d$,$1.2*R_d$	$1.2*Q_d$,$0.8*R_d$

Table 6.9 Grid interaction index of PV/WT/BDG system – two-way sensitivity analysis

Variable	**Output - Grid interaction index**				**Corresponding input variable**	
	Low	High	Swing	Variance	Low output	High output
Wind velocity& Other load	0.476	1.156	0.680	38.84%	0.8*Vd,0.8*Wd	1.2*Vd,1.2*Wd
Cooling load & Wind velocity	0.513	1.123	0.610	31.25%	0.8*Qd,0.8*Vd	1.2*Qd,1.2*Vd
Solar radiation & Wind velocity	0.494	1.028	0.534	23.96%	1.2*Rd, 0.8*Vd	0.8*Rd, 1.2*Vd
Cooling load & Other load	0.630	0.848	0.218	4.00%	0.8*Qd, 0.8*Wd	1.2*Qd, 1.2*Wd
Solar radiation & Other load	0.633	0.762	0.129	1.39%	1.2*Rd, 0.8*Wd	0.8*Rd, 1.2*Wd
Cooling load & Solar radiation	0.670	0.751	0.081	0.55%	0.8*Qd,1.2*Rd	1.2*Qd,0.8*Rd

Table 6.10 00Combined objective of PV/WT/BDG system – two-way sensitivity analysis

Variable	**Output – Combined objective**				**Corresponding input variable**	
	Low	High	Swing	Variance	Low output	High output
Wind velocity& Other load	0.867	1.009	0.142	20.43%	1.2*Vd,0.8*Wd	0.8*Vd, 1.2*Wd
Cooling load& Wind velocity	0.870	1.008	0.138	19.26%	0.8*Qd,1.2*Vd	1.2*Qd,0.8*Vd
Solar radiation& Wind velocity	0.877	0.962	0.085	7.23%	1.2*Rd, 1.2*Vd	0.8*Rd, 0.8*Vd
Cooling load & Other load	0.853	1.019	0.166	27.82%	0.8*Qd, 0.8*Wd	1.2*Qd, 1.2*Wd
Solar radiation& Other load	0.862	0.979	0.117	13.86%	1.2*Rd, 0.8*Wd	0.8*Rd, 1.2*Wd
Cooling load & Solar radiation	0.873	0.980	0.106	11.39%	0.8*Qd,1.2*Rd	1.2*Qd,0.8*Rd

The results of two-way sensitivity analysis concerning each output are shown in Table 6.7-6.10, which list the low and high output values, the swing/variance values and the corresponding input variables. The maximum ranges of performance outputs under the variation of wind velocity & other load, are between 39,842.7 and 52,792.9 USD for the operation cost, between -31,387.5 and 56,825.4 kg/kWh for CO_2 emissions, and between 0.476 and 1.156 for the grid interaction index, respectively. The variations of other two pairs, i.e. solar radiation & other load and cooling load & solar radiation, have less effects on the above outputs with the variances of less than 10%.

Regarding the combined objective, the most significant pair is cooling load & other load (variance = 27.82%) and the maximum range of the combined objective is between 0.853 and 1.019. Wind velocity & other load (variance = 20.43%), cooling load & wind velocity (variance = 19.26%) are also two important influential pairs.

Figure 6.5 shows the tornado charts of the two-factor sensitivity analysis, arranged downward according to the values of the variances. The sensitivity order for the operation cost is: wind velocity & other load > cooling load & wind velocity > cooling load & other load > solar radiation & wind velocity > solar radiation & other load > cooling load & solar radiation. The sensitivity orders for the other two outputs are the same (but slightly different from that for the operation cost). Regarding the combined objective, the sensitivity order is: cooling load & other load > wind velocity & other load > cooling load & wind velocity > solar radiation & other load > cooling load & solar radiation > solar radiation & wind velocity.

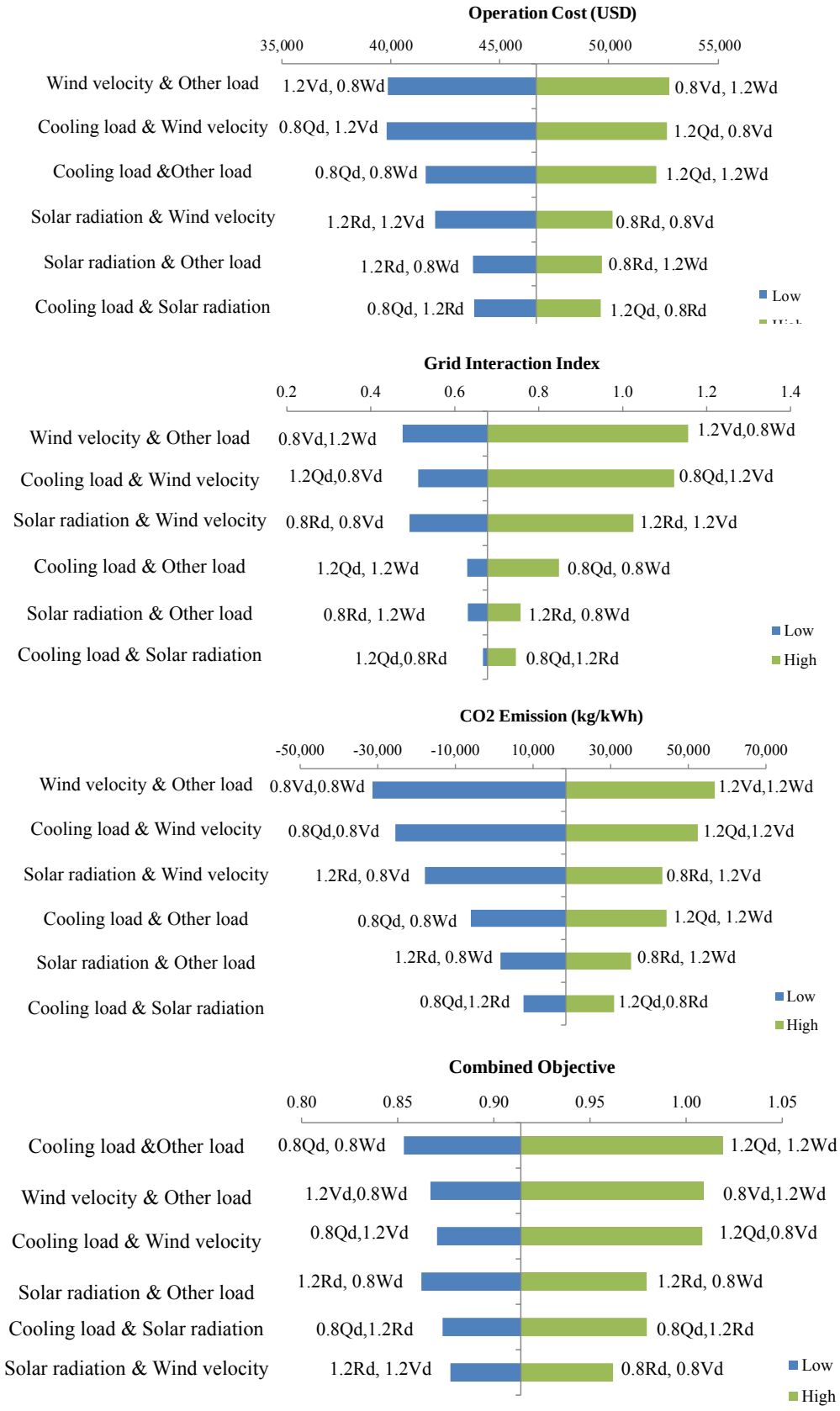

Figure 6.5 Two-way tornado diagrams for outputs sorted by variances

6.4.3 Multiway Sensitivity Analysis of PV/WT/BDG System

The multiway sensitivity analysis is conducted to assess the extreme cases when all of the input variables varied simultaneously to their 'best' and 'worst' values. Figure 6.6-6.9 show the multiway sensitivity analysis tornado charts for the outputs of the PV/WT/BDG system, arranged downward according to the values of the variances. The swing values of outputs corresponding to the single-factor and two-factor, which have the most significant impacts on the outputs, are also presented in the figure for comparison. With respect to the combined objective, the ranges of the output are between 0.85 and 1.09 when all of the input variables varied simultaneously, between 0.87 and 0.96 when two input variables varied simultaneously, and between 0.85 and 1.02 when only one input variable varied at a time.

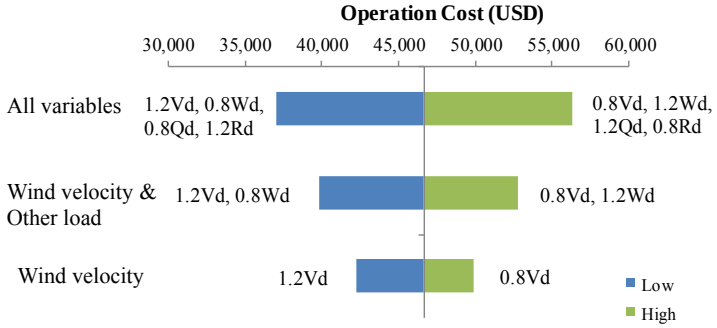

Figure 6.6 Comparison of operation cost for PV/WT/BDG system

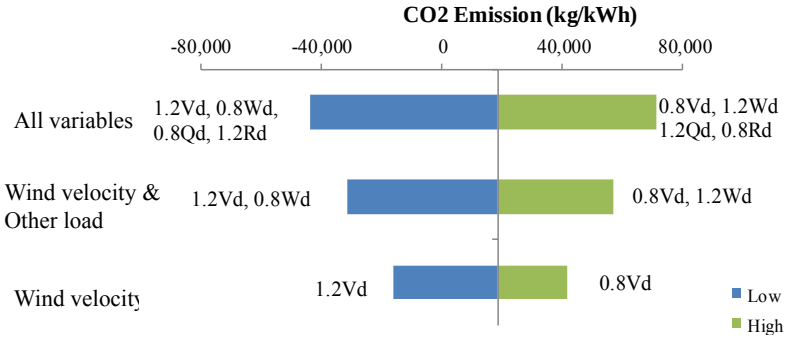

Figure 6.7 Comparison of CO2 emissions for PV/WT/BDG system

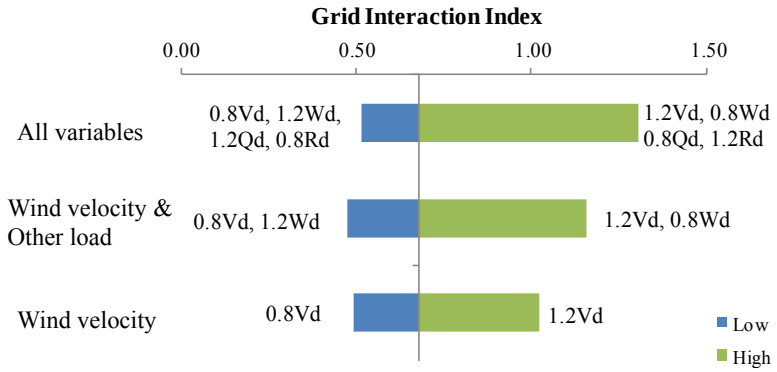

Figure 6.8 Comparison of GII for PV/WT/BDG system

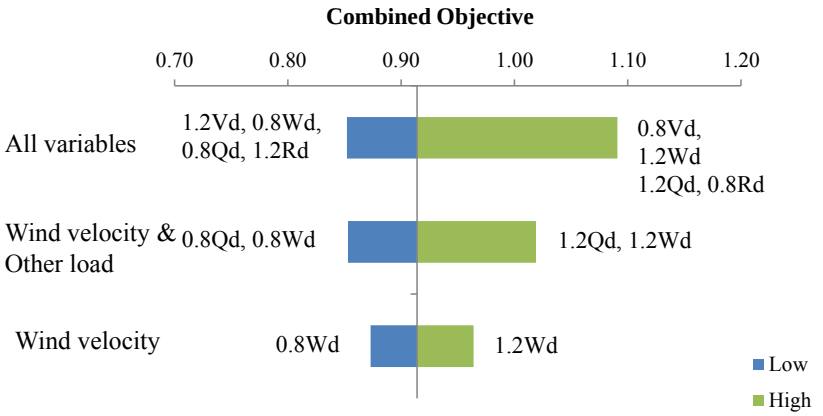

Figure 6.9 Comparison of combined objective for PV/WT/BDG system

6.5 Sensitivity Analysis of Different Design Options

Multiway sensitivity analysis for four design options is performed to investigate the performance robustness of the building with the four design options under extreme conditions. The results are presented in Table 6.11-6.12, which list the low/high output values (in the form of the percentages of their corresponding baseline values), swing and variance values.

Table 6.11 Comparison of operation cost/CO2 emissions of four design options

	Dimensionless operation cost				**Dimensionless CO_2 emissions**			
System	Low	High	Swing	Variance	Low	High	Swing	Variance
PV/WT	-226.3%	210.4%	436.7%	98.2%	"-∞"	"∞"	"∞"	-
PV/WT/BDG	-20.6%	20.7%	41.3%	0.9%	-338.5%	284.9%	623.3%	55.5%
WT/BDG	-17.4%	16.2%	33.6%	0.6%	-252.0%	214.3%	466.3%	31.1%
PV/BDG	-11.8%	12.1%	23.9%	0.3%	-147.3%	159.5%	306.8%	13.4%

Table 6.12 Comparison of grid interaction index/ combined objective of four design options

	Dimensionless grid interaction index				**Dimensionless combined objective**			
System	Low	High	Swing	Variance	Low	High	Swing	Variance
PV/WT	-21.61%	71.15%	92.76%	18.97%	-15.37%	30.2%	45.5%	63.9%
PV/WT/BDG	-24.14%	92.84%	116.98%	30.17%	-6.73%	19.3%	26.1%	21.0%
WT/BDG	-28.62%	85.22%	113.83%	28.57%	-5.38%	15.9%	21.2%	13.9%
PV/BDG	-34.65%	65.9%	100.5%	22.3%	-0.10%	6.1%	6.2%	1.2%

Figure 6.10 presents a comparison between performance robustness of four design options, represented by the swings of outputs to variation of input variables. Concerning the sensitivities of the performance index except the grid interaction index, the order is: PV/WT > PV/WT/BDG > WT/BDG > PV/BDG. For the PV/WT system, the swing range of the dimensionless operation cost could reach between -226.3% and 210.4% when all the input variables vary simultaneously and their impacts are at the

same directions, indicating that the building integrated with PV/WT system may have poor performance robustness (in terms of the operation cost) compared with the buildings adopting other three design options. Furthermore, the swing of the dimensionless CO_2 emissions is infinite for the PV/WT system. This is because CO_2 emissions of nZEBs are zero at baseline design values and even a small variation in the outputs will cause an infinite variation of the dimensionless CO_2 emissions.

The results indicate that the PV/WT system is the most sensitive system concerning the variations in the input variables while the performance of PV/BDG system is the most robustness in terms of the operation cost, CO_2 emissions and combined objective. It is observed that the performance of the renewable energy system integrated with active electricity generation systems, e.g. BDG, is less sensitive to the variations of input variables. It is most likely due to that active electricity generation systems can be controlled according to the changes of operation conditions, which may alleviate fluctuations in the outputs to some extent. Similar observation can be found also in the work of Zhou et al (2013). He pointed out that the negative impacts of energy load and generation uncertainties are reduced after introducing the energy storage and/or grid connection for a building. In this study, the BDG is operated following the thermal load and therefore the variation of cooling load could be undertaken by the BDG to some extent. When only passive renewable energy systems, especially the wind turbine, are used for building electricity generation, the building may have a high risk of poor performance robustness under the variations of operation conditions. However, it is not the case for the grid interaction index since its swings and variances do not change significantly under different design options.

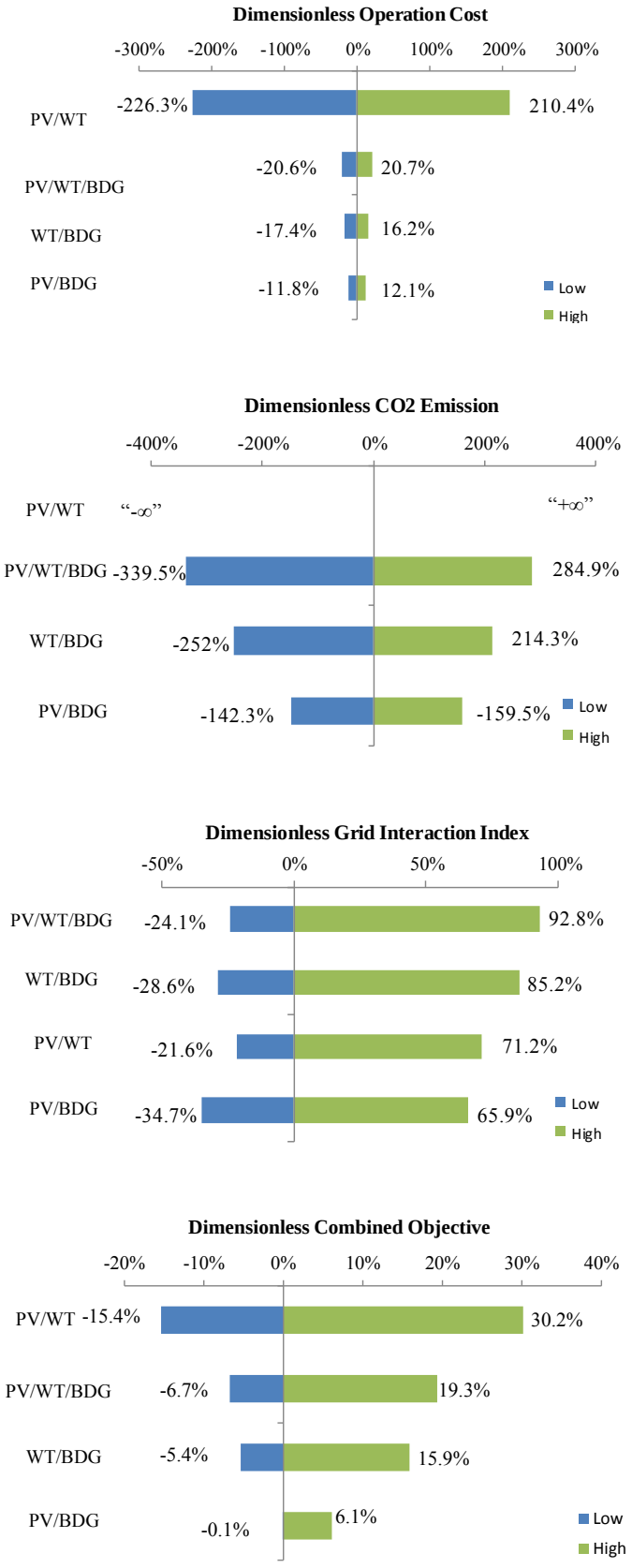

Figure 6.10 Comparison between performance robustness of four design options

6.6 Summary

In this chapter, four renewable energy system combinations for a grid-connected net zero energy building are studied. One-way sensitivity analysis, two-way sensitivity analysis and multiway sensitivity analysis are performed for the typical design options to identify the most significant factors that affect the building performance.

With the inputs variations of 20%, the maximum change of the comprehensive performance (i.e. combined objective) is 26.2%. The results of the one-way sensitivity analysis show that wind velocity is the key factor that significantly affects the three outputs (operation cost, CO_2 emissions and grid interaction index), with the variances of more than 50%. It is followed by the other load and building cooling load. The variances of the outputs caused by the variation of solar radiation are very small (less than 1%), showing that the effect of the variation in solar radiation is negligible. In contrast, the comprehensive performance is most sensitive to other load rather than wind velocity, followed by cooling load. This is because the increase of wind velocity results in reduced operation cost and CO_2 emissions, but a dramatically increased grid interaction index. Thus the effect of wind velocity variation on the comprehensive performance is not significant due to compensation effects. The results of two-way sensitivity analysis further indicate that cooling load & other load, wind velocity & other load, cooling load & wind velocity are the three major pairs which affect the comprehensive performance significantly. In summary, more attention should be paid on the accuracy of wind velocity prediction regarding the total cost/operation cost and/or CO_2 emissions. But the accuracy of building loads prediction should be the

priority to be concerned during the design stage concerning the robustness of the comprehensive performance.

The results of multiway sensitivity analysis on four design options indicate that the PV/BDG system may have a worse comprehensive performance under the design condition, but its performance in the real operation is most robustness. In addition, the introduction of active electricity generation systems in buildings could increase the performance robustness of the building energy systems.

Sensitivity analysis at the early stage of the design process could provide important information to identify the design/operation inputs/parameters on which designers should pay more attention in the later phases. Sensitivity analysis also provides designers additional but important information on the performance robustness of different design options for making design decisions.

CHAPTER 7 OPTIMAL SCHEDULING OF ENERGY SYSTEMS IN nZEBs USING NONLINEAR PROGRAMMING

Optimal scheduling of building energy systems is essential to achieve operation cost saving and to achieve grid-friendly buildings, particularly for nZEBs. However, the integration of renewable energy systems and energy storage systems in buildings results in more complex energy systems, which poses the complexity and great challenges for the optimal control of these integrated energy systems. In the buildings integrated with CCHP systems, “following the thermal load” (FTL) and “following the electric load” (FEL) are the two basic control strategies for CCHP systems in applications. However the mismatch problems of the thermal and electric loads are still difficult to be solved by both two strategies.

This chapter presents an optimal scheduling using nonlinear programming for the control of energy systems in nZEBs. The proposed scheduling strategy is tested and validated on the same reference building used in design optimization (presented in Chapter 5) after adding a thermal storage. Same energy system models presented in Chapter 4 are also used in this study. *Section 7.1* presents an overview on optimal scheduling methods for energy systems. In *Section 7.2*, the optimization problem is formulated to minimize the daily operation cost, taking into account the characteristics and interaction between energy systems as well as the constraints of practical

applications. The nonlinear programming algorithm, used in this study, was also introduced. *Section 7.3* presents two case studies, i.e. selling electricity to grid is allowed (Case 1) and selling electricity to grid is forbidden (Case 2), to evaluate the optimal scheduling strategy. A summary and limitations of the proposed scheduling strategy is provided in *Section 7.4*.

7.1 Introduction of Optimal Scheduling Methods for Energy Systems

It is acknowledged that the rule-based control method have been widely used in practical operation and control of building energy systems for many years. However, it often provides poor performance and does not offer optimal control for the energy systems. Model predictive control (MPC) method involves the information of dynamic modeling and occupancy prediction when it is used for the scheduling of building energy systems. It can lead to further energy savings. There are several advantages by using the MPC as the control methods. It takes into account disturbance predictions (e.g. weather, electricity price, occupancy profiles) when trying to regulate appropriately (Oldewurtel 2010). It can also shift and minimize the peak power loads within certain period to achieve the least operational cost according to the tariff selected (Ma et al 2012).

The main steps of predictive control are as follows. At the current time k, the optimal control variables are obtained on a fixed horizon for the next period, say [k, $k+N$]. Among the optimal controls on the fixed horizon [k, $k+N$], only the first one k+1 is adopted as the current control law. The procedure is then repeated at the next time, say [$k+1$, $k+1+N$]. This procedure is called 'receding horizon' since the horizon recedes

as time proceeds (Kwon and Han 2005). The scheduling strategy adopted in this study is considered as "intervalwise receding horizon control" since the horizon recedes intervalwise or periodically as time proceeds. This procedure is shown in Figure 7.1. At the beginning of a day, say at 00:00 am on day 1, the optimal strategy is activated and the schedules of the energy systems are obtained on a finite fixed horizon of 24 hours. The schedule trajectories of control variables obtained are adopted as the next 24 hours (Day 2) control law. The procedure is then repeated at beginning of the next day (Day 3).

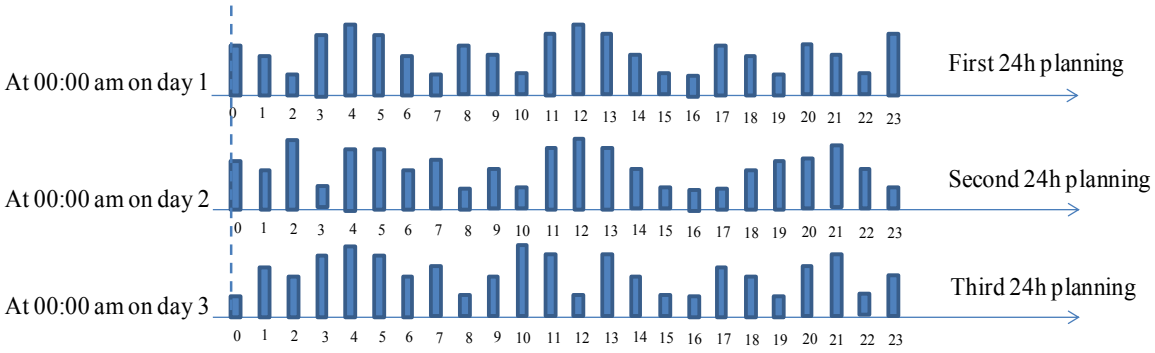

Figure 7.1 Illustration of one day-ahead (24 hours) scheduling

This study intends to address the optimal scheduling of the energy systems (both active and passive energy systems) in buildings connected to a grid under the time-sensitive electricity pricing. A MPC-based strategy is developed using NLP algorithm to optimize the power generation/use and the TES charge/discharge for the nZEB.

7.2 MPC-based Optimal Scheduling Strategy using Nonlinear Programming

7.2.1 Description of Energy Systems

The same building and energy system, the reference building used in design optimization (described in Chapter 5), revised on the basis of Hong Kong Zero Carbon Building (ZCB) are used for the validation of the scheduling strategy proposed. In additional to the revision made for constructing the above reference building, one more assumption is made on the energy system, i.e. the fire pool with a volume of 125 m^3 is assumed as the stratified chilled water storage tank in this building.

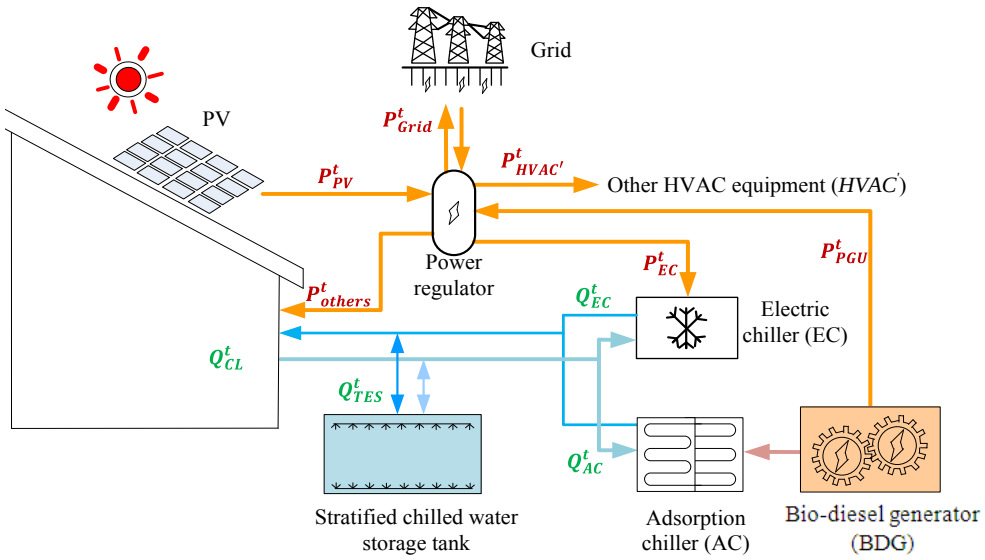

Figure 7.2 Energy flows among the energy systems in the building studied

Figure 7.2 illustrates the energy flows among energy systems in the studied building. The building electricity demand, including electricity consumed by the electric chillers, HVAC and other devices (lighting, computers, etc.), is supplied by the on-site generation systems, i.e. PV and combined cooling and power unit. The grid power can

be considered as an electricity storage, which provides electricity when on-site generation is not sufficient and receives electricity when surplus electricity is generated on site. The building cooling demand is satisfied mainly by the electric and absorption chillers. Thermal energy storage system stores cooling when surplus cooling is provided by chillers and discharges cold when the electricity price is high. The specifications and parameters of the energy systems are listed in Table 7.1.

Table 7.1 Specifications of the energy systems in the building studied

Symbol	Equipment	Amount	Specification
TES	Chilled water storage tank	1	Volume = 125 m^3
BDG	Bio-diesel generator	1	Rated power=100 kW, Rated efficiency=0.33
AC	Absorption chiller	1	Rated capacity=130 kW, COP_N=0.8
EC	Electric chiller	3	Rated capacity=70 kW, Nominal COP_N=4.2
PV	Photovoltaic system	1	Area=1015 m^2

Figure 7.3 and 7.4 show the solar radiation/outdoor air temperature and electricity generations/ consumptions in a typical day in August, which is retrieved from the BMS installed in the ZCB. The outdoor temperature varied from 27 to 35℃ and peak solar radiation was about 900 W/m^2 in that day. Corresponding to the weather conditions, the BDG was running at rated capacity with electricity generation of 100 kW and the daily peak generation by PV was approximately 90 kW. The electricity consumptions

of HVAC system and other devices (lighting, computers, etc.) were about 60 kW and 30 kW respectively during office hours.

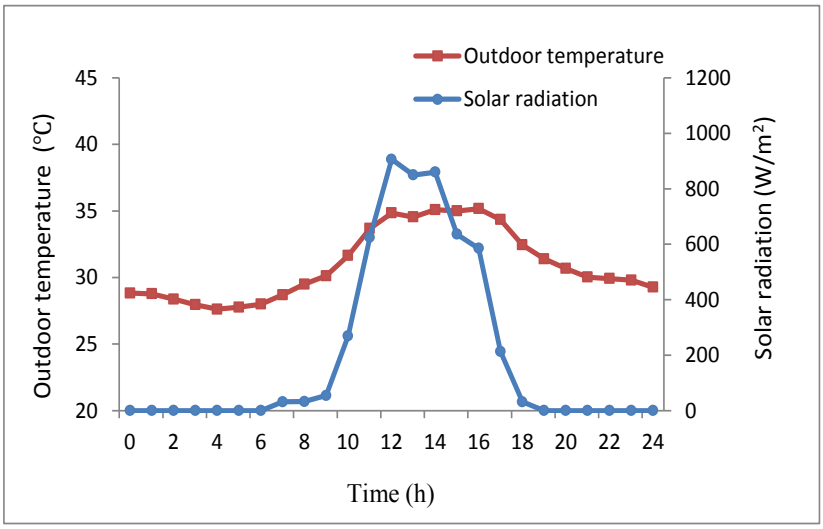

Figure 7.3 Ambient conditions in a typical day in August

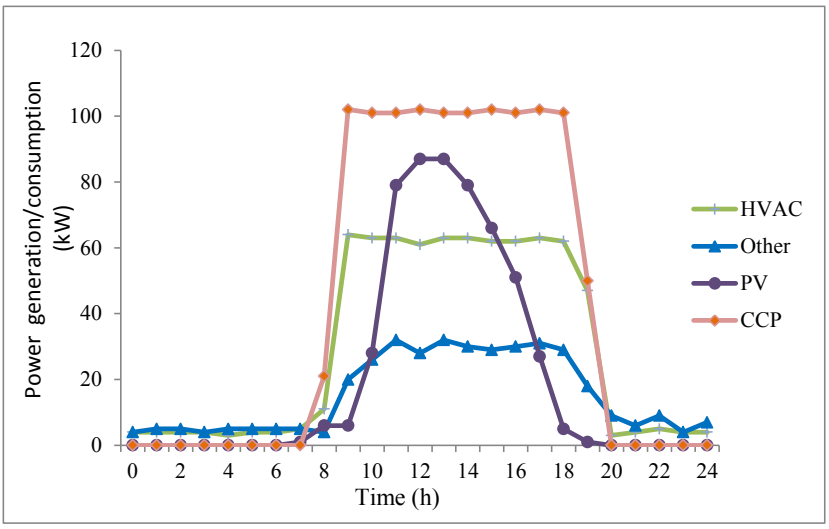

Figure 7.4 Power generation/consumptions in a typical day in August

7.2.2 Description of the Optimization Problem and Approach

Figure 7.5 illustrates the general approach for scheduling the building energy systems based on forecasted weather (e.g. outside air temperature, solar radiation) and

electricity price given by the grid. The optimization objective is to serve the building electric load and cooling load in the control trajectories with least electricity cost. The values of day-ahead building cooling load (Q^t_{cl}), electricity consumption of the building (P^t_{others}+$P^t_{HVAC'}$) and PV power generation (P^t_{PV}) in the interval of one hour are the input variables for the proposed scheduling strategy. The strategy minimizes daily operation cost comprising of the electricity bills from grid (c^t_{elec}×P^t_{grid}), the gas consumed by BDG (C^t_{gas} ×V^t_{gas}). The gas usage by the BDG (V^t_{gas}) and the cooling provided by the electric chillers (Q^t_{EC}) are the two input control variables. The prediction horizon considered in this study is 24 hours. Therefore, there are 48 values (2×24) of the two input control variables. Finally, 96 values (4×24) of four control variables (cooling charged/discharged by TES (Q^t_{TES}), the gas usage by BDG (V^t_{gas}), the cooling provided by electric chillers (Q^t_{EC}), and electricity received/delivered from/to the grid (P^t_{grid})) in the next 24 hours are determined by the strategy. In this study, the electricity price is proposed based on the day-ahead pricing in New York in 2013, as no such pricing is used in Hong Kong. The ratio of the average electricity price in New York to average electricity price in Hong Kong is used to form the day-ahead electricity price for Hong Kong used in this study (The New York Independent System Operator). It is assumed that the selling electricity price is the same as the buying price.

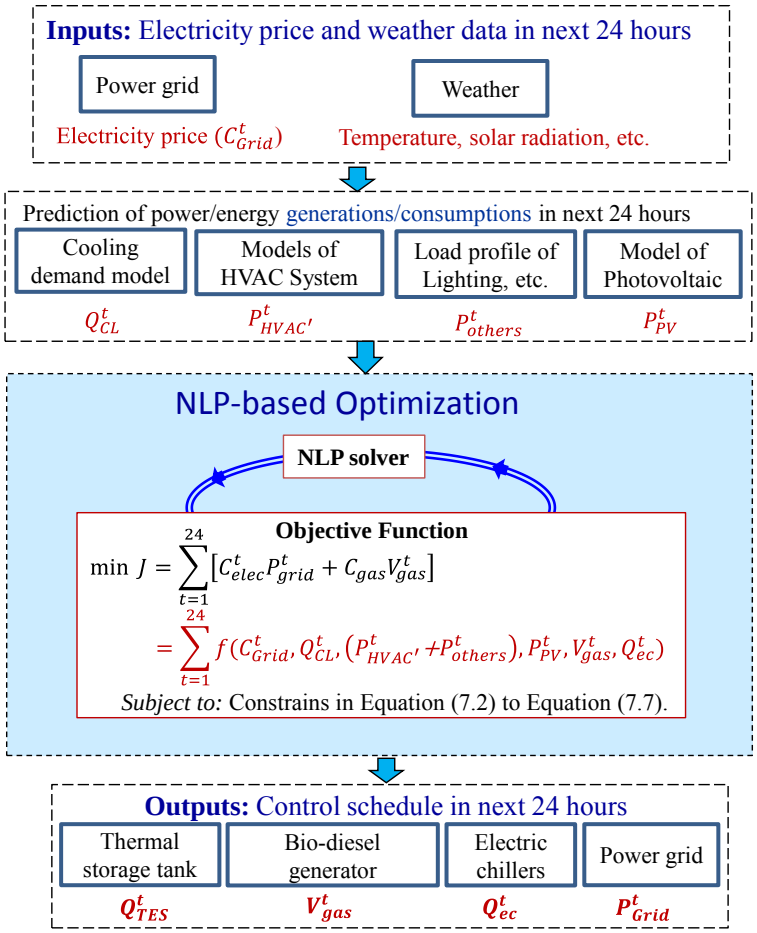

Figure 7.5 Optimal scheduling based on predicted loads/generations of building energy systems and electricity price

7.2.3 Nonlinear Programming (NLP) Algorithm and Its Implementation

Nonlinear programming is a kind of mathematical programming as a branch of optimization theory. NLP problems are widespread in engineering, economics, physical sciences and mathematics, etc. The general NLP problem can be stated simply as follows (Bazaraa et al. 2006):

$$\text{Minimize} \quad f(x)$$

$$\text{Subject to} \quad g_i(x) \leq 0 \quad \text{for } i=1,\ldots,m_1$$

$$h_j(x) = 0 \text{ for } j=1,\ldots,m_2$$

$$x \in X \subseteq R^n$$

where, f, g_i and h_j are functions defined on R^n. X is a subset of R^n. $x = [x_1,x_2,\ldots,x_n]^T$ is a vector of n decision variables. f is the objective function. The set X generally defines the lower and upper bounds for each variables. Each of the constraints $g_i(x) \leq 0$ is called an inequality function. Each of the contraints $h_j(x) = 0$ is called an equality function. Solving above problem is to find the values of x that minmize the objective function f and the meanwhile statisfy the restrictions of constraints. It becomes a NLP problem if any of the constraints or the objective function is nonlinear. Otherwise, it is a linear programming problem.

There are many methods for solving the NLP problems, e.g., gradient projection method (Rosen 1960), reduced gradient method (Wolf 1963) and penalty function method (Bazaraa 2006). Many software tools are also available, such as Matlab optimization toolbox (Matlab Optimization Toolbox), Lingo (LINDO Systems) and Bonmin (Bonmin–COIN-OR Project). In this chapter, the Matlab optimization toolbox is introduced to solve such a NLP problem.

7.2.4 Objective Function and Constraints

The operation energy cost includes the electricity cost of the power from the grid and the cost of gas. The strategy provides the day-ahead optimal scheduling of the energy systems. A few assumptions are made as follows when developing the strategy.

- Equipment capacity selection is not considered and equipment capacities are given.

- The electricity price from the grid varies as a time-based profile, which is given 24 hours in advance.
- The weather forecast can provide 24 hour data of solar radiation, ambient temperature and relative humidity, etc.

Objective function

The simplified physical models described in the Chapter 4 are used to predict the energy system operation performance responding to the four input variables. The objective function used in the optimization is shown as the Equation (7.1).

$$\min J = \sum_{t=1}^{n}\left[C_{ele}^{t}P_{grid}^{t} + C_{gas}V_{gas}^{t}\right] \quad (7.1)$$

Constraint and balance equations

i. Electricity balance:

$$P_{grid}^{t} = P_{ec}^{t} + P_{HVAC'}^{t} + P_{others}^{t} - P_{PV}^{t} - P_{BDG}^{t} \quad (7.2)$$

ii. Cooling load balance:

$$Q_{cl}^{t} = Q_{ec}^{t} + Q_{ac}^{t} + Q_{TES}^{t} \quad (7.3)$$

iii. Power generator of the BDG unit:

$$0 \le V_{gas}^{t} \le V_{gas,max} \quad (7.4)$$

iv. Electric chiller:

$$0 \le Q_{ec}^{t} \le Q_{ec,max} \quad (7.5)$$

v. Absorption chiller:

$$0 \leq Q_{ac}^{t} \leq Q_{ac,max} \tag{7.6}$$

vi. Thermal storage tank:

$$0 \leq m_{TES}^{t} \leq m_{TES,max} \tag{7.7}$$

It is worth noting that the BDG, electric chillers and absorption chiller usually have their own minimum load ratio. The TES also should have the minimum water flow rate. Equation (7.2) - Equation (7.7) do not include those performance limits. In addition, the electric chiller cannot work when Q^{t}_{ec} is lower than a certain load ratio, e.g. 30% of $Q_{ec,max}$. Equation (7.8) is therefore more physically meaningful compared with Equation (7.7)

$$0.3Q_{ec,max} \leq Q_{ec}^{t} \leq Q_{ec,max}, \text{ or } Q_{ec}^{t} = 0 \tag{7.8}$$

However, equations in the form of Equation (7.8) make the optimization problem to be a MINLP (mixed-integer nonlinear programming) problem which is more complex to be solved mathematically. But as MINLP is complex for real application, therefore it is simplified as a NLP problem in the first step of the optimal scheduling study. These components (BDG, electric chillers and absorption chiller) are actually set to have rather poor performance when part load ratios are lower than their lower limits, trying to avoid the systems operating at those unrealistic conditions in simulation trials.

7.3 Test and Evaluation of the Optimal Scheduling Strategy

7.3.1 Case 1: Selling Electricity to Grid Allowed

In the summer test day, the optimized schedule of the hourly electricity consumption/generation is shown in Figure 7.6. The BDG operated at full load when the grid electricity price was higher than the electricity cost of BDG (0.239 USD/kWh), i.e. between 12:00pm and 16:00pm. Meanwhile, the surplus electricity was sold to the grid. The TES was fully charged when the grid electricity price was low in the off-peak period (between 1:00am and 7:00am). Three electric chillers operated at full load when the grid electricity price was low (0.037 USD/kWh) between 4:00am and 6:00am. Where, a positive value of electricity in the figure stands for generating by itself or buying electricity from grid, and a negative value of electricity stands for consuming or selling electricity to grid.

The optimal scheduling of the hourly cold generation/consumption is shown in Figure 7.7. The absorption chiller served a large portion of the cooling load of the building when the BDG operated at full load between 12:00pm and 16:00pm while the TES served the rest portion of the cooling load. Between 11:00am and 12:00pm, the cooling load was partially served by the TES while TES had high priority as the grid electricity price was high. In the rest of the office hour (9:00am - 11:00am), the building cooling was served by the electric chillers. However, the electric chillers and absorption chiller was assigned to operate at very low loads occasionally (i.e. between 7:00am and 8:00pm and between 20:00pm and 24:00pm), while it is practically not possible for chillers to operate at such low load. This is the problem of using NLP as it cannot

handle the discrete ranges of variables. It is also worth noticing that the amount of chilled water in TES was initialized to $m_{TES,min}$ in all test cases.

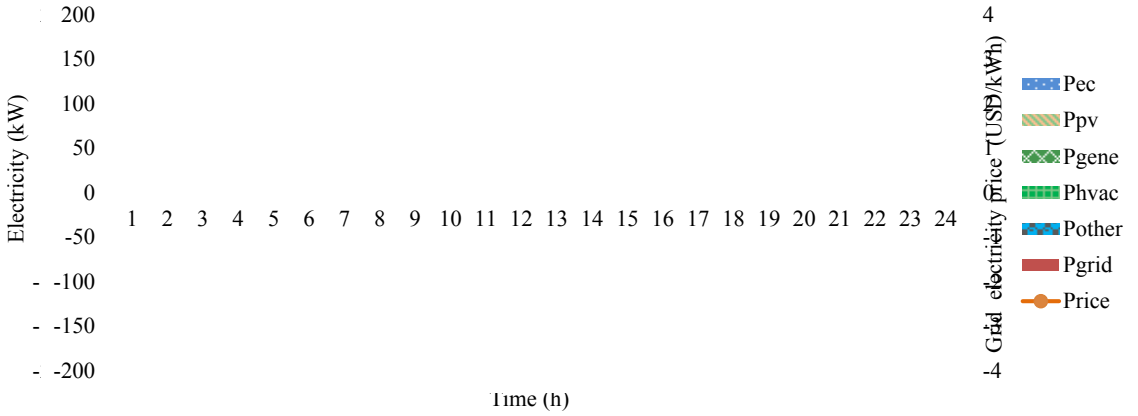

Figure 7.6 Schedule of the hourly electricity consumption/generation in summer test day - Selling electricity to grid allowed

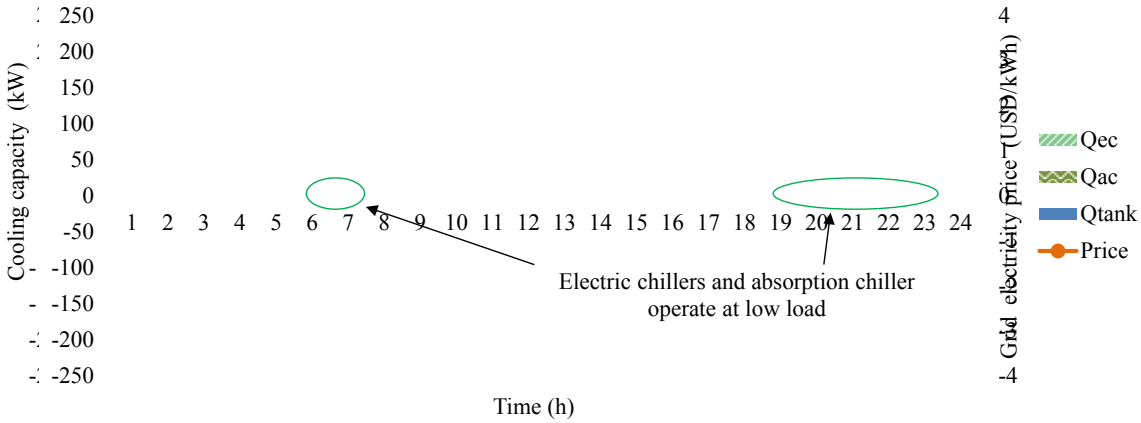

Figure 7.7 Schedule of the hourly cold consumption/generation in summer test day - Selling electricity to grid allowed

The CDE, PEC and the operation cost of the building in the summer test day are calculated in four different situations according the availabilities of PV, TES and BDG, as shown in Table 7.2. The first situation (A), which stands for the building with PV system, is used as the benchmark. The application of TES (B) resulted in the increase

of both CDE and PEC by 2% respectively and reduction of operation cost by 18%. There was no surplus electricity from PV system in the cases. Therefore, there was no actual interoperation between PV system and TES system. It is why the effects of adding TES to PV were the same as shown in Table 7.2 and Table 7.4, as well as Table 7.3 and Table 7.5. The use of BDG (C) resulted in significantly reductions of CDE (27%) and PEC (15%) since the exhaust gas was well utilized. Compared with the third situation using BDG (C), the use of both BDG and TES (D) resulted in slight higher CDE (2%) and PEC (1%), but the operation cost saving was significant (i.e. 29%).

Table 7.2 CDE, PEC and operation cost in summer test day-Selling electricity to grid allowed

Situation	CDE (kg)	CDE saving	PEC (kWh)	PEC saving	Cost (USD)	Cost saving
A: PV	643	-	3747	-	253	-
B: PV+TES	654	-2%	3812	-2%	208	18%
C: PV+BDG	468	27%	3167	15%	215	15%
D: PV+TES+BDG	479	25%	3232	14%	180	29%

In the cloudy spring test day, the optimized schedule of the hourly electricity consumption/generation is as shown in Figure 7.8. The grid electricity price has two peaks. The BDG operated at full load once the grid electricity price was higher than the electricity cost given by BDG (11:00am-14:00pm and 17:00pm-21:00pm). It is worth noting that the BDG still operated between 20:00pm and 21:00pm to sell electricity to grid since the electricity price was still high. The TES allowed BDG to

do so since it stored all of the cold from the absorption chiller. The BDG did not work between 14:00pm and 17:00pm although the electricity price was slightly higher than the cost of the BDG. During this period, it could not save operation cost if the BDG was in operation since the surplus cold would be stored in TES and would not be used till the end of this day.

The optimized schedule of the hourly cold generation/consumption is shown in Figure 7.9. The TES offers advantages in storing the surplus cold from the absorption chiller. Benefited from the use of TES, the BDG worked longer to reduce the operation cost and CO_2 emission. The electric chillers and absorption chiller also operated at very low load occasionally, i.e. between 5:00am and 8:00pm and between 20:00pm and 24:00pm, which is not practical as mentioned before.

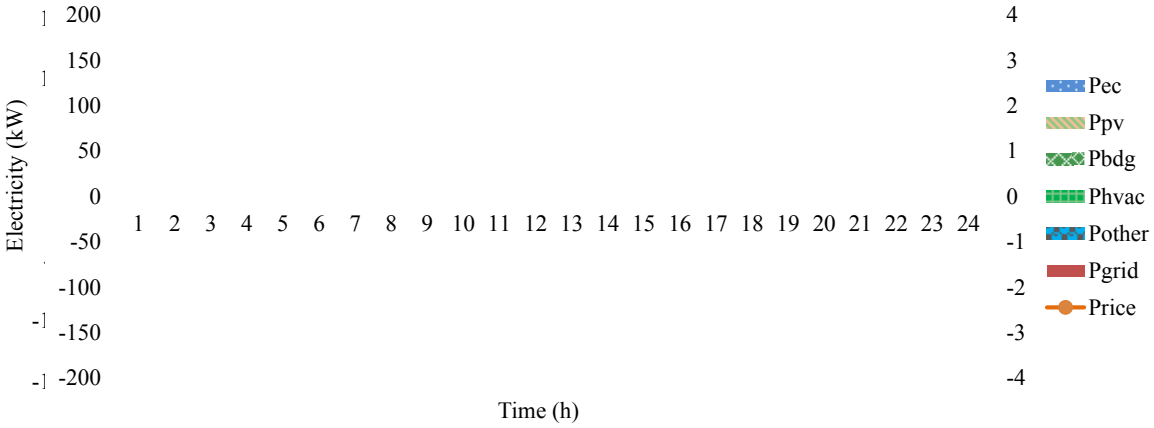

Figure 7.8 Schedule of the hourly electricity consumption/generation in cloudy spring test day - Selling electricity to grid allowed

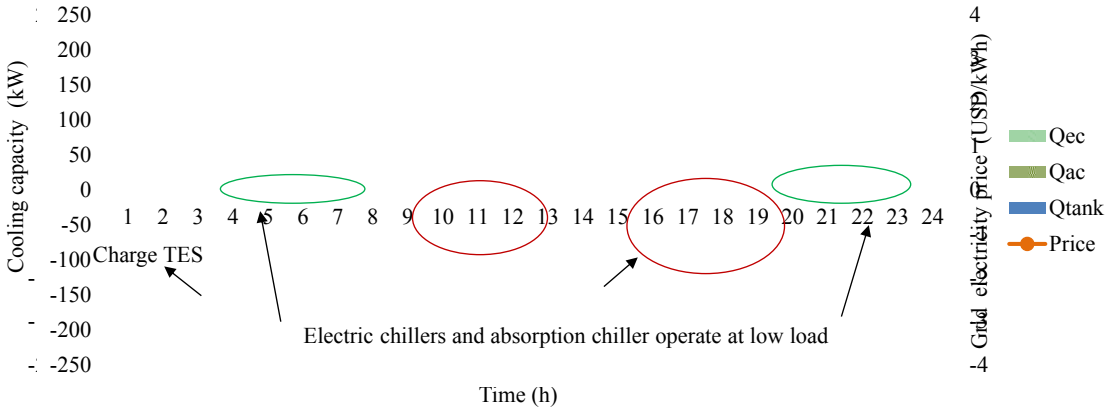

Figure 7.9 Schedule of the hourly cooling consumption/generation in cloudy spring day-Selling electricity to grid allowed

Table 7.3 CDE, PEC and operation cost in cloudy spring test day - Selling electricity to grid allowed

Situation	CDE (kg)	Saved CDE	PEC (kWh)	Saved PEC	Cost (USD)	Saved Cost
A: PV	494	-	2883	-	257	-
B: PV+TES	506	-2%	2948	-2%	227	12%
C: PV+BDG	293	41%	2216	23%	203	21%
D: PV+TES+BDG	255	48%	2243	22%	185	28%

The CDE, PEC and operation cost of the building in the cloudy spring test day in the four situations are presented in Table 7.3. The use of TES (B) resulted in the increase of CDE and PEC by 2% respectively, and the reduction of the operation cost by 18%. The use of BDG (C) resulted in significant saving of CDE (55%) and PEC (23%). Compared with the situation using BDG (C), the use of both BDG and TES (D) resulted in more saving of CDE (69%) and similar saving of PEC (23%). The operation cost saving was also significant (28%). It is worth noting that a portion of

cold in the TES can be used in the next day. The calculated performance should be better if the cold left in the TES is considered in the calculation of CDE, PEC and operation cost.

7.3.2 Case 2: Selling Electricity to Grid Forbidden

In the summer test day, the optimized schedule of the hourly electricity consumption/generation is shown in Figure 7.10. During the peak hours of the grid electricity price (12:00pm-17:00pm), the BDG worked at partial load providing a portion of electricity (the other portion was provided by the PV system).

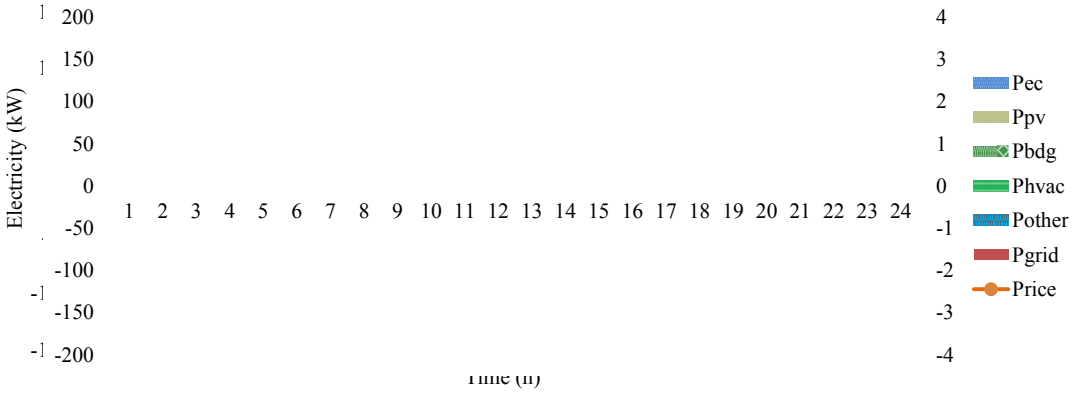

Figure 7.10 Schedule of the hourly electricity consumption/generation in summer test day - Selling electricity to grid forbidden

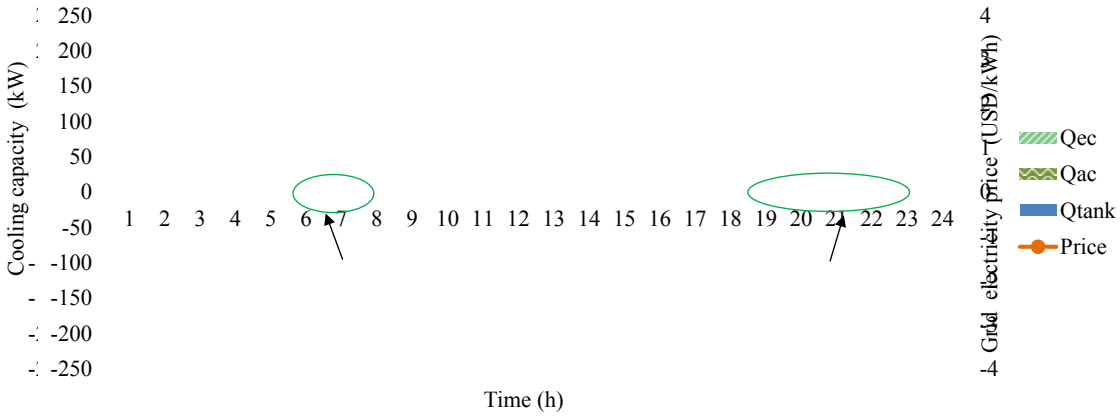

Figure 7.11 Schedule of the hourly cooling consumption/generation in summer test day - Selling electricity to grid forbidden

The optimized schedule of the hourly cold generation/consumption is shown in Figure 7.11. The absorption chiller and TES provided the cold during the peak hours. During the office hours, the electric chillers worked longer time compared with the Case I since more cold from TES was consumed during the peak hours.

The CDE, PEC and operation cost of the building in the summer test day in the four situations are shown in Table 7.4. The use of BDG (C) reduced CDE and PEC by 19% and 11% respectively. Compared with the situation using BDG (C), the use of both BDG and TES (D) reduced less CDE (12%) and PEC (6%). But the operation cost saving was more significant (i.e. 24%).

Table 7.4 CDE, PEC and operation cost in summer test day - Selling electricity to grid forbidden

Situation	CDE (kg)	Saved CDE	PEC (kWh)	Saved PEC	Cost (USD)	Saved Cost
A: PV	642	-	3747	-	253	-
B: PV+TES	654	-2%	3812	-2%	208	18%
C: PV+BDG	523	19%	3350	11%	227	10%
D: PV+TES+BDG	567	12%	3524	6%	194	24%

Table 7.5 CDE, PEC and operation cost in cloudy spring test day - Selling electricity to grid forbidden

Situation	CDE (kg)	Saved CDE	PEC (kWh)	Saved PEC	Cost (USD)	Saved Cost
A: PV	494	-	2883	-	257	-
B: PV+TES	506	-2%	2948	-2%	227	12%
C: PV+BDG	293	41%	2216	23%	204	21%
D: PV+TES+BDG	304	38%	2293	20%	197	23%

In the cloudy spring test day, the optimized schedule of the hourly electricity consumption/generation is shown in Figure 7.12. Compared with the Case I, the BDG did not work in the non-office hour (20:00pm-21:00pm) since it was forbidden to sell electricity to the grid. The optimized schedule of the hourly cold generation is shown in Figure 7.13. The surplus cold from the absorption chiller was stored in the TES. It offered benefit as the BDG could then work at full capacity during the peak hours. There was still cold left in the TES which could be used in the next day. The electric chillers and absorption chiller also operated at very low loads occasionally, between 5:00am and 8:00pm and between 20:00pm and 24:00pm. The CDE, PEC and operation cost of the building in the cloudy spring test day are shown in Table 7.5. Compared with the situation using BDG (C), the use of both BDG and TES (D) resulted in less CDE and PEC savings (-3% and -3% respectively). The cost saving was slightly higher (increased by 2%).

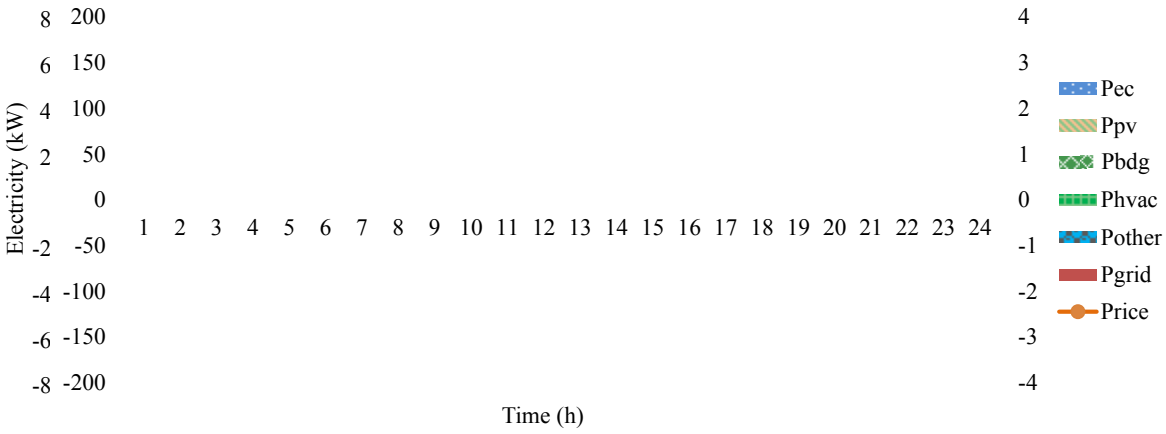

Figure 7.12 Schedule of the hourly electricity consumption/generation in cloudy spring test day - Selling electricity to grid forbidden

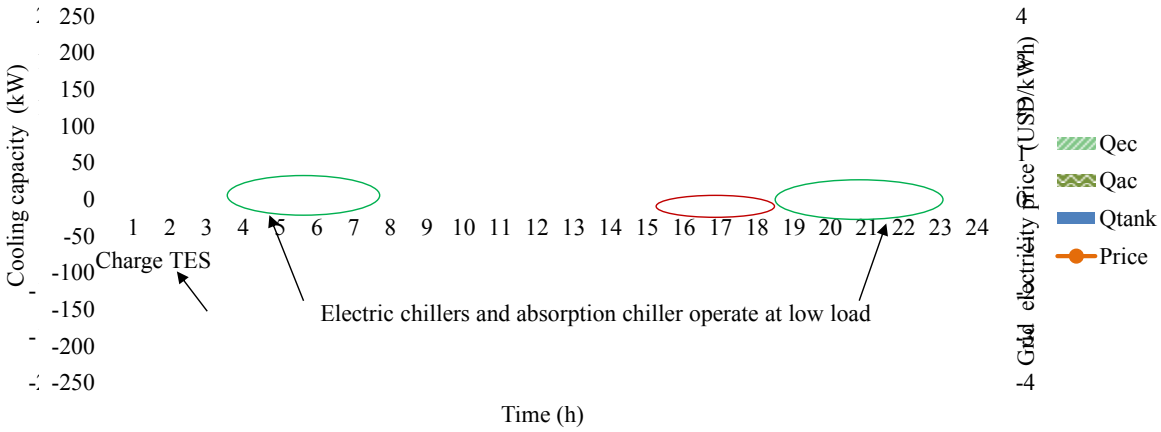

Figure 7.13 Schedule of the hourly cold consumption/generation in cloudy spring test day - Selling electricity to grid forbidden

In the case of using BDG (C) in the cloudy spring test day, the savings of CDE, PEC and cost were the same as shown in Table 7.3 and Table 7.5. It is because the cooling load in the spring day was small and the cold from absorption chiller (Q_{ac}) could satisfy the entire cooling load (Q_{cl}). The BDG worked in partial load to make Q_{ac} equal to Q_{cl}. Therefore, the schedules of hourly electricity consumption/generation were the same in both spring cases. In the case of using BDG (C) in the sunny summer test day, the reductions of CDE, PEC and cost were different as shown in Table 7.2 and Table 7.4. It is because the cooling load in the summer test day was high. The cold from absorption chiller (Q_{ac}) could not satisfy the entire cooling load (Q_{cl}). In Case I, the BDG worked in full load to sell the surplus electricity since selling electricity to grid was allowed. In Case II, the BDG could not work in full load since selling electricity to grid was forbidden. Therefore, the schedules of hourly electricity consumption/generation are different in two summer test cases. It is of interest to evaluate how the system works when the PV system provides excess electricity. The optimized schedule of the hourly electricity consumption/generation was therefore

evaluated in the sunny spring test day, as shown in Figure 7.14. The electric chiller worked to consume the surplus electricity. The surplus cold from the electric chiller was stored in the TES, as shown in Figure 7.15. The TES helped to avoid the waste of electricity. Such situation might also exist in Case I when the grid electricity price was low while the PV system generated surplus electricity.

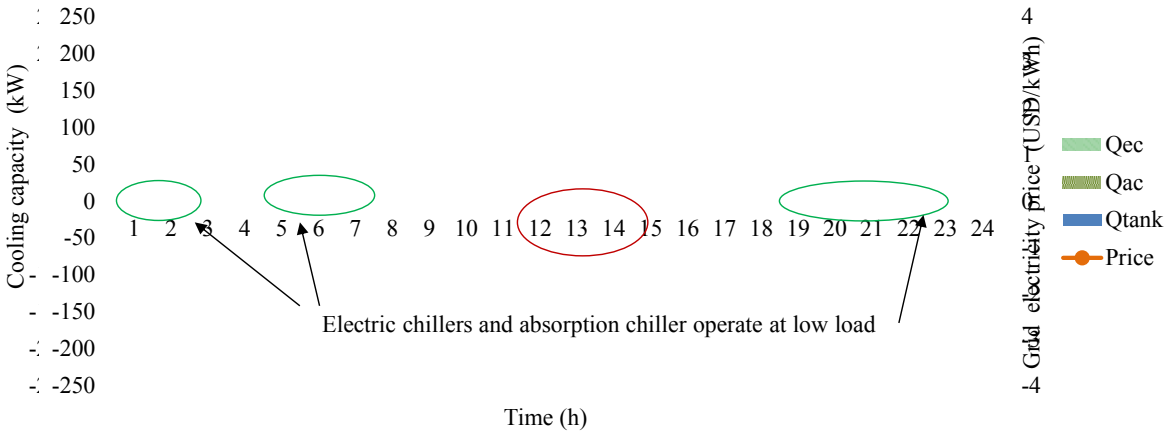

Figure 7.14 Schedule of the hourly electricity consumption/generation in sunny spring test day - Selling electricity to grid forbidden

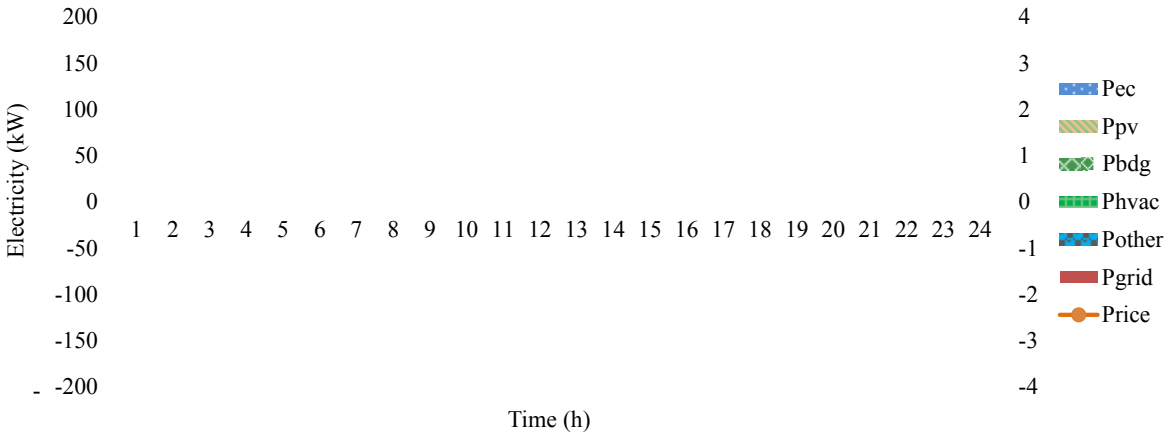

Figure 7.15 Schedule of the hourly cooling consumption/generation in sunny spring test day - Selling electricity to grid forbidden

7.3.3 Sensitivity Analysis

In the above study, the MPC-based method determines 96 values (4x24) of the four output variables on the basis of the 96 values (4x24) of the four input variables for the coming 24 hours. Uncertainties in the 96 input values would affect the output values. In the study presented here, Monte Carlo simulation method (Binder and Landau 2000) was used to assess the effects of uncertainties. The basic idea is to run simulations many times over with uncertainties in inputs in order to obtain the distributions of the unknown probabilistic results, i.e. CDE, PEC and cost. Such a simulation is repeated 1000 times. CDE, PEC and cost in all simulations are analyzed in a statistic way.

The simulations are on the basis of the following assumptions:

- The Q^t_{cl}, P^t_{PV}, P^t_{others}+P^t_{HVAC}, and c^t_{elec} used in Case I and Case II are assumed to be the true values in the coming 24 hours;
- The errors in the predicted values are assumed to be normal distributed. The predicted values are simulated by adding normal distributed noises to the true values.
- The predicted values are used as inputs instead of the true values.
- Two uncertainty levels are considered according to a survey of prediction models, i.e. 5% and 10%. 5% means the error is 5% of the mean of true values.
- Noises are added for the first three variables during the office hours (9:00am-19:00pm). Noises are added into c^t_{elec} during 0:00am-19:00pm.
- The electricity prices in the next day during 0:00am-5:00am are revised to be smaller than the values during 20:00pm-24:00pm in the day concerned. It is

because TES would be charged for the next day if c^t_{elec} is too small during 20:00pm-24:00pm.

The system is operated as follows: firstly, the energy usage is rescheduled once at the beginning of each hour for the coming 24 hours on the basis of the amount of chilled water left in TES and the new predictions for the coming 24 hours. It benefits to take the deviations caused by uncertainties in previous hours into consideration in the optimal schedule in the current hour. In the current hour, the system works according to the schedules which are generated under uncertainties. The actual operating condition presents the true values of Q^t_{cl}, P^t_{PV}, P^t_{others}+P^t_{HVAC}, and c^t_{elec}. For instance, the actual cooling load in hour t equals to the Q^t_{cl} in Case I or Case II. At the end of current hour, the amount of chilled water in TES is calculated which will be used as initial value for the MPC-based schedule and actual operation in the next hour.

Due to uncertainties, the system cannot work exactly as the schedules. Some revisions are made for the actual operation strategy. In the case when selling to grid is allowed, among the four output variables, two of them are the same as the schedules, i.e. gas consumption of the power generator (V^t_{gas}) and cold provided by electric chillers (Q^t_{EC}). Sometimes, V^t_{gas} and Q^t_{EC} are adjusted to the limit values if their values are larger than the maximum limits. The remaining two output variables, i.e. tank discharging/charging (Q^t_{TES}) and electricity import/export from/to the grid (P^t_{grid}), are calculated according to the cold balance and electricity balance. In the case when selling electricity to grid is forbidden, if P^t_{grid} is scheduled to be zero, V^t_{gas} is adjusted to maintain P^t_{grid} to be zero in actual operation unless V^t_{gas} achieves its maximum value. Tank discharging/charging (Q^t_{TES}) is calculated according to the cold balance.

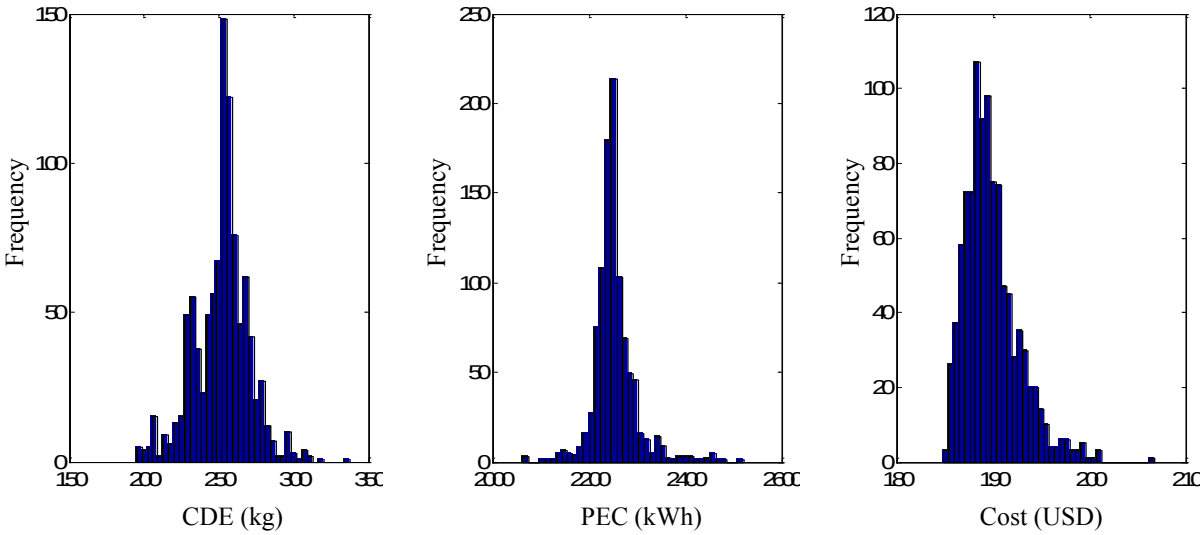

Figure 7.16 Histograms of CDE, PEC and cost of 1000 Monte Carlo simulations in the cloudy spring day with uncertainties (10%) in input variables -Selling electricity to grid allowed

Figure 7.16 illustrates the histograms of CDE, PEC and cost of 1000 Monte Carlo simulations in the cloudy spring day with uncertainties (10%) in input variables, in the case when selling electricity to grid is allowed. The CDE and PEC were almost normal distributed. The costs were not normally distributed. Almost all costs under uncertainties were higher than the corresponding ideal values. Table 7.6 shows the results of Monte Carlo simulations in the case when selling electricity to grid is allowed. It is found that CDE, PEC and cost varied in small ranges. It is mainly because TES and grid have reduced the negative effects of uncertainties. Uncertainties in the predicted Q^t_{cl} are adjusted by TES. Uncertainties in the predicted P^t_{PV} and predicted P^t_{others}+$P^t_{HVAC'}$ are eliminated by grid. Uncertainties in predicted c^t_{elec} and Q^t_{EC} affect CDE, PEC and cost significantly. For instance, if predicted c^t_{elec} is higher than electricity cost of BDG (0.239 USD/kWh) but the true c^t_{elec} is lower than that value, BDG will fully open which will lead to high cost and low CDE, PEC.

Table 7.7 shows the results of Monte Carlo simulations in the case when selling electricity to grid is forbidden. The CDE, PEC and cost, each with a small variation range, reflect little fluctuations when uncertainties are considered. Results demonstrate that uncertainties can be partially handled by the actual operation strategy. The actual operation strategy contributed to maintain CDE, PEC and cost at near optimal levels. TES enhances robustness of this system which makes the adjustments of BDG operation to be possible. It reduces the negative effects of uncertainties.

Table 7.6 Results of Monte Carlo simulations with uncertainties in input variables - Selling electricity to grid allowed

Day	Uncertainty level	Item	Min	Max	Mean	Ideal value
Spring test day	5%	CDE	231	270	253	255
		PEC	2218	2290	2243	2243
		cost	185	191	187	185
	10%	CDE	195	338	253	255
		PEC	2063	2521	2254	2243
		cost	185	207	190	185
Summer test day	5%	CDE	437	520	472	479
		PEC	3100	3377	3217	3232
		cost	180	187	181	180
	10%	CDE	375	570	467	479
		PEC	2894	3545	3200	3232
		cost	180	193	185	180

Table 7.7 Results of Monte Carlo simulations with uncertainties in input variables - Selling electricity to grid forbidden

Day	Uncertainty level	Item	Min	Max	Mean	Ideal value
Spring test day	5%	CDE	294	340	312	304
		PEC	2265	2416	2326	2293
		cost	197	203	199	197
	10%	CDE	283	370	324	304
		PEC	2221	2540	2371	2293
		cost	197	207	202	197
Summer test day	5%	CDE	487	590	545	567
		PEC	3246	3611	3458	3524
		cost	194	198	196	194
	10%	CDE	488	614	548	567
		PEC	3269	3689	3468	3524
		cost	194	202	198	194

It is concluded that uncertainties in the four input variables do not affect the performance of the proposed method significantly. Uncertainties can be reduced by the actual operation strategy, TES and grid.

7.4 Summary and Limitations

In this chapter, an optimal scheduling strategy using nonlinear programming is proposed for the control of energy systems in nZEBs. Evaluation tests are conducted in a reference building. Results show that the strategy can solve the power generation/demand mismatch problem of the nZEB by scheduling their operation in an optimal manner, and reduce the building operation cost significantly. When selling

electricity to the grid is allowed, reductions of 25% and 48% in carbon dioxide emissions (CDE), 14% and 22% in primary energy consumption (PEC), 29% and 28% in operation cost are achieved in the summer test day and the cloudy spring test day respectively, compared with situation without BDG and cold storage. When selling electricity to the grid is forbidden, reductions of 12% and 38% in CDE, 6% and 20% in PEC, 24% and 23% in operation cost are achieved in test days respectively in the same situation. Results also show that the benefit of using cold storage together with distributed energy systems in the nZEB. It helps to fully utilize the BDG system and reduces CDE, PEC and operation cost by storing the surplus cold from the absorption chiller. Sensitivity analysis shows uncertainties in the inputs do not affect the performance of the proposed method significantly. The effects of uncertainties in inputs can be reduced by the actual operation strategy, TES and grid.

It is also worth noticing that NLP algorithm can consider the nonlinear input-output characteristics of energy systems (i.e. electric chillers and absorption chiller), but it ignores the discrete working ranges of the energy systems. Therefore, the scheduled cooling loads for electric chiller and absorption chiller are very low occasionally, which is not practically applicable in the actual operation as the chillers cannot work at such low loads. It is essential to schedule the cooling appropriately for electric/absorption chillers by using an improved algorithm which is proposed in the further study presented in Chapter 8.

CHAPTER 8 ENHANCED OPTIMAL SCHEDULING OF ENERGY SYSTEMS IN nZEBs USING MIXED-INTEGER NONLINEAR PROGRAMMING

In Chapter 7, an optimal scheduling using nonlinear programming for the control of energy systems in nZEBs was proposed to improve the performance of energy systems operation. Considerable reductions of in carbon dioxide emissions (CDE), primary energy consumption (PEC) and operation cost are obtained. However, limitations of using NLP are also revealed from the results.

This chapter therefore presents an enhanced optimal scheduling using mixed-integer nonlinear programming for the control of energy systems in nZEBs. *Section 8.1* presents the characteristics of the NLP and its weakness, which answers why mixed-integer nonlinear programming is used in this study. In *Section 8.2*, the general form of an MINLP is provided, in which a cost penalty concerning the plant start/stop is added into the objective function to improve the lifetime of the devices. The sub-systems are subject to the constraints of operating above their minimum load ratios. In order to evaluate the proposed strategy, the performance of energy systems scheduled by the MINLP-based optimization approach is compared with that using a rule-based strategy and the NLP strategy respectively in *Section 8.3*. The summary is given in *Section 8.4*.

8.1 Why Mixed-integer Nonlinear Programming?

In chapter 7, a model predictive control method using NLP algorithm is proposed to optimize the scheduling of building energy systems. However, the scheduled cooling loads for electric chiller and absorption chiller are very low occasionally, which is not practically applicable in actual operations as the chillers will be switched off for protecting themselves at such low loads.

The energy systems often have strong non-linear characteristics and have discrete working ranges, the outputs of BDG unit, electric chillers and TES should not be over their design capacities and should not be less than their minimum load ratios. If the very low loads are removed from the searching ranges, it becomes optimization problem involving discrete working ranges. NLP algorithm can consider the nonlinear input-output characteristics and the upper limits of loads. But, it cannot handle the discrete working ranges of energy systems. Furthermore, the on/off frequencies of active energy devices (i.e. BDG and chillers) have a negative effect on the lifetime of the devices, but it is not considered properly in the existing studies on the scheduling problems.

An improved optimal scheduling strategy is therefore presented, which is based on MINLP considering both the nonlinear input-output characteristics and the discrete working ranges of the active energy systems, for building energy systems to minimize the daily operation cost. A cost penalty is introduced to consider the on/off number of the active energy systems and therefore reduce their on/off switching frequencies.

8.2 MPC-based Optimal Scheduling using Mixed-Integer Nonlinear Programming Algorithm

8.2.1 MINLP Algorithm and Its Implementation

Many optimization problems in engineering, scientific and industry applications are related to discrete decisions and nonlinear system characteristics that have great influence on the quality of the decisions. Mixed-integer nonlinear programming (MINLP) is one of the most general optimization methods, which includes both mixed-integer linear programming (MILP) and nonlinear programming (NLP). The general form of an MINLP can be conveniently expressed as Equation (8.1) (Mixed-Integer Nonlinear Optimization 2012):

$$\text{Minimize } f(x, y) \tag{8.1}$$

$$\text{Subject to: } g(x, y) \leq 0,\ x \in X,\ y \in Y$$

$$(Y \text{ is an integer})$$

where, the function f: $R^{n+s} \rightarrow R$ and g: $R^{n+s} \rightarrow R^m$ are possibly nonlinear objective function and constraint function respectively. The variables *x* and *y* are the decision variables and *y* is required to be an integer. The sets $X \subseteq R^n$ and $Y \subseteq R^s$ are bounding-box-type restrictions on the variables.

The integer variable y is called 0-1 or binary integer variables that can be used to model yes/no decisions, such as whether to operate a plant. However, integer variables make an optimization problem non-convex and far more difficult to solve. In this study,

the nonlinear problems with integer constraints are solved by the branch and bound method that runs the Generalized Reduced Gradient (GRG). The MultiStart check box on the GRG Nonlinear tab is used to start from several different sets of initial values. This can increase the chance that a possible near 'optimal solution' is found.

8.2.2 Objective Function and Constraints

The optimal scheduling problems of MINLP-based strategy here is to minimize the operation energy cost in the coming 24 hours, as shown in Equation (8.2a), subject to all the operation technical constraints (i.e., Equation (8.3)-(8.7)). The optimal scheduling problem is formulated as a mixed-integer nonlinear programming (MINLP) problem and solved using Generalized Reduced Gradient (GRG) algorithm.

The objective function is shown in Equation (8.2a). By correlating the predicted values and two input variables, it can be reformed as Equation (8.2b).

$$\min J = \sum_{t=1}^{n} \left[C_{ele}^{t} P_{grid}^{t} + C_{oil} V_{oil}^{t} \right] \tag{8.2a}$$

$$\min J = \sum_{t=1}^{24} f\left(C_{Grid}^{t}, Q_{cl}^{t}, \left(P_{HVAC'}^{t} + P_{others}^{t}\right), P_{PV}^{t}, V_{oil}^{t}, Q_{ec}^{t}\right) \tag{8.2b}$$

To consider the sequence control of chillers and BDG, which is more realistic and feasible from an operation point of view, a cost penalty ($C_{seq}N_{seq}$) is added into the objective function. In order to minimize the value of the objective, the number of start/stop of chillers and BDG would be reduced since a cost is added on the number. The value of C_{seq} is determined by trial calculation based on experience. The overall operation cost, including operation energy cost and cost penalty concerning the plant start/stop, is shown in Equation (8.2c).

$$\min J' = \sum_{t=1}^{n}\left[C_{elec}^{t}P_{grid}^{t} + C_{oil}V_{oil}^{t} + C_{seq}N_{seq}^{t}\right] \quad (8.2c)$$

The operation of the sub-system is subject to the constraints as listed in Equation (8.3)-(8.7). The outputs of the sub-systems (BDG unit, electric chillers and TES) should not be over their design capacities and should not be less than their minimum load ratios (i.e. Equation (8.3)-(8.5)). The electricity consumed by the sub-systems (electric chillers, other HVAC systems, other devices) during control interval is equal to the power provided by the PV, BDG and grid, as shown by Equation (8.6). The cooling consumed during each control interval is equal to that provided by the electric chillers, absorption chiller (driven by the BDG) and the thermal energy storage, as shown in Equation (8.7).

Operation range of BDG unit:

$$0.3 \times F_{oil,max} \leq F_{oil}^{t} \leq F_{oil,max},\ or F_{oil}^{t} = 0 \quad (8.3)$$

Operation range of electric chillers:

$$0.3 \times Q_{ec,max} \leq Q_{ec}^{t} \leq Q_{ec,max}, or\ Q_{ec}^{t} = 0 \quad (8.4)$$

Operation range of thermal energy storage:

$$0 \leq m_{TES}^{t} \leq m_{TES,max} \quad (8.5)$$

Electricity balance of building energy system:

$$P_{PV}^{t} + P_{CCP}^{t} + P_{grid}^{t} = P_{EC}^{t} + P_{HVAC}^{t} + P_{others}^{t} \quad (8.6)$$

Cold energy balance of building:

$$Q_{cl}^{t} = Q_{ec}^{t} + Q_{ac}^{t} + Q_{TES}^{t} \quad (8.7)$$

8.3 Test and Evaluation of the Enhanced Optimal Strategy

Energy systems used for the tests of the enhanced strategy are the same systems described in Chapter 7. It is therefore not discussed in this chapter again. Detail information of the building model, energy system models as well as renewable energy system models can be found in Chapters 3, 4 and 7.

8.3.1 Comparison between Enhanced Optimal Control Strategy with Rule-based Control Strategy

Table 8.1 lists the combinations of the systems and strategies in the four scenarios studied. The performances of the energy systems using the enhanced optimal scheduling control strategy (Scenario S1, S3) are evaluated and compared with that using the rule-based control strategy (Scenario S0, S2). Under Scenario S1 and S3, the enhanced optimal control strategy is used, which provides a long-term operation planning for 24 hours in advance. Under scenario S0, the BDG is controlled according to the building cooling load. The absorption chiller is driven by the BDG and its cooling ability depends on the operation of BDG. When the building cooling demand excesses the maximum capacity of the absorption chiller, the extra cooling load is provided by the electric chillers. This control strategy is also named as “following thermal load” control strategy which is independent from the electricity price. Under scenario S2, the chillers are operated in early morning, when the electricity price is low, to charge the storage tank in order to meet the buildings demand in the office

hour that day. Electric chillers will operate when the absorption chiller cannot satisfy the cooling demand.

Table 8.1 System and control strategy of four scenarios studied

Scenarios	System	Strategy
S0	PV+BDG	Rule-based
S1	PV+BDG	MINLP
S2	PV+BDG +Tank	Rule-based
S3	PV+BDG +Tank	MINLP

In order to validate the enhanced optimal scheduling strategy in realistic working condition, the real cooling load of Hong Kong ZCB recorded by the BMS on-site was also used in the validation tests. The schedules of hourly cooling generations determined by the strategies under different scenarios are shown in Figure 8.1. Under scenario S0 (Figure 8.1a), the absorption chiller served a large portion of the building cooling load and only a small portion was served by the electric chillers (i.e. at 9:00am, 16:00am -18:00am). Under scenario S1 controlled by the MINLP-based strategy (Figure 8.1b), the electric chillers undertook a large portion of cooling load when the grid electricity price was not very high (8:00am-11:00am and 16:00pm-18:00pm). The absorption chiller served the cooling load only at the peak period (12:00am-16:00pm).

Under scenario S2 (Figure 8.1c), using the rule-based control strategy, the TES was fully charged by the electric chillers in the off-peak period (1:00am-7:00am) and it was completely discharged first to provide cooling before switching on the absorption/electric chillers. When the capacity of absorption chiller was not sufficient,

the electric chillers will be switched on as the supplementary (16:00pm-18:00pm). Under scenario S3 (Figure 8.1d), using MINLP-based control strategy, the electric chillers operated continuously, providing a small portion of cooling (8:00am-10:00am) after the TES was fully charged. The absorption chiller provided the cooling when the electricity price was high (12:00am-17:00pm), and the TES was discharged to provide the cooling at the rest of the time. Note, there was a very small amount of TES discharge in the figures when TES was not used, which was actually the cold loss.

The schedules of the hourly electricity consumptions/generations determined by the control strategies under different scenarios in the same test day are shown in Figure 8.2. Under scenario S0 (Figure 8.2a), the BDG operated to provide electricity in the entire office hours between 8:00am and 18:00pm. Surplus electricity generated by the BDG was sent to the grid during this period and a large amount of surplus electricity (433.5 kWh, see Table 8.2) was sent to the grid in that day. Under scenario S1 using the optimal strategy (Figure 8.2b), the BDG operated to provide electricity (and heat for the absorption chiller) only when the grid electricity price was high (12:00pm-15:00pm) and electric chillers therefore consumed much more electricity in the test day. Surplus electricity generated by the BDG was sent to the grid only in this short period and a large amount of electricity (121.5 kWh) was taken from the grid in that day.

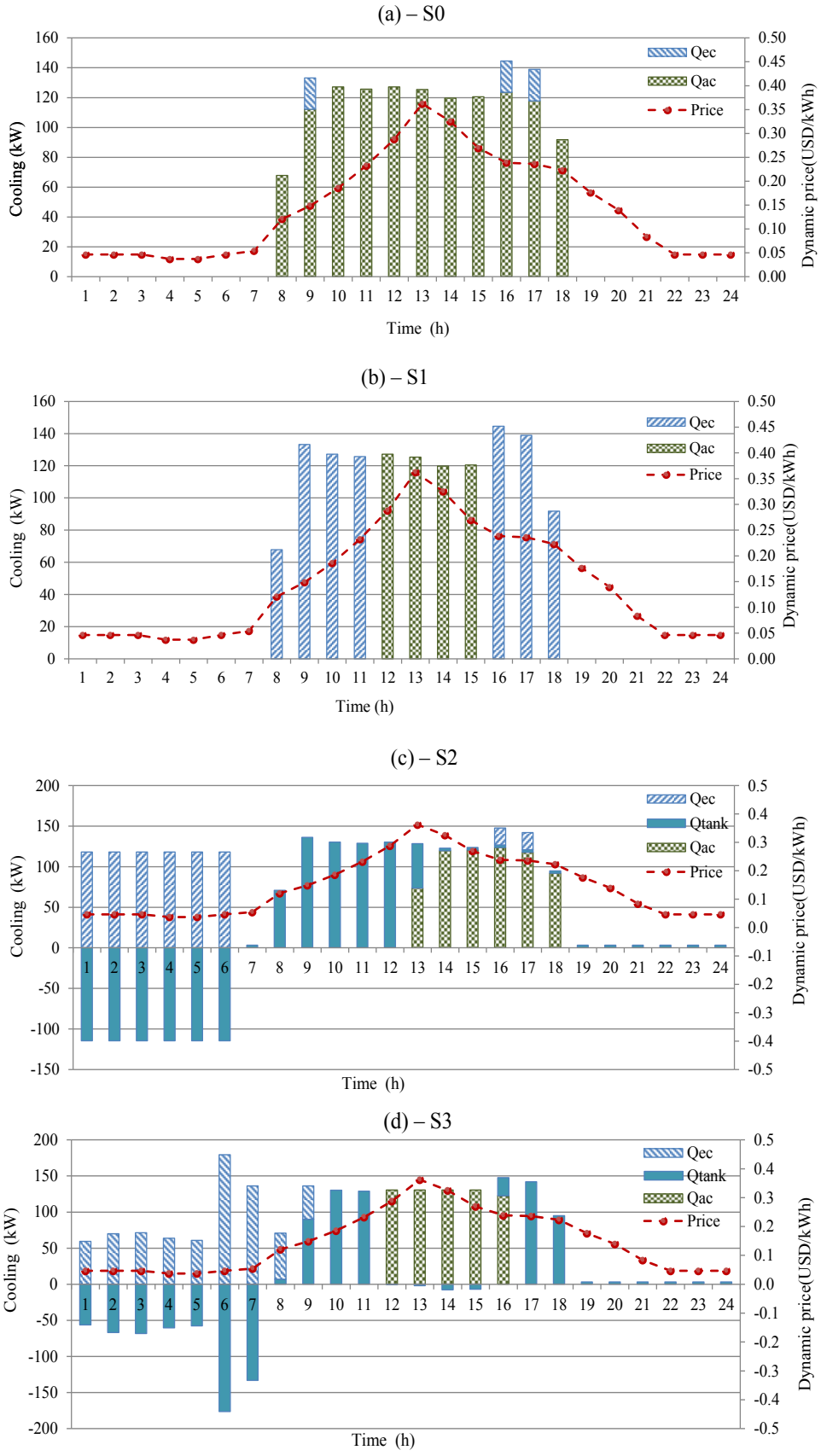

Figure 8.1 Schedule of hourly cooling generations in a day under different scenarios

Under scenario S2 (Figure 8.2c), the electric chillers consumed about 40kWh electricity per hour to charge the TES during off-peak period (1:00am-7:00am). The BDG kept running to provide electricity for six hours (13:00pm-19:00pm) after the cold stored in the TES was completely discharged. Under scenario S3 (Figure 8.2d), using the enhanced optimal control strategy, electricity consumed (and cold generated) by the electric chillers not scheduled as constant (1:00am-9:00am). The BDG was scheduled to operate at its rated power for five hours (12:00pm-17:00pm) when the electricity price was high.

The schedule of the TES charge/discharge in a day and in a week is shown in Figure 8.3. The TES was charged at the beginning of the day under both scenario S2 and scenario S3 when electricity price was low. Under scenario S2, the TES discharged to provide cooling until the cooling stored in the TES reached its minimum level based on rule-based strategy, while, under scenario S3, the TES discharged to provide cooling during non-peak periods (i.e. 8:00am-11:00am, 16:00pm-18:00pm).

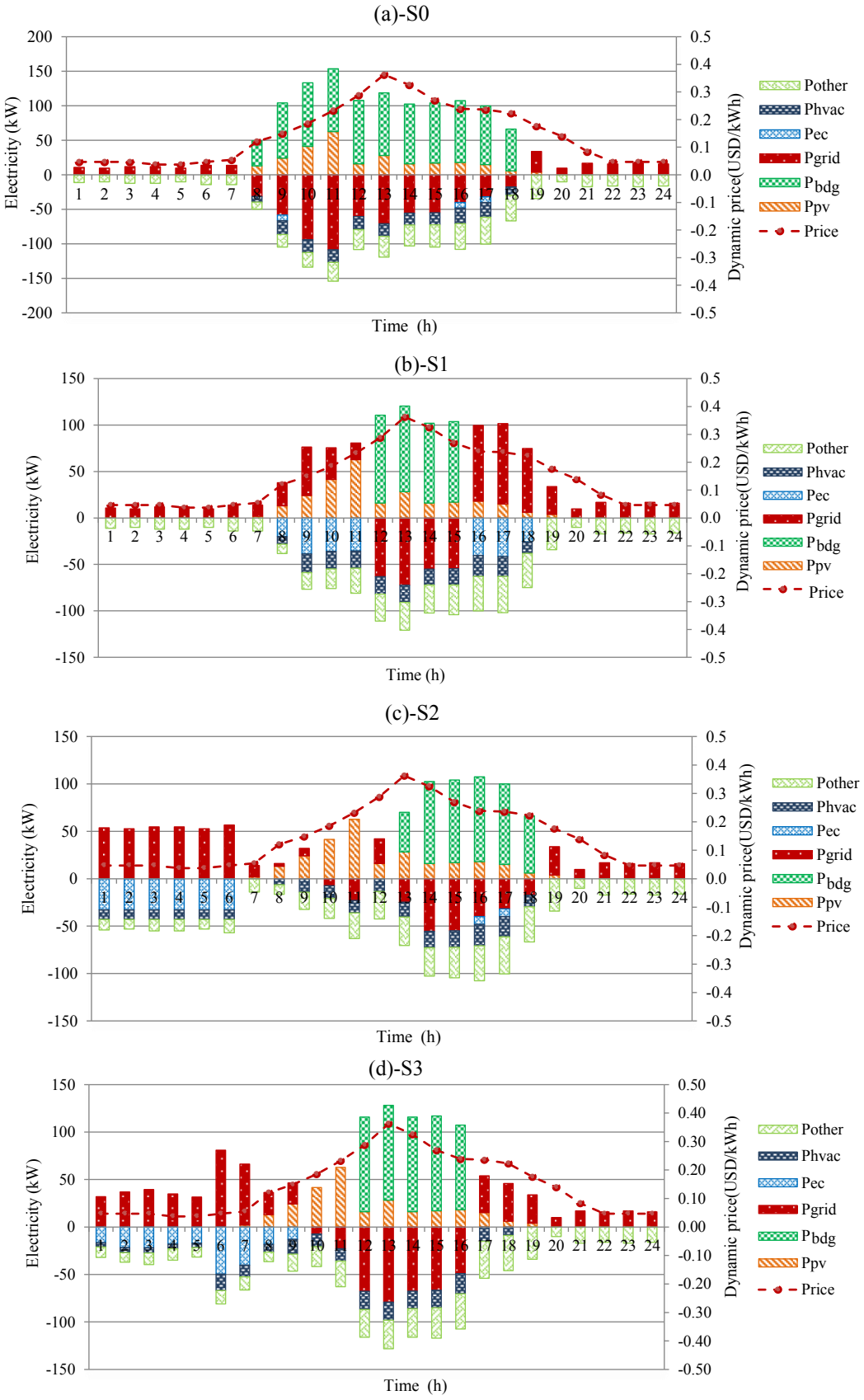

Figure 8.2 Schedule of the hourly electricity generation/consumption in a day

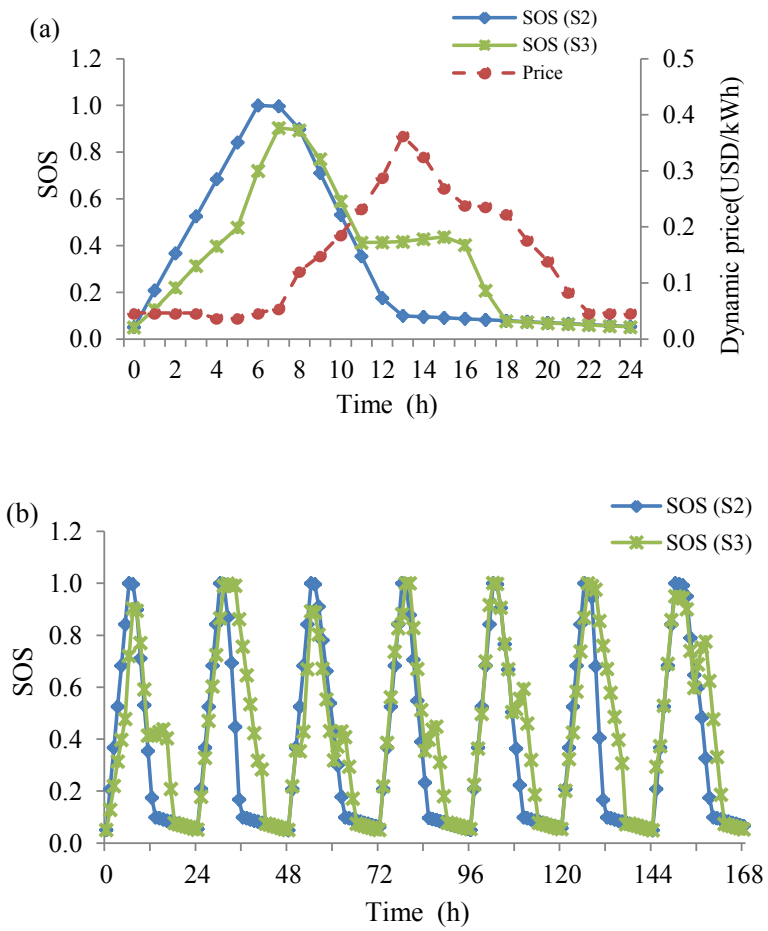

Figure 8.3 TES charge/discharge schedule in a day (a) and in a week (b)

Table 8.2 lists the daily operation costs and cost savings under four different scenarios. Under scenario S0, the daily operation cost in that week was between 111.4 USD and 185.3 USD, and the total operation cost in the week was 1,011.5 USD. Compared with scenario S0, the daily cost saving obtained was between 10.1% and 22.7% when the MINLP-based strategy was applied in the PV+BDG system under scenario S1. Under scenario S2, daily operation costs and total operation cost in the week were reduced significantly when the TES was used in the building. The daily cost saving achieved (under S2) was around 29.5% (between 26.2% and 33.4%) compared with that under scenario S0. Under scenario S3, when the TES and the MINLP-based

optimal strategy were used, both daily operation costs and total operation cost in the week were reduced dramatically compared with that under scenario S0 (i.e. the total operation cost in the week reduced from 1,011.5 USD to 536.15 USD). The total operation cost saving in the week under scenario S3 was 36.2% compared with that under scenario S1 when TES was not used in the building, and 24.8% compared with that under scenario S2 when TES and rule-based control strategy were used.

Table 8.3 summaries the effects of the MINLP-based optimal scheduling strategy and the TES on the cost saving. The use of MINLP-based control achieved a saving of 16.9% on the energy system without TES and a saving of 24.8% on the energy system with TES. The use of TES achieved a saving of 29.5% under rule-based control and a saving of 36.2% under MINLP-based control. When using both MINLP-based control and TES, the saving achieved in the week was as high as 47%.

The oil consumption and net electricity input from the grid (electricity received from grid minus electricity delivered to grid) under the four scenarios are shown in Table 8.4. Under the scenario S0, the oil consumption was about two times of that under the scenario S1, S2 and S3. This may be positive to the grid since the grid could receive surplus electricity generated from the building when the load of the grid is high. Under the scenario S1 and S2, the oil consumptions were reduced significantly since the TES and MINLP-based scheduling strategy were used respectively. The grid provided about 2,000 kWh of electricity in the week. Under the scenario S3, the oil consumption was the lowest, which was benefited from the effects of both TES and MINLP-based scheduling strategy.

Table 8.2 Daily and weekly operation costs and saving under different scenarios

Day	S0	S1		S2		S3			
	Cost (USD)	**Cost** (USD)	**Saving** (S1 *vs* S0)	**Cost** (USD)	**Saving** (S2 *vs* S0)	**Cost** (USD)	**Saving** (S3 *vs* S2)	**Saving** (S3 vs S1)	**Saving** (S3 vs S0)
1	158.8	132.7	16.5%	116.6	26.6%	92.5	20.7%	30.3%	41.8%
2	175.9	149.5	15.0%	117.7	33.1%	90.5	23.1%	39.5%	48.5%
3	125.7	98.4	21.8%	87.2	30.6%	61.6	29.5%	37.4%	51.0%
4	132.7	102.5	22.7%	88.3	33.4%	67.2	24.0%	34.5%	49.4%
5	121.7	97.0	20.3%	86.7	28.8%	60.6	30.1%	37.5%	50.2%
6	185.3	166.6	10.1%	134.0	27.7%	109.9	18.0%	34.0%	40.7%
7	111.4	94.0	15.6%	82.3	26.2%	54.0	34.3%	42.6%	51.5%
Average	144.5	120.1	17.4%	101.8	29.5%	76.6	25.7%	36.5%	47.6%
Total	1011.5	840.6	16.9%	712.8	29.5%	536.2	24.8%	36.2%	47.0%

(S0: PV+BDG (Rule-based), S1: PV+ BDG (MINLP), S2: PV+ BDG +Tank (Rule-based), S3: PV+ BDG +Tank (MINLP))

Table 8.3 Effects of the TES and the enhanced optimal scheduling strategy

Control Strategy	**PV+BDG**	**PV+ BDG +TES**	**Cost saving**
Rule-based	1011.5 (USD)	712.8 (USD)	29.5%
MINLP-based	840.6 (USD)	536.2 (USD)	36.2%
Cost saving	16.9%	24.8%	47.0%

Table 8.4 Oil consumption and net electricity input from grid

	S0		**S1**		**S2**		**S3**	
Day	Oil (kg)	Electricity (kWh)	Oil (kg)	Electricity(kWh)	Oil (kg)	Electricity(kWh)	Oil (kg)	Electricity (kWh)
1	229.5	-433.5	125.5	121.5	117.4	227.9	97.6	321.5
2	252.9	-483.9	121.8	222.6	166.5	29.3	119.6	253.0
3	155.5	-192.3	60.3	288.1	44.9	440.5	48.8	395.6
4	196.2	-355.5	72.9	300.0	81.1	318.2	68.3	377.8
5	178.5	-275.5	70.3	286.8	65.9	377.0	68.4	347.7
6	239.3	-325.7	65.7	607.7	162.1	135.1	122.0	327.5
7	171.0	-271.6	91.0	142.9	59.1	381.0	67.0	322.6
Average	203.3	-334.0	86.8	281.4	99.6	272.7	84.5	335.1
Total	1423.0	-2337.9	607.4	1969.6	697.0	1909.0	591.7	2345.8

8.3.2 Comparison between MINLP and NLP Optimization Approaches

Compared with the NLP method, the MINLP approach requires additional computational effort since it combines algorithms from linear programming, nonlinear programming and integer programming. However, it should be noted that the results obtained using MINLP approach are more feasible and realistic, since the devices (i.e. electric chillers, BDG) usually have their own minimum load ratios while the devices may also have off-status in practice (i.e. discrete working ranges). It can be observed from Figure 8.4 that the load of the electric chillers assigned by NLP was less than the 21 kW (i.e. less than the minimum load (30%) of a chiller) between 16:00 pm and 17:00 pm, which is unacceptable from an operational point of view. The effects of the MINLP and NLP approaches on outputs of optimization are investigated by comparing the operation energy costs of the building when using the two optimization approaches. The differences between the operation energy costs of the system scheduled by two optimization approaches were very small in most of the test days (less than 4.00%) and could be negligible (Table 8.5). However, the load of the electric chillers scheduled by NLP was sometimes lower than its minimum load resulting that the schedules determined by the NLP optimization approach cannot be practically implemented. The MINLP approach can well address these problems since the integer variables, which handle capacity ranges of devices as discrete variables, are available. This allows that the schedules determined by the MINLP optimization approach can be practically implemented in practical operation.

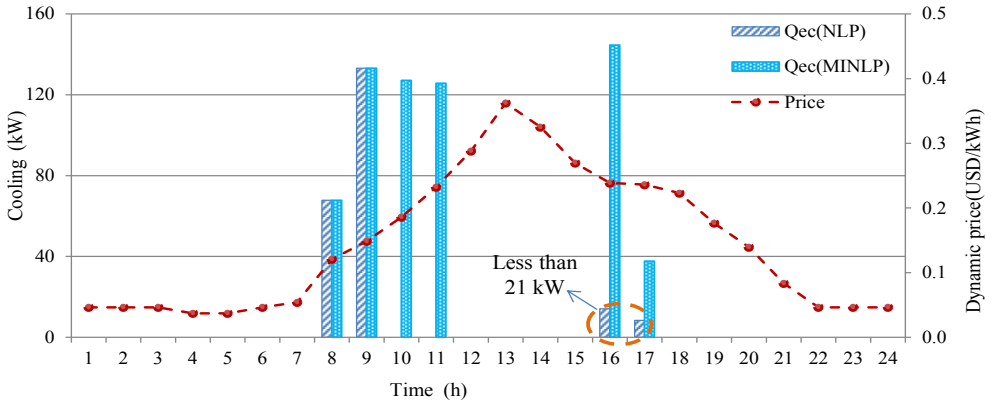

Figure 8.4 Comparison of the cooling distribution for electric chillers using MINLP and NLP

Table 8.5 Comparison between the energy costs obtained by MINLP and NLP

	Cost (USD)			Cost(USD)		
Days	NLP	MINLP(S1)	Saving	NLP	MINLP(S3)	Saving
1	137.9	132.7	3.77%	92.4	92.5	-0.11%
2	146.4	149.5	-2.12%	90.7	90.5	0.22%
3	98.4	98.4	0.00%	61.6	61.5	0.16%
4	102.5	102.5	0.00%	67.1	67.1	0.00%
5	97.0	97.0	0.00%	62.6	60.6	3.19%
6	162.5	166.6	-2.52%	110.2	109.9	0.27%
7	93.0	94.0	-1.08%	53.5	54.0	0.93%
Total	837.7	840.6	-0.35%	538.0	536.1	0.35%

8.3.3 The Effect of Plant Start/Stop Penalty on System Performance

Considering the start/stop frequency of the electric chillers and BDG, a plant start/stop cost penalty is included in the objective function to prohibit frequent on/off switching of the electric chillers and BDG. The effects of including the cost penalty on the

operation energy cost and start/stop number of chillers and BDG are shown in Table 8.6. The daily start/stop number of the electric chillers was reduced significantly (16.7%-60%) when the start/stop cost penalty was included. The effect of including the start/stop cost penalty on the operation energy cost is not significant since the energy cost saving is sometimes positive and sometimes negative (varying between -2.64% and 2.53%). Therefore, the introduction of the cost penalty had a significant contribution to reducing the start/stop frequency of electric chillers, which could help to avoid irregular operating patterns and hence benefit to the service life of the devices. It is worth noticing that the effect of the start/stop cost penalty of the BDG can be ignored in the case studied since the optimal schedule of BDG had always only two on/off switches in each of the test days due to the electricity price profile used.

Table 8.6 Effects of plant start/stop cost penalty under scenario S3

Day	**Cost penalty not concerned**		**Cost penalty concerned**		**Cost Saving**	**Reduction of start/stop number**
	Energy cost (USD)	*Start/Stop number*	*Energy cost (USD)*	*Start/Stop number*		
1	94.97	14	97.47	8	-2.64%	42.9%
2	90.68	30	90.51	12	0.19%	60.0%
3	61.33	12	61.55	10	-0.35%	16.7%
4	66.39	14	67.15	6	-1.15%	57.1%
5	61.24	12	60.59	6	1.06%	50.0%
6	112.72	22	109.87	12	2.53%	45.5%
7	53.85	14	54.01	8	-0.29%	42.9%

8.4 Summary

In this chapter, an enhanced strategy based on the mixed-integer nonlinear programming is presented to optimize the operation schedule of building energy systems. The performance of two energy systems using the enhanced optimal scheduling control strategy (Scenario S1, S3) are evaluated and compared with that using the rule-based control strategy (Scenario S0, S2). The enhanced optimal control strategy could achieve an operation energy cost saving of 16.9% and a cost saving of 24.8% when applied on the energy systems without and with thermal energy storage respectively. The use of thermal energy storage in the building energy system studied could achieve a cost saving of 29.5% under rule-based scheduling control and a cost saving of 36.2% under enhanced optimal (MINLP-based) scheduling control. The proposed scheduling strategy together with the thermal energy storage could eventually achieve a cost saving of up to 47%.

The performance of energy systems scheduled by the MINLP-based optimization approach is also compared with that scheduled by another optimization approach, namely nonlinear programming (NLP). The NLP-based approach can consider the nonlinear input-output characteristic of energy systems but the forbidden working ranges of the energy systems are ignored. Thus the load of electric chillers scheduled by the NLP optimization approach is sometimes lower than their minimum load, resulting in that the optimal scheduled trajectories cannot be implemented in practical operation. The MINLP-based approach has well addressed these problems as observed in the tests since the capacity ranges of the energy systems are handled as discrete variables, which truly reflects the actual operation constraints.

CHAPTER 9 SUMMARIES AND RECOMMENDATIONS

nZEBs, integrated with smart grid, is becoming a future trend for constructing new buildings and renovating existing buildings. The aim of this present thesis is to develop design optimization approach and optimal scheduling strategy for the control of energy systems in nZEBs. This Chapter summarizes the main conclusions as in the following Section, *Section 9.1* presents the main contributions of this thesis, *Section 9.2* presents the main conclusions of all the researches done in the thesis, and *Section 9.3* presents recommendations for future works.

9.1 Summary of Main Contributions

The main contribution of the work in this thesis can be summarized as following:

1. The annual energy performance of Hong Kong ZCB is evaluated based on on-site data collection. The building energy performance is compared with its designed values, which provides an elementary evaluation on energy performance for this building and indicates the direction of improving the building performance.

2. Simulation platform for nZEBs is developed for optimal designing and controlling of energy systems in nZEBs. The energy system models are developed in a way that considers the interaction between building energy systems and renewable energy systems.

3. The simulation-based design optimization for nZEBs is proposed based on TRNSYS and MATLAB softwares. Three most important performance indices are investigated using single objective optimization and multi-objectives optimization methods. The capability and effectiveness of the two methods are compared in terms of design optimization of energy systems in nZEBs.

4. MPC-based optimal scheduling strategies are proposed for scheduling energy systems in the next 24 hours for nZEBs. It shows some advantages to the rule-based control methods for energy systems. The proposed optimal scheduling strategy can achieve significant reductions in carbon dioxide emission, primary energy consumptions and operation cost.

5. The recommendations for the future work in the direction of optimal design and control of nZEBs is provided based on the comprehensive review on the design and control strategies/technologies as well as the development of nZEB projects. This provides nZEB professionals with the basic information on selecting efficient and suitable design options as well as optimization techniques for design/control optimization since there is no exact approach at present for designing and controlling the buildings to achieve nearly/net zero energy targets.

9.2 Conclusions

9.2.1 Design Optimization of Renewable Energy Systems in nZEBs

Genetic Algorithm (GA) method and non-dominated sorting Genetic Algorithm-Ⅱ (NSGA-Ⅱ) approach are applied for optimal design of renewable energy systems in nZEBs. The results of the single objective optimization show that the optimal results obtained when minimizing the combined objective (objective=0.82/0.82, for LEB and ZEB respectively), minimizing CO2 emissions only (objective=-0.46/0.13) and minimizing the grid interaction index only (objective=0.32/0.45) for both low energy building and zero energy building are much better than the corresponding performance (objective=1.0) in the benchmark building. When only the total cost is concerned in optimization, the total cost of low/zero energy buildings (objective=1.9/1.83) is about 2 times of that for the benchmark building. When using multi-objective optimization, three objectives (i.e. total cost, CO_2 emissions and grid interaction index) are considered in parallel and a subset of pareto-optimal solutions is identified in a single run. For the low energy building, the reduction in the renewable energy system investment results in a dramatical increase of CO_2 emissions and lower grid interaction index. However, the cost, CO_2 emissions and grid integration index for the zero energy building have little variations when different design options are selected, due to the constraint of zero annual energy balance. By comparing these optimal design solutions of renewable energy system, decision makers could understand the trade-off relationship among the three objectives and the effects of the design parameters on the objectives.

9.2.2 Impacts of Operation Variables on nZEB Performance Robustness

Sensitivity analysis is conducted on an optimized system to investigate the impacts of the operation variables on nZEB performance. The results show that with 20% variations in the four variables, the maximum change of the combined objective is 26.2%.

The results of the one-way sensitivity analysis show that wind velocity is the key factor that significantly affects the three outputs (operation cost, CO_2 emissions and grid interaction index), with the variances of more than 50%. It is followed by other load and building cooling load. The variances of the outputs caused by the variation of solar radiation are very small (less than 1%), showing that the effect of the variation in solar radiation is negligible. In contrast, the comprehensive performance is most sensitive to other load rather than wind velocity, followed by cooling load. This is because the increase of wind velocity results in reduced operation cost and CO_2 emissions, but a dramatically increased grid interaction index. Thus the effect of wind velocity variation on the comprehensive performance is not significant due to compensation effects. The results of two-way sensitivity analysis further indicate that cooling load & other load, wind velocity & other load, cooling load & wind velocity are the three major pairs which affect the comprehensive performance significantly. In summary, more attention should be paid on the accuracy of wind velocity prediction regarding the total cost/operation cost and/or CO_2 emissions. But the accuracy of building loads prediction should be the priority to be concerned during the design stage concerning the robustness of the comprehensive performance.

The results of multiway sensitivity analysis on four design options indicate that the PV/BDG system may have a worse comprehensive performance under the design condition, but its performance in the real operation is most robustness. In addition, the introduction of active electricity generation systems in buildings could increase the performance robustness of the building energy systems.

9.2.3 Optimal Scheduling for Energy Systems Using Nonlinear Programming

An optimal scheduling using nonlinear programming is proposed for the control of nZEBs. Evaluation tests are conducted in a reference building. Results show that the strategy can solve the power generation/demand mismatch problem of a building involving PV system, combined cooling and power generation (BDG) and cold storage by scheduling their operation in an optimal manner, and reduce building operation cost significantly.

When selling electricity to the grid is allowed, reductions of 25% and 48% in carbon dioxide emission (CDE), 14% and 22% in primary energy consumption (PEC), 29% and 28% in operation cost are achieved in a summer day and a cloudy spring day respectively, compared with situation without BDG and cold storage. When selling electricity to the grid is forbidden, reductions of 12% and 38% in CDE, 6% and 20% in PEC, 24% and 23% in operation cost are achieved in the same situation. Results also show that the use of cold storage together with distributed energy systems in low/zero energy buildings, which fully utilizes the BDG system, can reduce CDE, PEC and operation cost by storing the surplus cold from the adsorption chiller.

Sensitivity analysis shows uncertainties in the inputs do not affect the performance of the proposed method significantly. Uncertainties can be reduced by the actual operation strategy, TES and grid.

9.2.4 Optimal Scheduling for Energy Systems Using Mixed-integer Nonlinear Programming

Based on the optimal scheduling using NLP, an improved scheduling using MINLP is proposed. Results show that the improved strategy could achieve an operation energy cost saving of 16.9% and a cost saving of 24.8% when applied on the energy systems without and with thermal energy storage respectively. The use of thermal energy storage in the building energy system studied could achieve a cost saving of 29.5% under rule-based scheduling control and a saving of 36.2% under MINLP-based scheduling control. The proposed scheduling strategy together with the thermal energy storage could eventually achieve a cost saving of up to 47%.

Comparison is made on the performances of the energy systems scheduled by the MINLP-based and NLP-based optimization approaches. The NLP-based approach can consider the nonlinear input-output characteristic of energy systems but the forbidden working ranges of the energy systems are ignored. Thus the load of electric chillers scheduled by the NLP optimization approach is sometimes lower than their minimum load, resulting in that the optimal schedule determined cannot be implemented in practical operation. The MINLP-based approach has well addressed these problems as observed in the tests since the capacity ranges of the energy systems are handled as discrete variables, which truly reflects the actual operation.

9.3 Recommendations for Future Work

The present PhD works make great efforts on developing design optimization method and optimal control strategy for energy systems in nZEBs. Major efforts can be made on the following aspects to improve the contribution of the research related in the future.

1. The design optimization in this thesis focuses on finding the optimal options and combinations of renewable energy system sizes only. The embodied energy is not considered, which is usually higher than that in normal buildings. Actually, the embodied energy of a low energy building may represent more than 70% of the total of embodied and operational energy over 100 years. Therefore, more parameters need to be considered in the design optimization if the scope is extended to cover the embodied energy and the effects of operation strategies used in future studies.

2. The sensitivity analysis in this study focuses on the impacts of operation variables on the performance of nZEBs. Fixed changes are supposed to be given to the four input variables concerned. That is to say, all input variables are increased and decreased by 20%, 10% and 5% from their baseline values. The limitation of this method is that only a small portion of the possible space of input variables is explored. Probabilistic uncertainty analysis is worth to be introduced to improve the assessment method rather than assigning a single value to each input for sensitivity analysis.

3. The study of design optimization is conducted based on a fixed control strategy, while optimal control strategy is conducted based on a fixed system size. In fact, system optimization should be conducted taking into account both system design and control strategy. It is necessary to develop a generic decision tools that move the design and control of nZEBs towards a holistic view.

REFERENCES

Aelenei, L., and H. Gonçalves. 2014. From solar building design to net zero energy buildings: Performance insights of an office building. *Energy Procedia* 48:1236–1243.

Agarwal, N., A. Kumar and Varun. 2013. Optimization of grid independent hybrid PV–diesel–battery system for power generation in remote villages of Uttar Pradesh, India. *Energy for Sustainable Development* 17(3):210–219.

Ai, B., H.X. Yang, H. Shen and X.B. Liao. 2003. Computer-aided design of PV/wind hybrid system. *Renewable Energy* 28(10):1491–1512.

Al-Sanea, S.A., M.F. Zedan and S.N. Al-Hussain. 2012. Effect of thermal mass on performance of insulated building walls and the concept of energy savings potential, *Applied Energy* 89 (January (1)):430–442.

Askari, I.B. and M. Ameri. 2012. Techno-economic feasibility analysis of stand-alone renewable energy systems (PV/bat, Wind/bat and Hybrid PV/wind/bat) in Kerman, Iran. *Energy Sources, Part B: Economics, Planning, and Policy* 7(1):45–60.

Aste, N., R.S. Adhikari and C. Del Pero. 2011. Photovoltaic technology for renewable electricity production: towards net zero energy buildings. *International Conference on Clean Electrical Power (ICCEP)*, Ischia, June 14-16.

Attia, S., E. Gratia, A. De Herde and J.L.M. Hensen. 2012. Simulation-based decision support tool for early stages of zero-energy building design. *Energy and Buildings* 49:2–15.

Avril, S., G. Arnaud, A. Florentin, and M. Vinard. 2010. Multi-objective optimization of batteries and hydrogen storage technologies for remote photovoltaic systems. *Energy* 35(12):5300–5308.

Baglivo, C., P.M. Congedo, A. Fazio and D. Laforgia. 2014. Multi-objective optimization analysis for high efficiency external walls of zero energy buildings (ZEB) in the Mediterranean climate. *Energy and Buildings* 84:483–492.

Bambrook, S.M., A.B. Sproul and D. Jacob. 2011. Design optimization for a low energy home in Sydney. *Energy and Buildings* 43(7):1702–1711.

Barley, C.D., C.B. Winn, L. Flowers and H.J. Green. 1995. Optimal control of remote hybrid power systems. *Part I. Simplified model. In: Proceedings of WindPower'*. Washington, DC.

Barley, C.D. and C.B. Winn. 1996. Optimal dispatch strategy in remote hybrid power systems. *Solar Energy* 58(4–6):165–79.

Beaudin, M. and H. Zareipour. 2015. Home energy management systems: A review of modelling and complexity. *Renewable and Sustainable Energy Reviews* 45:318–335.

Bekele, G. and G. Tadesse. 2012. Feasibility study of small Hydro/PV/Wind hybrid system for off-grid rural electrification in Ethiopia. *Applied Energy*; 97:5-15.

Berkenkamp, F., and M. Gwerder. 2014. Hybrid model predictive control of stratified thermal storages in buildings, *Energy and Buildings* 84: 233–240.

Bernal-Agustín, J.L. and R. Dufo-López. 2009. Simulation and optimization of stand-alone hybrid renewable energy systems. *Renewable and Sustainable Energy Reviews* 13(8): 2111–2118.

Bilodeau, A. and K. Agbossou. 2006. Control analysis of renewable energy system with hydrogen storage for residential applications. *Journal of Power Sources* 162(2):757-764.

Bio-diesel price 2015. http://www.globalpetrolprices.com/Hong-Kong/diesel_prices/

Blengini, G.A., T. Di Carlo. 2010. The changing role of life cycle phases, subsystems and materials in the LCA of low energy buildings. *Energy and Buildings* 42(6): 869–880.

Bonmin–COIN-OR Project. https://projects.coin-or.org/Bonmin

Borowy, B.S. and Z.M. Salameh. 1996. Methodology for optimally sizing the combination of a battery bank and PV array in a wind/PV hybrid system. *IEEE Transactions on Energy Conversion* 11(2):367–373.

Bucking, S., R. Zmeureanu and A. Athienitis. 2014. A methodology for identifying the influence of design variations on building energy performance. *Journal of Building Performance Simulation* 7(6): 411–426.

Cai, W.G., Y. Wu, Y. Zhong and H. Ren. 2009. China building energy consumption: situation, challenges and corresponding measures. *Energy Policy* 37(6):2054-2059.

Candanedo, J.A., and A.K. Athienitis. 2011. Predictive control of radiant floor heating and solar-source heat pump operation in a solar house. *HVAC& Research* 17:235-256.

Cardona, E., and A. Piacentino. 2003. A methodology for sizing a trigeneration plant in Mediterranean areas. *Applied Thermal Engineering* 23:1665–1680.

Chandan, V., A-T. Do, B. Jin, F. Jabbari, J. Brouwer and I. Akrotirianakis, et al. 2012. Modeling and optimization of a combined cooling, heating and power plant system. *In: American control conference (ACC)*, Canada, June 27-29, 2012. pp: 3069–74.

CO2 emission factors 2010. http://www.sunearthtools.com/tools/CO2-emissions-calculator.php

Costanzo, G.T., G.C. Zhu, M.F. Anjos, G. Savard. 2012. A system architecture for autonomous demand side load management in smart buildings. *IEEE Transactions on Smart Grid* 3(4):2157–2165.

Crawley, D., S. Pless and P. Torcellini. 2009. Getting to net zero. *ASHRAE Journal* 51(9):18-25.

Deb, K., A. Pratap, S. Agarwal and T. Meyarivan. 2002. A fast and elitist multiobjective Genetic Algorithm: NSGA-II. *IEEE Transactions on Evolutionary Computation* 6:182-197

Dehnad, A., and H. Shakouri. 2013. A novel model of intelligent electrical load management by goal programming for smart houses, respecting consumer preferences. *Energy Power Engineering* 5(10):622–627.

Dekker, J., M. Nthontho S. Chowdhury and S.P. Chowdhury. 2012. Economic analysis of PV/diesel hybrid power systems in different climatic zones of South

Africa. *International Journal of Electrical Power & Energy Systems* 40(1): 104–112.

Deng, S., R.Z. Wang and Y.J. Dai. 2014. How to evaluate performance of net zero energy building – A literature research. *Energy* 71: 1–16.

Depecker, P., C. Menezo, J. Virgone and S. Lepers. 2001. Design of buildings shape and energetic consumption. *Building and Environment* 36: 627–635.

Doostizadeh, M. and H. Ghasemi. 2012. A day-ahead electricity pricing model based on smart metering and demand-side management. *Energy* 2012; 46(1):221–230.

Doust, N., G. Masera, F. Frontini, and M. Imperadori. 2012. Cost optimization of a nearly net zero energy building: a case study. In SIMUL 2012, *The Fourth International Conference on Advances in System Simulation* (pp. 44–49).

Dufo-López, R., J.L. Bernal-Agustín and J. Contreras. 2007. Optimization of control strategies for stand-alone renewable energy systems with hydrogen storage. *Renewable Energy* 32(7):1102–1126.

EBPD 2010. The Directive 2010/31/EU of the European Parliament and of the Council of 19 May 2010 on the energy performance of buildings, *Official Journal of the European Union*.

Ekren, O., B.Y. Ekren. 2010. Size optimization of a PV/wind hybrid energy conversion system with battery storage using simulated annealing. *Applied Energy* 87(2): 592–598.

Elliott, M.S. 2008. Decentralized model predictive control of a multiple evaporator HVAC system [MSc thesis]. College Station, Texas, United States: Texas A&M University.

El-Temtamy, S.A. and T.S. Gendy. 2014. Economic evaluation and sensitivity analysis of some fuel oil upgrading processes. *Egyptian Journal of Petroleum* 23(4): 397-407.

Eshraghi, J., N. Narjabadifam, N. Mirkhani, S. Sadoughi Khosroshahi and M. Ashjaee. 2014. A comprehensive feasibility study of applying solar energy to design a zero energy building for a typical home in Tehran. *Energy and Buildings* 72:329–339.

Evins, R. 2013. A review of computational optimization methods applied to sustainable building design. *Renewable and Sustainable Energy Reviews* 22:230-245.

Facci, A.L., L. Andreassi, S. Ubertini and E. Sciubba. 2014. Analysis of the influence of thermal energy storage on the optimal management of a trigeneration plant. *Energy Procedia* 45:1295–1304.

Fang, F., Q.H. Wang and Y. Shi. 2012. A Novel Optimal Operational Strategy for the CCHP System Based on Two Operating Modes. *IEEE Transactions on Power Systems* 27(2):1032–1041.

Fong, K.F. and C.K. Lee. 2014. Investigation on hybrid system design of renewable cooling for office building in hot and humid climate. *Energy and Buildings* 75:1–9.

Fong, K.F. and C.K. Lee. 2012. Towards net zero energy design for low-rise residential buildings in subtropical Hong Kong. *Applied Energy* 93:686–694.

Frey, H.C., S.R. Patil. 2002. *Risk Anal* 22 (3): 553–578

Fumo, N., P.J. Mago and L.M. Chamra. 2009. Emission operational strategy for combined cooling, heating, and power systems. *Applied Energy* 86(11):2344–2350.

Gans, W., A. Alberini, A. Longo. 2013. Smart meter devices and the effect of feedback on residential electricity consumption: Evidence from a natural experiment in Northern Ireland. *Energy Economics* 2013; 36:729–743.

Ghedamsi, K. and D. Aouzellag. 2010. Improvement of the performances for wind energy conversions systems. *International Journal of Electrical Power & Energy System* 32: 936-945.

Gordon, J.M. 1987. Optimal sizing of stand-alone photovoltaic solar power systems. *Solar Cells* 20(4):295–313.

Gu, Q.Y., H.B. Ren, W.J. Gao and J.X. Ren. 2012. Integrated assessment of combined cooling heating and power systems under different design and management options for residential buildings in Shanghai. *Energy and Buildings* 51:143–152.

Guo, L., W. Liu, J. Cai, B. Hong and C. Wang. 2013. A two-stage optimal planning and design method for combined cooling, heat and power microgrid system. *Energy Conversion and Management* 74:433-445.

Hamdy, M., A. Hasan and K. Siren. 2011. Applying a multi-objective optimization approach for design of low-emission cost-effective dwellings. *Building and Environment* 46(1):109–123

Hamdy, M., A. Hasan and K. Siren. 2013. A multi-stage optimization method for cost-optimal and nearly-zero-energy building solutions in line with the EPBD-recast 2010. *Energy and Buildings* 56: 189–203.

Hassoun, A., and I. Dincer. 2014. Development of power system designs for a net zero energy house. *Energy and Buildings* 73: 120–129.

Hazran, H. and A.I.A.A. Rani. 2005. Review on operation of ventilation air - conditioning system at Kompleks Sains & Teknologi, Universiti Teknologi MARA, Universiti Teknologi MARA, Shah Alam, Malaysia, April 2005.

Henze, G.P., C. Felsmannb and G. Knabeb. 2004. Evaluation of optimal control for active and passive building thermal storage. *International Journal of Thermal Sciences* 43(2):173–183.

Hong, T., L. Yang, D. Hill, W. Feng. 2014. Data and analytics to inform energy retrofit of high performance buildings. *Applied Energy* 126: 90-106.

Huang, G.S. 2011. Model predictive control of VAV zone thermal systems concerning bi-linearity and gain nonlinearity. *Control Engineering Practice* 19:700-710.

Iqbal, M.T. 2004. A feasibility study of a zero energy home in Newfoundland. *Renewable Energy* 29(2): 277–289.

Ismail, M.S., M. Moghavvemi and T.M.I. Mahlia. 2012. Design of a PV/diesel stand-alone hybrid system for a remote community Palestine. *Journal of Asian Scientific Research* 2(11): 599-606

Ismail, M.S., M. Moghavvemi and T.M.I. Mahlia. 2013. Techno-economic analysis of an optimized photovoltaic and diesel generator hybrid power system for remote houses in a tropical climate. *Energy Conversion and Management* 69: 163–173.

Rosen, J.B. 1960. The gradient projection method for nonlinear programming, *Journal of the Society for Industrial and Applied Mathematics* 8 (1):181–217.

Binder, K. and D.P. Landau. 2000. *A guide to Monte–Carlo simulations in statistical physics*, Cambridge University Press.

Kaabeche, A., M. Belhamel, R. Ibtiouen, S. Moussa and M.R. Benhadadi. 2006. Optimisation d'un système hybride (Eolien-photovoltaïque) totalement autonome. *Revuedes Energies Renouvelables* (3):199-209.

Kaabeche, A., M. Belhamel and R. Ibtiouen. 2011. Sizing optimization of grid-independent hybrid photovoltaic/wind power generation system. *Energy* 36(2): 1214–1222.

Kalantar, M. and S.M.G. Mousavi. 2010. Dynamic behavior of a stand-alone hybrid power generation system of wind turbine microturbine, solar array and battery storage. *Applied Energy* 87:3051–3064.

Kang, K.H. and D.J. Won. 2009. Power management strategy of stand-alone hybrid system to reduce the operation mode changes. *In Transmission & Distribution Conference & Exposition: Asia and Pacific, IEEE*(pp. 1–4).

Kapsalaki, M., V. Leal and M. Santamouris. 2012. A methodology for economic efficient design of Net Zero Energy Buildings. *Energy and Buildings* 55: 765–778.

Karaki, S.H., R.B. Chedid and R. Ramadan. 1999. Probabilistic performance assessment of autonomous solar-wind energy conversion systems. *IEEE Transactions on Energy Conversion* 14(3):766-772.

Kashima, T. and S. Boyd. 2013. Cost optimal operation of thermal energy storage system with real-time prices, *in: Proceedings of International Conference on Control, Automation, and Information Sciences (ICCAIS)*, November 2013:233–237.

Kellogg, W.D., M.H. Nehrir, G. Venkataramanan and V. Gerez. 1998. Generation unit sizing and cost analysis for stand-alone wind, photovoltaic and hybrid wind/PV systems. *IEEE Transactions on Energy Conversion* 13(1):70–75.

Khan, M.J. and Iqbal, M.T. 2005. Pre-feasibility study of stand-alone hybrid energy systems for applications in Newfoundland. *Renewable Energy* 30(6):835–854.

Khatib, T., A. Mohamed, K. Sopian and M. Mahmoud. 2011. Optimal sizing of building integrated hybrid PV/diesel generator system for zero load rejection for Malaysia. *Energy and Buildings* 43(12): 3430–3435.

Khelif, A., A. Talha, M. Belhamel and A. Hadj Arab. 2012. Feasibility study of hybrid Diesel–PV power plants in the southern of Algeria: Case study on AFRA power plant. *International Journal of Electrical Power & Energy Systems* 43(1):546–553.

Kilkis, S. 2007. A new metric for net- zero carbon buildings. Proceedings of ES2007. *Energy Sustainability.* Long Beach, California, pp. 219-224.

Kolokotsa, D., D. Rovas, E. Kosmatopoulos and K. Kalaitzakis. 2011. A roadmap towards intelligent net zero- and positive-energy buildings. *Solar Energy* 85(12): 3067–3084.

Koutroulis, E., D. Kolokotsa, A. Potirakis and K. Kalaitzakis. 2006. Methodology for optimal sizing of stand-alone photovoltaic/wind-generator systems using genetic algorithms. *Solar Energy* 80(9):1072–1088.

Kurnitski, J., A. Saari, T. Kalamees, M. Vuolle, J. Niemelä and T. Tark. 2011. Cost optimal and nearly zero (nZEB) energy performance calculations for residential buildings with REHVA definition for nZEB national implementation. *Energy and Buildings* 43(11): 3279–3288.

Kusakan, K. and H.J. Vermaak. 2014. Hybrid diesel generator/renewable energy system performance modeling. *Renewable energy* 67: 97-102.

Kwon, W.H. and S. Han. 2005. *Receding horizon control model predictive control for state models*. London: Springer-Verlag.

Li, C., X.F. Ge, Y. Zheng, C. Xu, Y. Ren, C.G. Song and C.X. Yang. 2013. Techno-economic feasibility study of autonomous hybrid wind/PV/battery power system for a household in Urumqi, China. *Energy* 55: 263–272.

Li, D.H.W., L. Yang and J.C. Lam. 2013. Zero energy buildings and sustainable development implications – A review. *Energy* 54: 1–10.

Li, X.W. and J. Wen. 2014. Net-zero energy impact building clusters emulator for operation strategy development. *ASHRAE Annual Conference*, at Seattle, WA, USA; June 28- July 02, 2014.

LINDO Systems. www.lindo.com

Liu, M.X., Y. Shi and F. Fang. 2012. A new operation strategy for CCHP systems with hybrid chillers. *Applied Energy* 95:164–173.

Long, Ha, D., H. Joumaa, S. Ploix and M. Jacomino. 2012. An optimal approach for electrical management problem in dwellings, *Energy and Buildings* 45:1–14.

Low Energy Buildings in Europe: Current State of Play, Definitions and Best Practice. 2009. Brussels.

Lü, H., L. Jia, S.L. Kong and Z.S. Zhang. 2007. Predictive functional control based on fuzzy T-S model for HVAC systems temperature control. *Journal of Control Theory and Applications* 5:94-98.

Lu, Y.H., S.W. Wang, Y.J. Sun and C.C. Yan. 2015. Optimal scheduling of buildings with energy generation and thermal energy storage under dynamic electricity pricing using mixed-integer nonlinear programming. *Applied Energy* 147:49–58.

Lu, Y.H., S.W. Wang, Y. Zhao and C.C. Yan. 2015. Renewable energy system optimization of low/zero energy buildings using single-objective and multi-objective optimization methods. *Energy and Buildings* 89: 61–75.

Lujano-Rojas Juan, M., C. Monteiro, D.L. Rodolfo and L.J.Bernal-Agustin. 2012. Optimum residential load management strategy for real time pricing (RTP) demand response programs. *Energy Policy* 45: 671–679.

Bazaraa, M.S., H.D. Sherali and L.M. Shetty, 2006. Nonlinear Programming: Theory andAlgorithms, John Wiley and Sons, New York.

Ma, J.R., J. Qin, T. Salsbury and P. Xu. 2011. Demand reduction in building energy systems based on economic model predictive control. *Chemical Engineering Science* 67:92-100.

Ma, T., H.X. Yang and L. Lu. 2014. A feasibility study of a stand-alone hybrid solar–wind–battery system for a remote island. *Applied Energy* 121:149-158.

Ma, Y., A. Kelman, A. Daly and F. Borrelli. 2012. Predictive control for energy efficient buildings with thermal storage: modeling, stimulation, and experiments. *IEEE Control Syst* 32(1):44–64.

Maclay William and Maclay architects. 2014. The new net zero - leading-edge design and construction of homes and buildings for a renewable energy future. Chelsea green publishing white river junction, Vermont.

Mago, P.J. and L.M. Chamra. 2009. Analysis and optimization of CCHP systems based on energy, economical, and environmental considerations. *Energy and Buildings* 41:1099-1106.

Mago, P.J., N. Fumo and L.M. Chamra. 2009. Performance analysis of CCHP and CHP systems operating following the thermal and electric load. *International Journal of Energy Research* 33(9):852–864.

Mago, P.J. and A.K. Hueffed. 2010. Evaluation of a turbine driven CCHP system for large office buildings under different operating strategies. *Energy and Buildings* 42:1628-1636.

Maheri, A. 2014. Multi-objective design optimisation of standalone hybrid wind-PV-diesel systems under uncertainties. *Renewable Energy* 66:650–661.

Markvart, T. 1996. Sizing of hybrid PV/wind energy systems. *Solar Energy* 59 (4):277-281.

Marszal, A.J., P. Heiselberg, J.S. Bourrelle, E. Musall, K. Voss, I. Sartori and A. Napolitano. 2011. Zero Energy Building – A review of definitions and calculation methodologies. *Energy and Buildings* 43(4): 971–979.

Matlab Optimization Toolbox. http://www.mathworks.com

Miland, H. 2005. Operational Experience and control strategies for a stand-alone power system based on renewable energy and hydrogen, PhD Dissertation, Norwegian University of Science and Technology, Trondheim.

Milo, A., H. Gaztañaga, I. Etxeberria-Otadui, S. Bacha and P. Rodríguez. 2011. Optimal economic exploitation of hydrogen based grid-friendly zero energy buildings. *Renewable Energy* 36(1): 197–205.

Missaoui, R., H. Joumaa, S. Ploix and S. Bacha. 2014. Managing energy Smart Homes according to energy prices: Analysis of a Building Energy Management System. *Energy and Buildings* 71:155–167.

Mitra, S., Sun, L. and I.E. Grossmann. 2013. Optimal scheduling of industrial combined heat and power plants under time-sensitive electricity prices, *Energy* 54:194–211.

Mixed-Integer Nonlinear Optimization 2012. http://www.mcs.anl.gov/papers/P3060-1112.pdf

Moghaddas-Tafreshi, S.M. and S.M. Hakimi. 2009. Optimal sizing of a stand-alone hybrid power system via particle swarm optimization for Kahnouj area in south-east of Iran, 2009. *Renewable Energy* 34:1855–1862.

Moldovan, M.D., I. Visa, M. Neagoe and B.G. Burduhos. 2014. Solar Heating &cooling energy mixes to transform low energy buildings in nearly zero energy buildings. *Energy Procedia* 48:924–937.

nZEBs database. http://iea40.buildinggreen.com/

O'Brien, W., A. Athienitis and T. Kesik. 2009. The development of solar house design tool. *In 11th International Building Performance Simulation Association (IBPSA) Conference* (pp. 27–30).

Oldewurtel, F., A. Parisio, C. Jones, M. Morari, D. Gyalistras and M. Gwerder, et al. 2010. Energy efficient building climate control using stochastic model predictive control and weather predictions. *In: Proceedings of American control conference*.

Oliveira Panão, M.J.N., M.P. Rebelo and S.M.L. Camelo. 2013. How low should be the energy required by a nearly Zero-Energy Building? The load/generation energy balance of Mediterranean housing. *Energy and Buildings* 61:161–171.

Ould Bilal, B., V. Sambou, P.A. Ndiaye, C.M.F. Kébé and M. Ndongo. 2010. Optimal design of a hybrid solar–wind–battery system using the minimization of the annualized cost system and the minimization of the loss of power supply probability (LPSP). *Renewable Energy* 35:2388–2390.

Özkan, H.A. 2015. A new real time home power management system. *Energy and Buildings* 97:56–64.

Pe´rez-Lombard, L., J. Ortiz and C. Pout. 2008. A review on buildings energy consumption information. *Energy and buildings* 40:394-398.

Wolf, P. 1963. Methods of nonlinear programming, in: Recent advances in mathematical programming, McGrew-Hill, New York.

Pacheco, R., J. Ordóñez and G. Martínez. 2012. Energy efficient design of building: A review. *Renewable and Sustainable Energy Reviews* 16(6):3559–3573.

Palonen, M., A. Hasan and K. Siren. 2009. A genetic algorithm for optimization of building envelope and HVAC system parameters. Eighth International Building Performance Simulation Association. *IBPSA Conference*: 159-166.

Pikas, E., M. Thalfeldt and J. Kurnitski. 2014. Cost optimal and nearly zero energy building solutions for office buildings. *Energy and Buildings* 74: 30–42.

Privara, S., J. Siroky, L. Ferkl and J. Cigler. 2011. Model predictive control of a building heating system: the first experience. *Energy and Buildings* 43: 564-72.

Ramoji, S.K. and B.J. Kumar. 2014. Optimal economical sizing of a PV-Wind hybrid energy system using genetic algorithm and teaching learning based optimization. *International Journal of Advanced Research in Electrical, Electronics and Instrumentation Engineering* 3(2): 7352–7367.

Rehman, S. and L.M. Al-Hadhrami. 2010. Study of a solar PV–diesel–battery hybrid power system for a remotely located population near Rafha, Saudi Arabia. *Energy* 35(12):4986–4995.

Rehrl, J. and M. Horn. 2011. Temperature control for HVAC systems based on exact linearization and model predictive control. *In: International Conference Control Applications (CCA)*. Denver, Colorado, USA. Pp. 1119-1124.

Ren, H.B., W.J. Gao and Y.J. Ruan. 2009. Economic optimization and sensitivity analysis of photovoltaic system in residential buildings. *Renewable Energy* 34(3):883–889.

Rezzouk, H. and A. Mellit. 2015. Feasibility study and sensitivity analysis of a stand-alone photovoltaic–diesel–battery hybrid energy system in the north of Algeria. *Renewable and Sustainable Energy Reviews* 43: 1134–1150.

Robert, A. and M. Kummert. 2012. Designing net-zero energy buildings for the future climate, not for the past. *Building and Environment* 55:150–158.

Rodriguez-Ubinas, E., C. Montero, M. Porteros, S. Vega, I. Navarro, M. Castillo-Cagigal, E. Matallanas and A. Gutiérrez. 2014. Passive design strategies and performance of Net Energy Plus Houses. *Energy and Buildings* 83: 10–22.

RTE 2011.: réseau de transport d'électricite, Bilan prévisionnel de l'équilibre offre demande d'électricite en france. http://www.rte-france.com

Salehi, F., Prasher, S.O., S. Amin, A. Madani, S.J. Jebelli, H.S. Ramaswamy and C.T. Drury. 2000. Prediction of Annual Nitrate-N Losses in Drain Outflows with Artificial Neural Networks. *Transactions of the ASAE* 2000; 43(5):1137-1143

Saltelli, A., K. Chan and E.M. Scott. 2000. Sensitivity analysis. John Wiley and Sons; Ltd.: West Sussex, England.

SHC TASK 40- ECBCS ANNEX 52. 2008. http://www.iea-shc.org/task40/

Silva, P.C.P., M. Almeida, L. Bragança and V. Mesquita. 2013. Development of prefabricated retrofit module towards nearly zero energy buildings. *Energy and Buildings* 56:115–125.

Skoplaki, E. and J.A. Palyvos. 2009. On the temperature dependence of photovoltaic module electrical performance: A review of efficiency/power correlations. *Solar Energy* 83: 614-624.

Sreeraj, E.S., K. Chatterjee and S. Bandyopadhyay. 2010. Design of isolated renewable hybrid power systems. *Solar Energy* 84(7):1124–1136.

Stephan, A., R.H. Crawford, and K. Myttenaere de. 2013. A comprehensive assessment of the life cycle energy demand of passive houses. *Applied Energy* 112: 23–34.

Sun, Y.J., P. Huang and G.S. Huang. 2015. A multi-criteria system design optimization for net zero energy buildings under uncertainties. *Energy and Buildings* 97: 196-204.

Sun, Y.J. 2015. Sensitivity analysis of macro-parameters in the system design of net zero energy building. *Energy and Buildings* 86: 464–477.

Sustainable buildings in Australia.

http://www.urbanecology.org.au/topics/energyefficientbuildings.html

Sustainable buildings in China.

http://www.som.com/projects/pearl_river_tower__mep

Sustainable buildings in Japan. http://www.sekisuihouse.com/zeh/eng/flash.html

Thalfeldt, M., E. Pikas, J. Kurnitski and H. Voll. 2013. Facade design principles for nearly zero energy buildings in a cold climate. *Energy and Buildings* 67: 309–321.

The New York Independent System Operator. http://www.nyiso.com

Tina, G., S. Gagliano and S. Raiti. 2006. Hybrid solar/wind power system probabilistic modelling for long-term performance assessment. *Solar Energy* 80(5): 578–588.

Torcellini, P., S. Pless, M. Deru and D. Crawley. 2006. Zero energy buildings: a critical look at the definition. ACEEE Summer Study, Pacific Grove, California. August 14-18.

U.S. Department of Energy. 2008. The smart grid: an introduction. Technical report. US Department of Energy.

Ulleberg, Ø. 2004. The importance of control strategies in PV–hydrogen systems. Solar *Energy* 76(1–3):323–329.

Visa, I., M.D. Moldovan, M. Comsit and A. Duta. 2014. Improving the renewable energy mix in a building toward the nearly zero energy status. *Energy and Buildings* 68:72–78.

Wang, J.J., Y.Y. Jing, C.F. Zhang and Z. Zhai. 2011. Performance comparison of combined cooling heating and power system in different operation modes. *Applied Energy* 88:4621-4631.

Wang, L., J. Gwilliam and P. Jones. 2009. Case study of zero energy house design in UK. *Energy and Buildings* 41(11):1215–1222.

Wang, S.W., X. Xue and C.C. Yan. 2014. Building power demand response methods toward smart grid. *HVAC&R Research* 20(6):665–687.

Wang, W., H. Rivard and R.G. Zmeureanu. 2003. Optimizing building design with respect to life-cycle environmental impacts. Eighth International Building Performance Simulation Association, *IBPSA Conference* 2003: 1355-1361.

Wang, W., R.G. Zmeureanu and H. Rivard. 2005. Applying multi-objective genetic algorithms in green building design optimization. *Building and Environment* 40: 1512-1525

World Map of nZEBs. 2013. http://batchgeo.com/map/net-zero-energy-buildings

Yang H.X., W. Zhou, L. Lu and Z.H. Fang. 2008. Optimal sizing method for stand-alone hybrid solar–wind system with LPSP technology by using genetic algorithm. *Solar Energy* 82:354–367.

Yang, H.X., J. Burnett and L. Lu. 2003. Weather data and probability analysis of hybrid photovoltaic/wind power generation systems in Hong Kong. *Renewable Energy* 28:1813-1824.

Yang, H.X., L. Lu and W. Zhou. 2007. A novel optimization sizing model for hybrid solar-wind power generation system. *Solar Energy* 81(1):76-84.

Yuan, S. and R. Perez. 2006. Multiple-zone ventilation and temperature control of a single-duct VAV system using model predictive strategy. *Energy and Building* 38:1248-1261.

Zebra. 2014. Nearly zero- energy building strategy 2020. September 26, 2014. http://zebra2020.eu/

Zero Carbon Building in Hong Kong. http://zcb.hkcic.org/Eng/index.aspx

Zhao, M., Künzel, H.M. and F. Antretter. 2015. Parameters influencing the energy performance of residential buildings in different Chinese climate zones. *Energy and Buildings* 96:64–75.

Zhao, Y., Y.H. Lu, C.C. Yan and S.W. Wang. 2015. MPC-based optimal scheduling of grid-connected low energy buildings with thermal energy storages. *Energy and Buildings* 86:415–426.

Zheng, C.Y., J.Y. Wu and X.Q. Zhai. 2014. A novel operation strategy for CCHP systems based on minimum distance. *Applied Energy* 128:325-335.

Zhou, G., G.P. Henze and M. Krarti. 2005. Parametric analysis of active and passive building thermal storage utilization. *Journal of Solar Energy Engineering* 127(1): 37–46.

Zhou, Z., J. Zhang, P. Liu, Z. Li and M.C. Georgiadis, E.N. Pistikopoulos. 2013. A two-stage stochastic programming model for the optimal design of distributed energy systems. *Applied Energy* 103:135–144.

Zhu, Z., S. Lambotharan, C.W. Hau and Z. Fan. 2012. Overview of demand management in smart grid and enabling wireless communication technologies. *IEEE Wireless Communications*. 48–56.